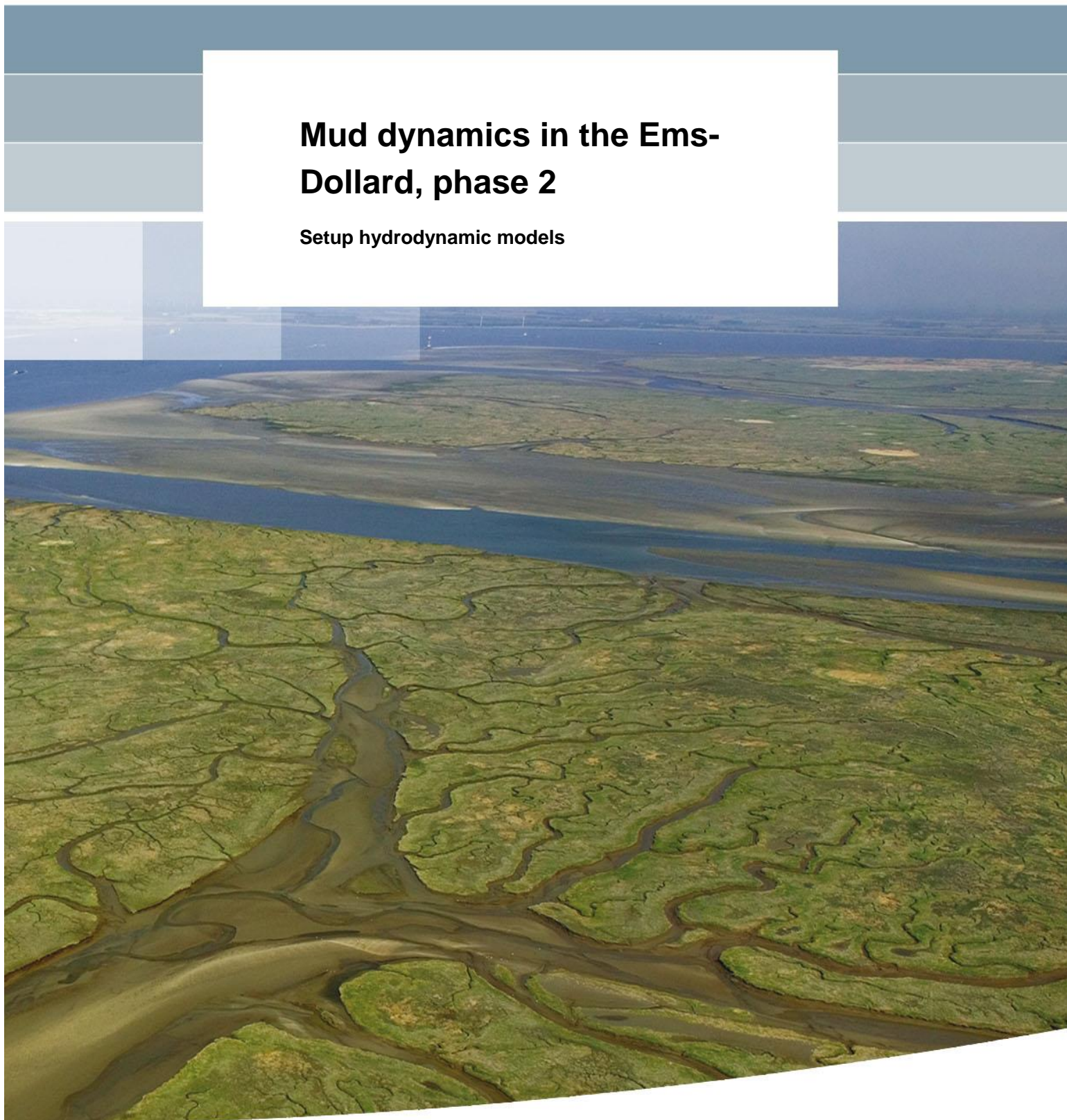


## **Mud dynamics in the Ems- Dollard, phase 2**

**Setup hydrodynamic models**





# **Mud dynamics in the Ems-Dollard, phase 2**

**Setup hydrodynamic models**

Bas van Maren  
Julia Vroom  
Thomas Vijverberg  
Marjolijn Schoemans  
Arnold van Rooijen

1205711-001





**Title**  
Mud dynamics in the Ems-Dollard, phase 2

<b>Client</b>	<b>Project</b>	<b>Reference</b>	<b>Pages</b>
Rijkswaterstaat	1205711-001	1205711-001-ZKS-0003-	108

**Keywords**

Lower Ems River, Ems Dollard Estuary, Water Framework Directive, Hydrodynamic model.

**Summary**

The Water Framework Directive (WFD) obliges the EU member states to achieve good status of all designated water bodies (rivers, lakes, transitional and coastal waters) by 2015. In the management plan for the implementation of the WFD (and Natura 2000) in the Netherlands, the context, perspectives, targets and measures for each designated water body (also including the Ems-Dollard) have been laid out. To achieve a good status of the Ems-Dollard Estuary (as the WDF obliges), knowledge on the mud dynamics in this region has to be improved, and the reasons for the increase in turbidity have to be identified before 2015. Therefore Rijkswaterstaat has initiated the project "Onderzoek slibhuishouding Eems-Dollard" (Research mud dynamics Ems-Dollard). This project explores the reasons for the historic increase in turbidity, and which measures can be designed to improve the water quality in the area.

Part of this research is the development of an effect-chain model. This report describes the set up of the hydrodynamic model of the effect-chain model. This model is used to drive the sediment transport model, the water quality model, and in a later stage of the project to explain the current state of turbidity in the Ems Estuary and quantify the effects of mitigating measures.

**References**

Offertenummer 1205711-000-ZKS-0004, toekenningbrief RWS/WD-2011/3497.

Version	Date	Author	Initials	Review	Initials	Approval	Initials
1.0	April 2013	Bas van Maren		Thijs van Kessel			
2.0	Oct 2013	Bas van Maren		Han Winterwerp			
3.0	June 2014	Bas van Maren		Han Winterwerp			
4.0	Sep 2014	Bas van Maren	BM	Marcel Taal		Frank Hoozemans	

**State**  
final



## Contents

<b>1</b>	<b>Introduction</b>	<b>3</b>
<b>2</b>	<b>Description of the models</b>	<b>7</b>
2.1	Introduction	7
2.2	Effect chain models	9
2.3	The Waddensea Ems Dollard (WED) model	10
2.4	The Ems River (ER) and Ems River Dollard (ERD) models	11
<b>3</b>	<b>Adaptation and validation of the WED model</b>	<b>13</b>
3.1	Introduction	13
3.2	The original WED model	14
3.3	Modifications	14
3.3.1	Boundary and initial conditions	15
3.3.2	Discharges	18
3.3.3	Various	18
3.4	Validation 2012	19
3.4.1	Waterlevels	19
3.4.2	Flow velocities	21
3.4.3	Residual flow	24
3.4.4	Salinity	26
3.5	Validation 2013	28
3.5.1	Waterlevels	28
3.5.2	Salinity	31
3.6	Wave modelling	32
3.6.1	Objectives and approach	32
3.6.2	Model set up	32
3.6.3	Model verification	35
3.6.4	Bed shear stress	39
3.6.5	2013 wave conditions	41
3.7	Model accuracy	43
3.8	Recommendations	44
3.9	Summary	45
<b>4</b>	<b>Set up and calibration of the ER and ERD models</b>	<b>47</b>
4.1	Introduction	47
4.2	Set up and calibration of the ERD model	47
4.2.1	Numerical grid and bathymetry	47
4.2.2	Boundary conditions	49
4.2.3	Miscellaneous	51
4.2.4	Calibration	52
4.3	Set up and calibration of the ER model	57
4.4	Model accuracy	63
4.5	Summary	64
<b>5</b>	<b>Historic scenarios</b>	<b>65</b>
5.1	Introduction	65
5.2	The WED model	65

5.2.1	Scenario set up	65
5.2.2	Hydrodynamic comparison	67
5.3	The ER model	72
5.3.1	Scenario set up	72
5.3.2	Calibration	77
5.4	Model accuracy	79
5.5	Summary	80
<b>6</b>	<b>Summary and recommendations</b>	<b>81</b>
6.1	The Ems Estuary	81
6.2	The lower Ems River	81
6.3	Model applicability	82
6.4	Recommendations	83
<b>7</b>	<b>Literature</b>	<b>85</b>
<b>Appendices</b>		
<b>A</b>	<b>Waterlevels WED model</b>	<b>87</b>
A.1	2012	88
A.2	2013	91
<b>B</b>	<b>Salinity WED model</b>	<b>95</b>
B.1	2012	95
B.2	2013	99
<b>C</b>	<b>Calibration waterlevels, ERD model, frequency domain</b>	<b>103</b>
C.1	Dukegat (top left: Cal 01, top right: Cal09, lower left: Cal14, lower right: Cal 16)	104
C.2	Knock (top left: Cal 01, top right: Cal09, lower left: Cal14, lower right: Cal 16)	105
C.3	Pogum (top left: Cal 01, top right: Cal09, lower left: Cal14, lower right: Cal 16)	107
C.4	Terborg (top left: Cal 01, top right: Cal09, lower left: Cal14, lower right: Cal 16)	108
C.5	Leerort (top left: Cal 01, top right: Cal09, lower left: Cal14, lower right: Cal 16)	109
C.6	Weener (top left: Cal 01, top right: Cal09, lower left: Cal14, lower right: Cal 16)	110
C.7	Papenburg (top left: Cal 01, top right: Cal09, lower left: Cal14, lower right: Cal 16)	111
<b>D</b>	<b>Calibration waterlevels ERD model, time domain</b>	<b>113</b>
<b>E</b>	<b>Salinity ERD model</b>	<b>117</b>
E.1	Knock	117
E.2	Pogum	118
E.3	Terborg	119
E.4	Leerort	120

## 1 Introduction

The Water Framework Directive (WFD) requires EU member states to achieve good ecological and chemical status of all designated water bodies (rivers, lakes, transitional and coastal waters) by 2015. In the management plan (Rijkswaterstaat, 2009) for the implementation of the WFD (and Natura 2000) in the Netherlands, the context, perspectives, targets and measures for each designated water body have been defined. The requirements for the Ems Estuary (see Figure 1.1 for location) are that the mud dynamics need to be better understood (before 2015), and driving forces for increase in turbidity need to be identified. Therefore Rijkswaterstaat has initiated the project 'Research mud dynamics Ems Estuary' (*Onderzoek slibhuishouding Eems-Dollard*). The aim of this project is to (I) determine if and why the turbidity in the Ems Estuary has changed, (II) to determine how the turbidity affects primary production, and (III) to investigate and quantify measures to reduce turbidity and improve the ecological status of the estuary – see also the flow chart of the project structure (Figure 1.2).

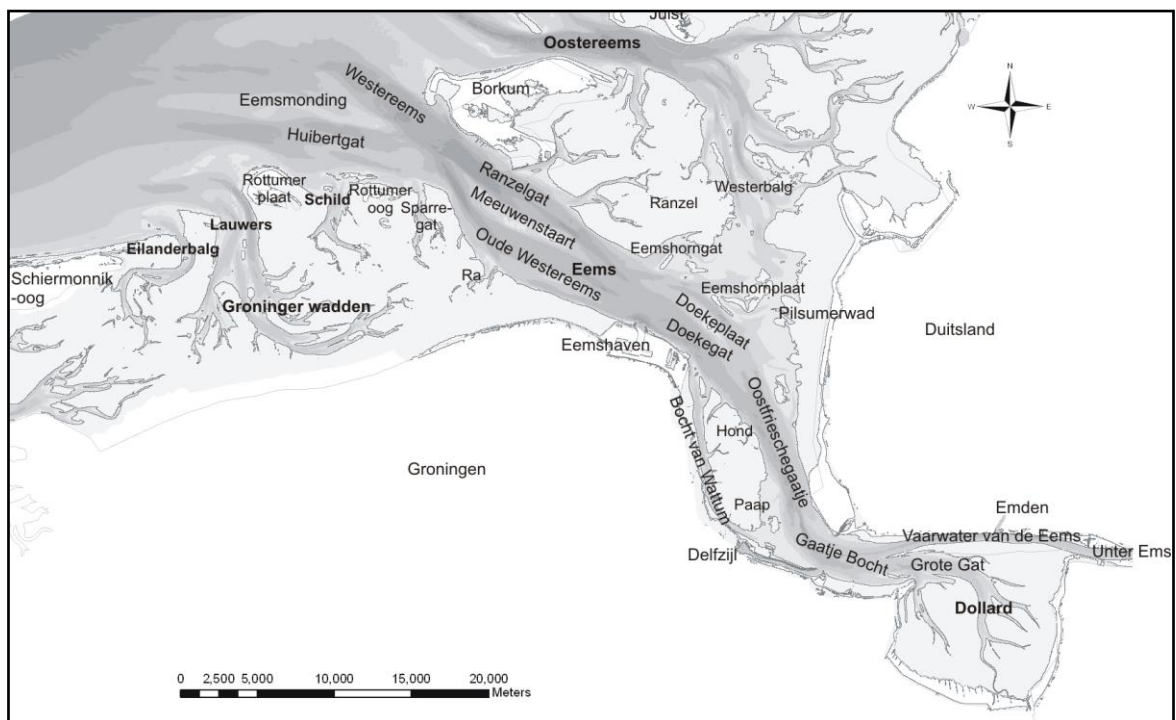


Figure 1.1 Map of Ems Estuary with names of the most important channels and flats (Cleveringa, 2008) in Dutch and German. The English name of the 'Vaarwater van de Eems' is the Emden navigation channel or Emden Fairway. The English name of 'Unter Ems' is the lower Ems River.

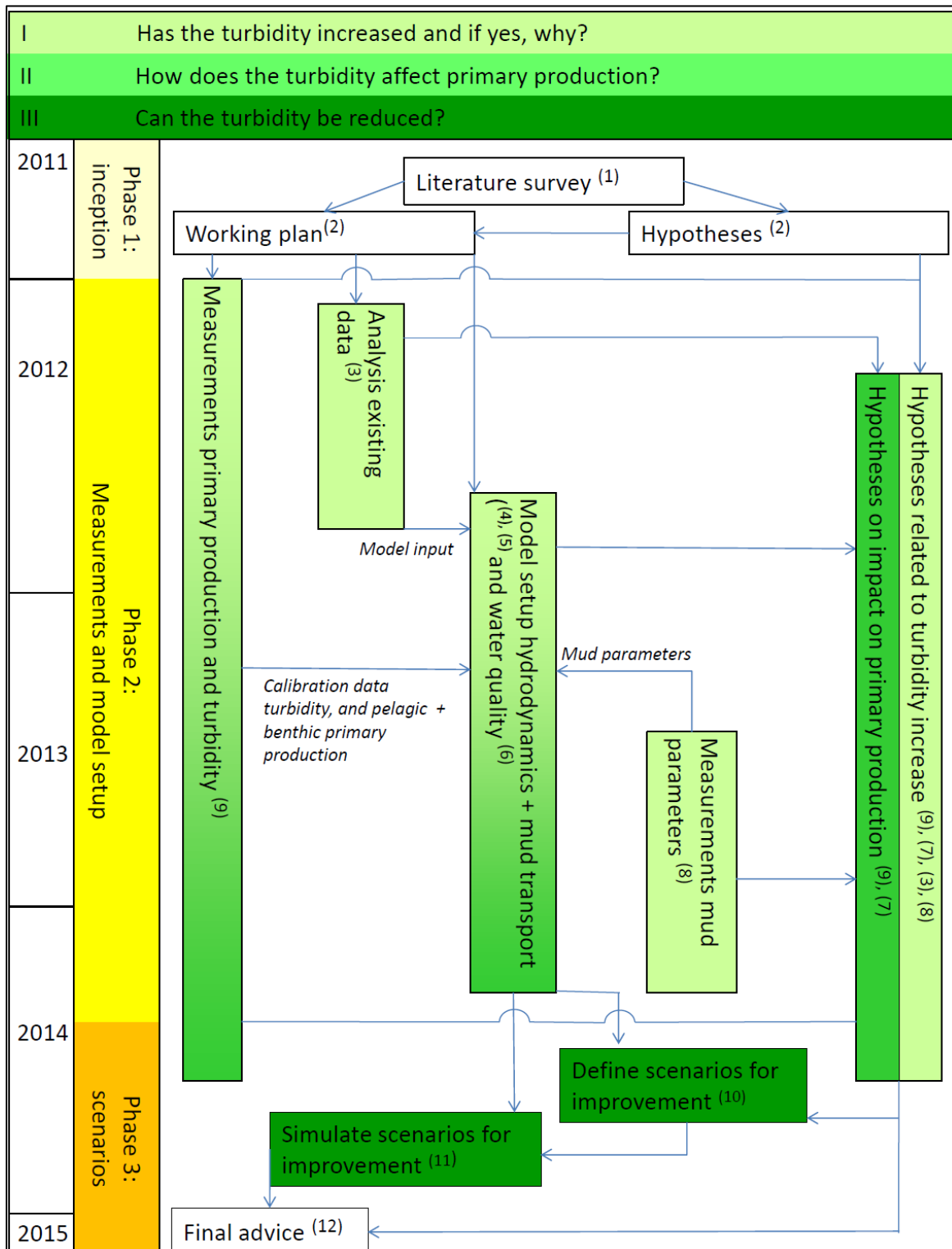


Figure 1.2 Flow chart for the structure and timetable of the study. Green colouring of the phase 2 activities relates to the colour of the main research questions I, II, and III. See Box 1 for a description and Table 1.1 for the references (1) – (12)

This research project explores mechanisms that may be responsible for the present-day turbidity of the estuary and identifies measures to reduce the turbidity. The long-term effect of human interventions on suspended sediment dynamics in an estuary such as the Ems Estuary is complex, and data supporting such an analysis is limited or non-existent. As an alternative to historic data analysis, an effect-chain model (relating human interventions to changes in hydrodynamics, sediment transport, and water quality) has been set up. Hereby maximal use was made of data that were already available and new data, collected within this project. Although the absolute values of the model predictions should be carefully interpreted, an effect-chain model provides a tool to investigate trends in system response to human interventions. This work provides indicative explanations for the current turbidity patterns and a first exploration of restoration options, but also reveals important gaps in knowledge and next steps to be taken. Additional research is required to further substantiate the results of this project.

The overall study is divided into three stages: an inception phase (phase 1) in which gaps in knowledge are identified and a research approach is defined; phase 2, in which measurements are done and models are set up and calibrated; and phase 3 in which the models are applied to investigate measures to improve the ecological and chemical status of the estuary. The overall structure and timeline of this study is summarized in Figure 1.2 and Box 1. An overview of the deliverables (reports and memos) produced during the project is given in Table 1.1. The numbers 1 to 12 of the deliverables are part of the project layout in Figure 1.2.

**BOX 1: SET UP OF THE STUDY (with Figure 1.2; references in Table 1.1)**

The primary objective of this study is to address the following:

q1: Has the turbidity increased and why?

q2: If yes, what is the impact on primary production?

q3: Can the turbidity be reduced?

These questions are presented in a flow chart (see Figure 1.2). During phase 1, existing gaps in knowledge were identified (see report 1 in Table 1.1), and a number of hypotheses were formulated related to q1 and q2 (report 2 in Table 1.1), to be addressed during phase 2 of the study.

Phase 2 consists of measurements, model set up and analysis. Measurements of primary production and turbidity are carried out from January 2012 to December 2013, and reported mid 2014 (report 9 in Table 1.1). These measurements are carried out to address hypotheses related to q1 and q2, and to calibrate the sediment transport and water quality models. Existing abiotic data (such as waterlevels, bed level, dredging, and sediment concentration) are analysed in this phase to address hypotheses related to q1 and to provide data for model calibration (report 3 in Table 1.1). Soil samples in the Ems estuary and Dollard basin have been collected to determine changes in mud content (hypotheses relates to q1) and determine parameter settings of the sediment transport model (report 8 in Table 1.1).

The effect-chain model set up for this study consist of three modules: a hydrodynamic module (report 4 in Table 1.1), a sediment transport module (report 5), and a water quality module (report 6). These models are applied to address the hypotheses related to q1, q2, and q3 (report 7 in Table 1.1).

In phase 3, a number of scenarios are defined to reduce turbidity / improve the water quality (q3) of the estuary (report 10 in Table 1.1). Their effectiveness is tested in reference (report 11). A final report, synthesizing the most important findings and recommendations (report 12) concludes the project.



Table 1.1 Reports / memos delivered during phase 1 to 3 of the Mud dynamics in the Ems estuary project (with numbers referencing to Figure 1.2). The current report is in bold.

Number	Year	Phase	Main research question	Report
1	2011	1	-	Literature study
2	2011	1	-	Working plan phase 2 and 3
3	2012	2	1	Analysis existing data
<b>4</b>	<b>2014</b>	<b>2</b>	-	<b>Set up hydrodynamic models</b>
5	2014	2	-	Set up sediment transport models
6	2014	2	-	Set up water quality model
7	2014	2	1, 2	Model analysis
8	2014	2	1	Analysis soil samples
9	2014	2	1, 2	Measurements primary production
10	2014	3	3	Scenario definition (memo)
11	2014	3	3	Model scenarios
12	2015	3	1, 2, 3	Final report

Part of phase 2 of the project is the set-up and analysis of numerical models. The models are used to better understand the historic changes and present-day conditions in the Ems Estuary (report 7 in Table 1.1) and to quantify the effect of measures to improve the functioning of the estuary (Phase 3; Report 11). The research questions to be addressed with the models cover a range of processes to be addressed, which have led to the development of multiple hydrodynamic and sediment transport models. This will be explained in more detail in Chapter 2. In Chapter 3, the adaptations to and validation of the hydrodynamic module of an existing effect-chain model are described. This model is less suitable for the lower Ems River, for which additional models have been setup (Chapter 4). In order to determine the historic changes in the Ems estuary, historic cases have been setup and calibrated (Chapter 5). The findings of the report are synthesized in Chapter 6.

## 2 Description of the models

This chapter provides a brief description of the applied models. More details about each model (such as modelling assumptions, domains, time and resolution etc.) are described in the dedicated model reports to sediment transport and water quality (reports 5 and 6 in Table 1.1). This is report 4 (setup of the hydrodynamic models).

### 2.1 Introduction

The objective of this study is to determine why turbidity has changed, what the impact is on primary production, and if / how this can be mitigated. These questions can be addressed using a combination of field data and numerical models. The most important gaps in knowledge, as identified in report 1, have been translated into a list of hypotheses (see report 2). These hypotheses cover a range of research objectives related to hydrodynamics, sediment transport, and water quality. For research questions addressing hydrodynamic processes, a hydrodynamic model is used. Modelling turbidity requires the use of a sediment transport model in combination with the hydrodynamic model. Primary production is dependent on turbidity, and therefore primary production is modelled with a hydrodynamic-sediment transport- primary production model. This is known as an effect-chain model, which is described in more detail in section 2.2.

The hypotheses formulated in report 2 will be tested with the numerical models, on which is reported in report 7. The ability of the models to test these hypotheses is determined by the physical and/or ecological processes the models reproduce. The most important processes (see for details report 1) are:

- a) Tidal propagation in the Ems Estuary and lower Ems River and changes therein as a result of deepening
- b) Residual flows resulting from river discharge, wind and salinity, and changes therein as a result of deepening
- c) Sediment transport mechanisms and typical sediment concentration levels as a result of tides, waves, and density-driven flows
- d) Sediment trapping in ports and the long-term effect of subsequent dredging and dispersal on the suspended sediment concentration in the estuary.
- e) Pelagic and benthic primary production under influence of light and nutrient availability

In each of the relevant reports, the applicability of the model to address the processes above will be addressed:

- a) and b) in this report (sections 3.7 (Ems Estuary), 4.4 (Ems River), and 5.4 (historic changes)) and in report 7;
- c) and d) in report 5 and 7;
- e) in report 6 and 7.

The starting point for the effect-chain model is the numerical model developed within the TO-KPP studies (see e.g. Van Kessel et al. (2013) for an overview). This model is originally based on a model developed by Alkyon (2008). This model is hereafter referred to as the WED model (Wadden Sea Ems Dollard). The original WED model was set up for the year 2005. In this project a large amount of monitoring data has been generated for the year 2012 and 2013. This includes the primary production and turbidity data, but also data of the continuous measurements near Eemshaven in the first half of 2012. Therefore, the model is recalibrated for the year 2012. Other aspects of the model that were improved are discussed in section 2.3.

The WED model is set up to simulate relatively long time periods and large spatial scales. Some of the research questions that need to be addressed cover smaller spatial scales and different process formulations. These questions require the use of more detailed models as the resolution of the WED model is insufficient to accurately model the dynamics in the lower Ems River and the exchange with the Ems Estuary. In order to better understand the changes in the lower Ems River (and exchange with the Ems Estuary), two models were set up: the Ems River Dollard (ERD) model and the Ems River (ER) model (see Figure 2.1). The ERD-model has a hydrodynamic model and the ER-model has both a hydrodynamic and a sediment-transport model (ER). See Table 2.1 for an overview of the modules for each model.

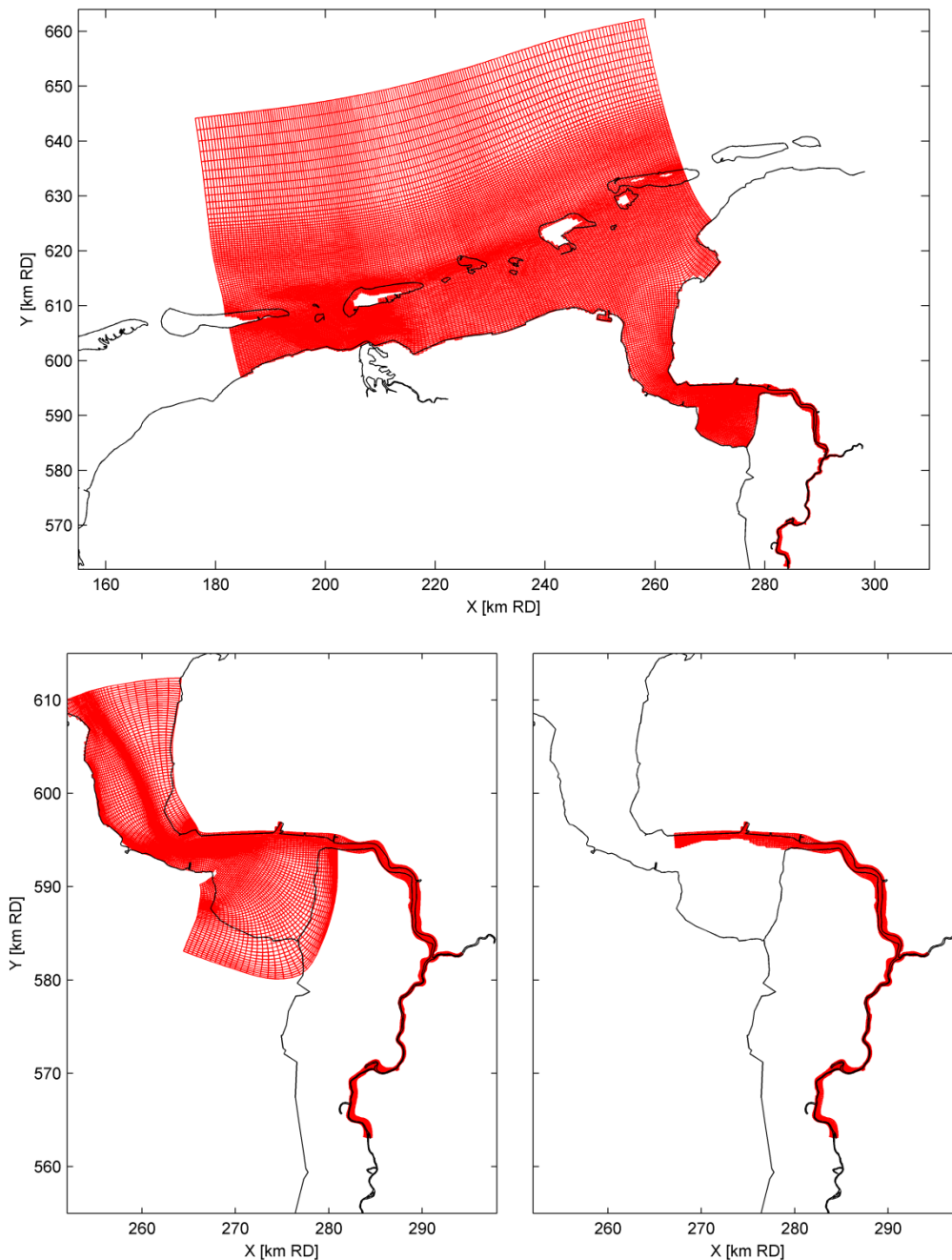


Figure 2.1 Computation grid of the WED model (top), the ERD model (lower left), and the ER model (lower right).

Table 2.1 Models adapted (WED) or developed (ER, ERD) within this project

Model	Hydro	Sediment transport	Waves	Water quality	Purpose
WED	yes	yes	yes	Yes	Simulates long-term changes in hydrodynamics, sediment transport, and water quality
ERD	yes	no	no	no	Simulates tidal processes in parts of the Ems Estuary, the Dollard, and the lower Ems River.
ER	yes	yes	no	no	Quantifies tidal and sediment transport processes within the lower Ems River and changes in sediment exchange between Ems river and Ems estuary

## 2.2 Effect chain models

An effect chain model is a set of models that describe jointly the effects of changes in the physical and morphological environment on chemical and biological variables. Each individual model describes a different set of processes within this chain of events. The basic idea of running different models is that each model component in itself can be optimally configured describing a limited set of processes. The alternative, one model describing all processes in one run, will have a higher computational demand and less flexibility, or a lower accuracy. Combining the results of the different models in a chain is necessary in order to take into account all relevant processes. In this study, the following three models were “chained” (Figure 2.2):

- A hydrodynamic model, producing time-dependent three-dimensional (3D) fields of salinity, temperature and other physical parameters such as bottom friction. This model is based on the open-source software Delft3D-Flow.
- A sediment model describing the transport and distribution of fine sediments, using the output of the hydrodynamic model as input. This model is based on the open-source software Delft3D-WAQ, configured for fine sediments.
- A water quality/primary production model describing cycling of nutrients, light distribution in the water, and primary production by phytoplankton and microphytobenthos. This model is based on the open-source software Delft3D- WAQ, configured for ecological processes. The water quality/primary production model component uses the output of both the hydrodynamic model and the sediment model as input.

For addressing the questions in this study, we follow an approach in which we assume that there is no significant feedback between hydrodynamics, sediment transport and water quality. This is elaborated in more detail in section 2.3. Therefore the coupling between the models is done off-line, meaning that each model is executed separately, using the output of the previous model in the chain as input. The hydrodynamic model exports files with hydrodynamic variables which are input for the sediment transport model. Subsequently, the sediment transport model generates files with sediment concentration fields that are (together with the hydrodynamic input files) used by the water quality model. This big advantage of this offline approach is that computational times remain manageable.

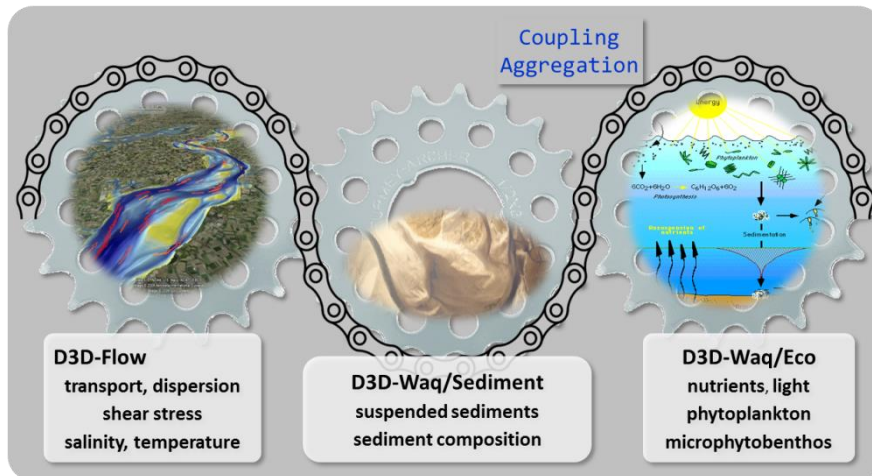


Figure 2.2 General set up of a linear effect-chain model.

### 2.3 The Waddensea Ems Dollard (WED) model

The combination of the hydrodynamic, sediment transport, and water quality models (the effect-chain model) will be used to explore the effects of natural variation and man-made changes in the nutrient loads and sediment dynamics of the estuarine waters on turbidity, primary production and phytoplankton biomass. This provides a tool which can be used to better understand the historic changes in the Ems Estuary (Report 7) but also to estimate the effect of proposed measures to improve the turbidity and primary production (Report 11). In order to adequately address the research questions formulated for this study (see section 1.1), the WED model developed in the TO-KPP studies needed to be improved on several aspects:

The computed salinity in the **hydrodynamic model** of the TO-KPP studies deviates considerably from the observed salinity. As salinity is a good approximation of computed dispersion and mixing, the salinity modelling needs to be improved for the current study. The mismatch of the model is probably the result of too strongly simplified boundary conditions. Therefore the freshwater sources are now implemented with more detail. In addition, the computed salinity is also verified with continuous measurements collected in the German part of the estuary and close to Eemshaven. These add to data collected at the Dutch MWTL stations). The second major improvement in the hydrodynamic model is the computation of wave-induced bed shear stresses with the SWAN wave model, instead of the less accurate fetch-length wave approach that was initially applied. The SWAN model generates a stronger along-estuary gradient in wave height and bed shear stress, which promotes up-estuary sediment transport.

The WED **sediment transport model** computes the transport of fine sediment (mud). One of the shortcomings of the TO-KPP sediment transport model was that the residual transport of sediment was directed down-estuary, whereas observations indicate that the Ems Estuary is importing. To achieve this, the wave model was improved, dredging and dumping was integrally modelled (sediment depositing in ports is regularly dredged and disposed on dumping locations through a dredging routine), and the sediment settings of the model were modified. Also, the original sediment transport model was only limitedly compared to observations. New observations were generated within the mud sampling programme (Report 8), the primary production measurements (Report 9), and the GSP measurements collected near Eemshaven to setup and validate the model. In addition to the turbidity measurements,

the model accuracy is determined by comparing modelled sediment fluxes with measured sediment fluxes (mainly using port siltation rates). Finally, the modelled sediment deposition is compared with observed sediment distribution patterns.

Within the Delft3D modelling suite, sediment can be modelled in Delft3D-FLOW sediment-online (with a full coupling between hydrodynamics, sediment transport and morphology) or in Delft3D-WAQ (which is coupled off-line, i.e. the sediment transport is computed after the hydrodynamic simulation). A coupling between hydrodynamics and morphology is needed when bed level changes significantly influence the hydrodynamics within the modelled timeframe, which is usually only required for sand and for decadal timescales. Morphological changes resulting from fine sediment erosion or deposition usually have limited impact on hydrodynamics. Fine sediment may influence the vertical mixing through suppression of turbulence at concentrations exceeding several 100 mg/l.

The WED sediment transport model is setup in Delft3D-WAQ, for 3 reasons. First, multi-year simulations are needed to develop a sediment transport model which is in dynamic equilibrium (where computed sediment concentrations are independent of initial conditions but determined by hydrodynamics, model settings, and boundary conditions), which is needed to compute the effect of perturbations to the system. Multi-year simulations are, however, problematic with a fully coupled model due to the associated computational times, as a fully coupled model is approximately 10 times slower than a non-coupled model. Secondly, in the majority of the Ems Estuary the concentrations are below several 100 mg/l and the bed level changes small. The sediment transport model therefore does not need to be fully coupled. And thirdly, in Delft3D-WAQ sediment transport processes are available (the buffering of fine sediment, using the model developed by van Kessel et al. (2011)) which are important for description of estuarine sediment dynamics.

The **water quality/primary production model** was further developed using a more detailed process description (Report 6), and using newly available monitoring data (Report 9). The implementation of a more detailed description of nutrient cycles including layered sediment with early diagenesis of organic material is needed to improve the calculation of phosphate compounds compared to the TO-KPP studies. The phosphate compounds show a strong sediment flux in summer in the inner parts of the estuary. Secondly, the monitoring programme carried out by IMARES (Report 9) provided a better approximation of phytoplankton growth process parameters, and validation data additional to the national monitoring programme.

## 2.4 The Ems River (ER) and Ems River Dollard (ERD) models

It is known that the lower Ems River became significantly more turbid in the last decades (e.g. de Jonge et al., 2014). At present the lower Ems River is a hyper-concentrated system with very limited ecological value. The exchange of sediment between the lower Ems River and the Ems Estuary may be important for the sediment dynamics in the Ems Estuary. This is also part of the hypotheses formulated in report 2. Also a more quantitative understanding of changes in the lower Ems River is needed to understand the current state of the Ems Estuary. The ecological state of the lower Ems River is not part of the current study.

The ERD model covers the Dollard and the Ems Estuary up-estuary of Eemshaven, whereas the ER model only covers the lower Ems River and the Emden navigation channel. The ERD model can, amongst others, be applied to model the effects of channel morphology and land reclamations in the lower Ems River, and investigate effects of changes in parts of the Ems Estuary (such as the Dollard) on the tidal dynamics.

The ER model only covers the lower Ems River and the Emden navigation channel, and is specifically set up to model the changes in tidal dynamics and sediment transport mechanisms that are caused by deepening of the Ems River. Section 2.3 explains that the sediment module of the WED model is executed in an off-line mode (without a dynamic feedback between hydrodynamics, sediment concentration, fluid density, and morphology). In the lower Ems River such a simplification is not valid, and therefore the hydrodynamics, morphology, and water density in the ER model are fully coupled.



### 3 Adaptation and validation of the WED model

#### 3.1 Introduction

This chapter describes adaptations made to the TO-KPP model (van Kessel et al., 2013), see Figure 3.1 for the model domain. The main changes made to the hydrodynamic module are the simulation period (2012 and 2013 instead of 2005, requiring different forcing for waterlevels, discharge, salinity, temperature, wind field imposed as boundary conditions) and the wave module (SWAN waves instead of a fetch length model). The changes to the model are formulated in section 3.3, and the validation against flow velocities, waterlevels and salinity presented in section 3.4. The set up of the wave model is described in section 3.6.

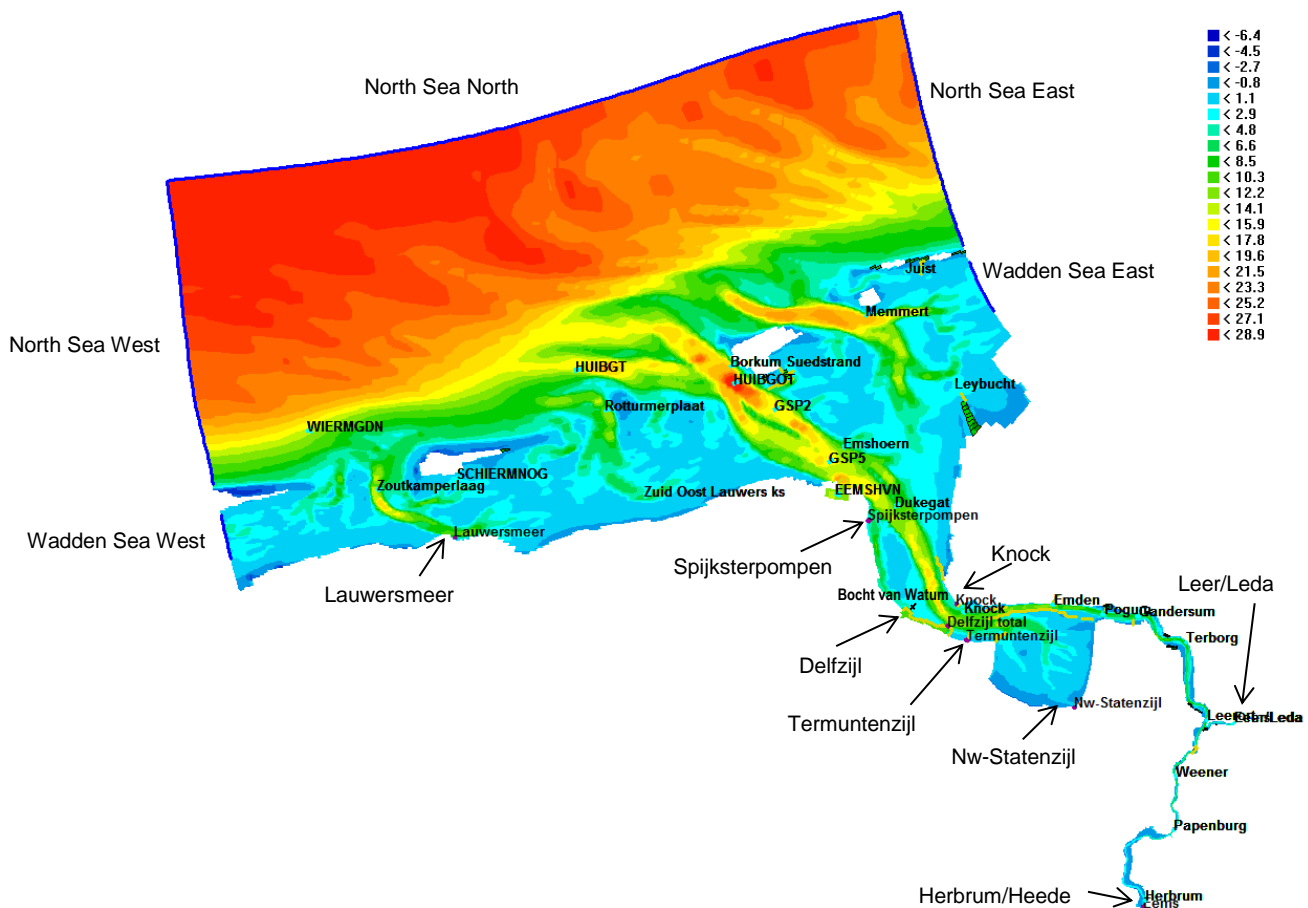


Figure 3.1 Domain of Waddensea-Eems-Dollard (WED) model with the colorscale denoting the bedlevel (relative to NAP). Model attributes are discharge points (arrows), observation points (blue or black crosses), thin dams (yellow line), dry points (green cells) and Geisedam (yellow line)

### 3.2 The original WED model

The TO-KPP WED model was set up and applied for the year 2005. The model was nested in a tide-forced North Sea model with boundaries along the North Sea and the Western Wadden Sea (see van Kessel et al., 2013). Fresh water discharges originated from Lauwersmeer, Delfzijl, Nieuwe Statenzijl, and the Eems at Herbrum and Leer. The model has 8 vertical  $\sigma$ -layers, increasing logarithmically in thickness from the bed to the surface (2, 3, 5, 8, 13, 19, 25 and 25%). The choice for 8 layers is a trade-off between computational efficiency (requiring a little cells as possible) and computational accuracy (with an increasing amount of grid cells the vertical variation in flow velocity, salinity, and sediment concentration (report 5) is more accurately resolved). Wave-induced bed shear stresses were generated with an offline fetch length model.

### 3.3 Modifications

The TO-KPP WED model has been modified on the following aspects (see Table 3.1) for the main settings):

- Boundary conditions (waterlevels, wind, discharges, salinity and temperature) have been obtained for the year 2012 and 2013.
- Discharge points have been added (Knock, Spijksterpompen, Termuntenzijl).
- The model is nested in an operational model which better aligns with the WED model grid ('Simona kust-fijn'). As a result, boundary conditions can be more rapidly obtained (without a need to specifically run an overall larger model) from an accurate and well-documented model.
- The model is forced with waterlevels instead of Riemann boundaries (a combination of flow velocity and waterlevels). Waterlevel boundaries may reduce the accuracy of the computed flow velocities in the North Sea, but do not differ from Riemann boundaries within the Ems Estuary itself. The advantage of waterlevel boundaries is that they are flexible to modify (add surge levels or sealevel rise) and allow nesting in operational (SIMONA) models. With the focus within this study being the Ems Estuary, and not the North Sea, waterlevel boundaries are therefore used.
- The eastern Wadden Sea is now an open boundary; in the previous WED model this boundary was closed for numerical stability reasons.
- The fetch length wave model is replaced by a SWAN wave model to compute local wave generation and propagation more accurately. The most important difference is a stronger seaward increase in wave-generated bed shear stress.
- The bed roughness in the lower Ems River is modified, based on the calibration of the ERD model (see chapter 4), resulting in a roughness distribution as in

Table 3.1 Main processes and parameter settings of the adapted hydrodynamic model.

Parameter	
Timestep (s)	30 seconds
Vertical layers	8 vertical $\sigma$ -layers (2, 3, 5, 8, 13, 19, 25 and 25%).
Horizontal viscosity	Uniform (1 m <sup>2</sup> /s)
Vertical mixing	k- $\epsilon$ turbulence model (with background viscosity of 1 10 <sup>-5</sup> m <sup>2</sup> /s)
Bed roughness	Spatially varying Manning's n (Figure 3.2).
Offshore Boundary conditions	Waterlevels (nested in operational model) and salinity (MWTL observations)
Discharges	Discharges (from waterboards and NLWKN) with (near)-zero salinity
Wind	Uniform but time-varying wind (measured at Beerta)

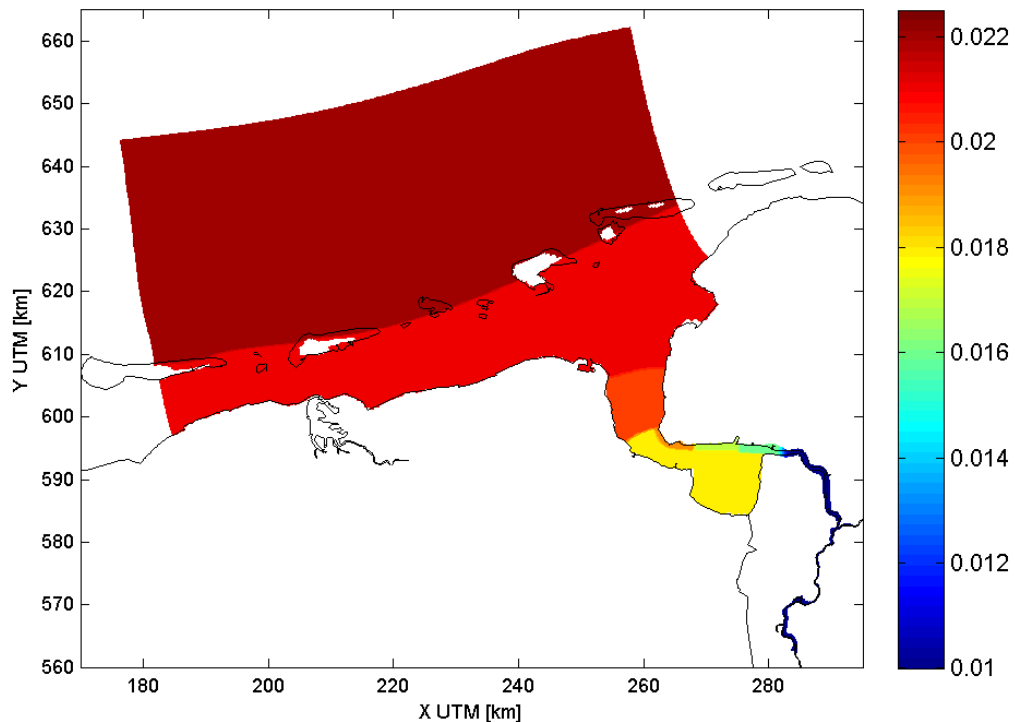


Figure 3.2 Spatial distribution of the Manning's roughness  $n$ .

### 3.3.1 Boundary and initial conditions

The WED model is forced at the boundaries with waterlevels, salinity and temperature. The waterlevel time series were derived from online available Simona kust-fijn model output<sup>1</sup>, see Figure 3.3, computed for 2012. For each point on the model boundary, the nearest Simona output point is used; see Figure 3.4 and Figure 3.5. The waterlevel time series have an interval of 10 minutes.

At locations Dantziggat and Rottumerplaat 50 (see Figure 3.3), measurements<sup>2</sup> are conducted in the MWTL measuring programme ('Monitoring Waterstaatkundige Toestand des Lands'; the Dutch survey programme to monitor its inland and coastal waters) once per month. The salinity and temperature observed at these stations are used to derive boundary conditions for the model by linearly interpolating the monthly observations. All North Sea boundaries are forced with salinity and temperature measured at Rottumerplaat 50 in 2012. Measurements at Dantziggat are used for the salinity and temperature at the Wadden Sea West and East boundary. The same values for the east and west boundaries are used because (1) there is no comparable dataset available near the east boundary, (2) the east-west gradient in salinity is relatively low, especially on the timescale that data is available, and (3) the salinity gradient on the North Sea is not essential for the hydrodynamics in the Ems Estuary. A 30 minute Thatcher-Harleman timelag is used to smoothly adjust initial inflow of salt and temperature conditions to the previous outflow phase.

<sup>1</sup> Accessible via [http://opendap-matrooms.deltares.nl/thredds/catalog/maps/normal/hmcn\\_kustfijn/catalog.html](http://opendap-matrooms.deltares.nl/thredds/catalog/maps/normal/hmcn_kustfijn/catalog.html).

<sup>2</sup> Accessible via [live.waterbase.nl](http://live.waterbase.nl) and/or available upon request at helpdesk Water.

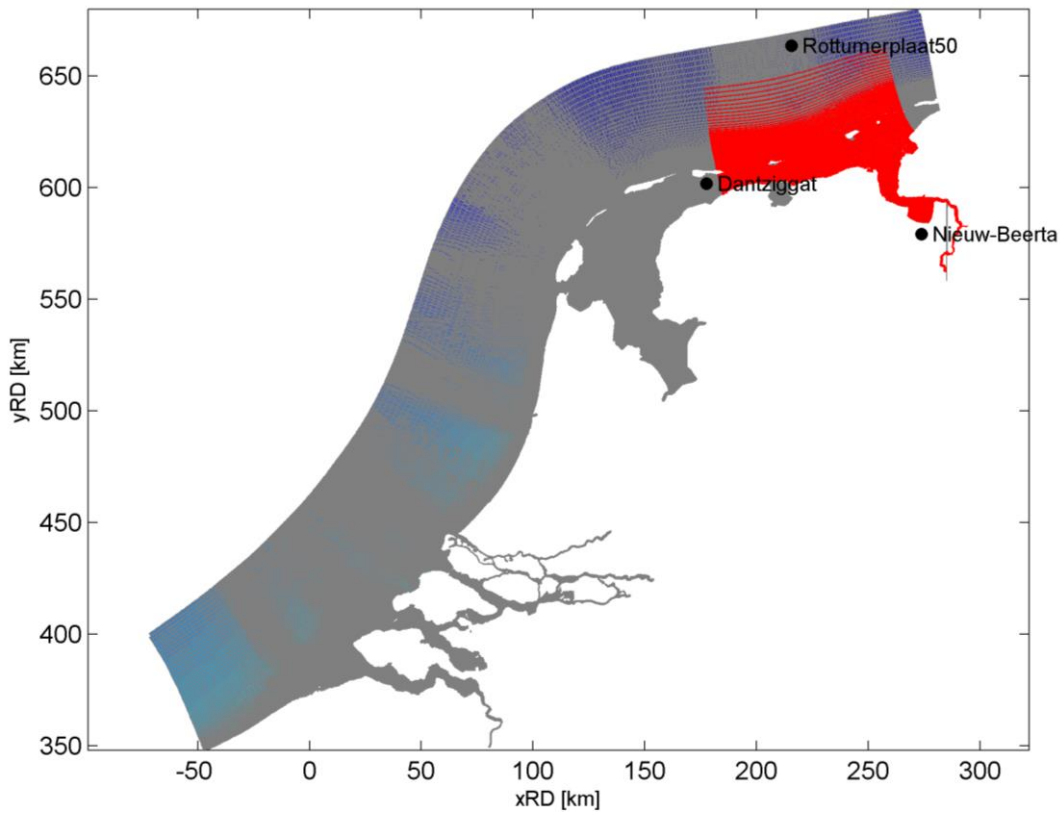


Figure 3.3 Simona 'kust-fijn' model (gray) and the WED model grid (red).

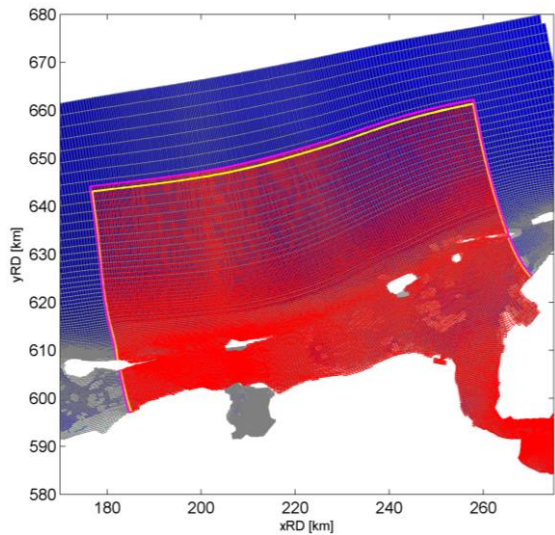


Figure 3.4 WED model grid (red) and boundaries (magenta) and Simona kust-fijn model (grey) and nearest grid points (yellow) used to construct boundary conditions.

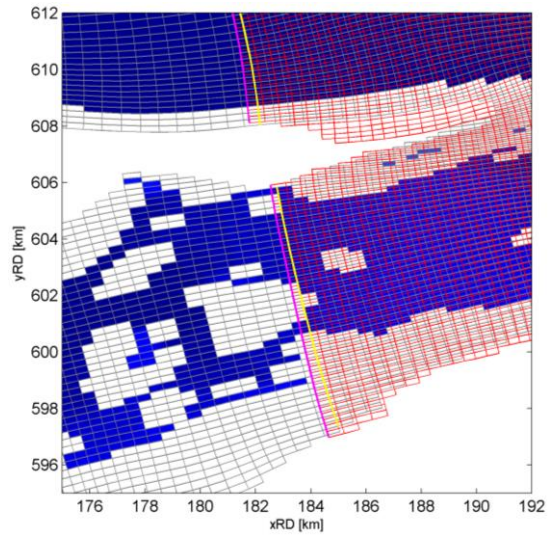


Figure 3.5 Detail of Figure 3.4 near Ameland. Blue cells in the Simona grid indicate (time-varying) active cells

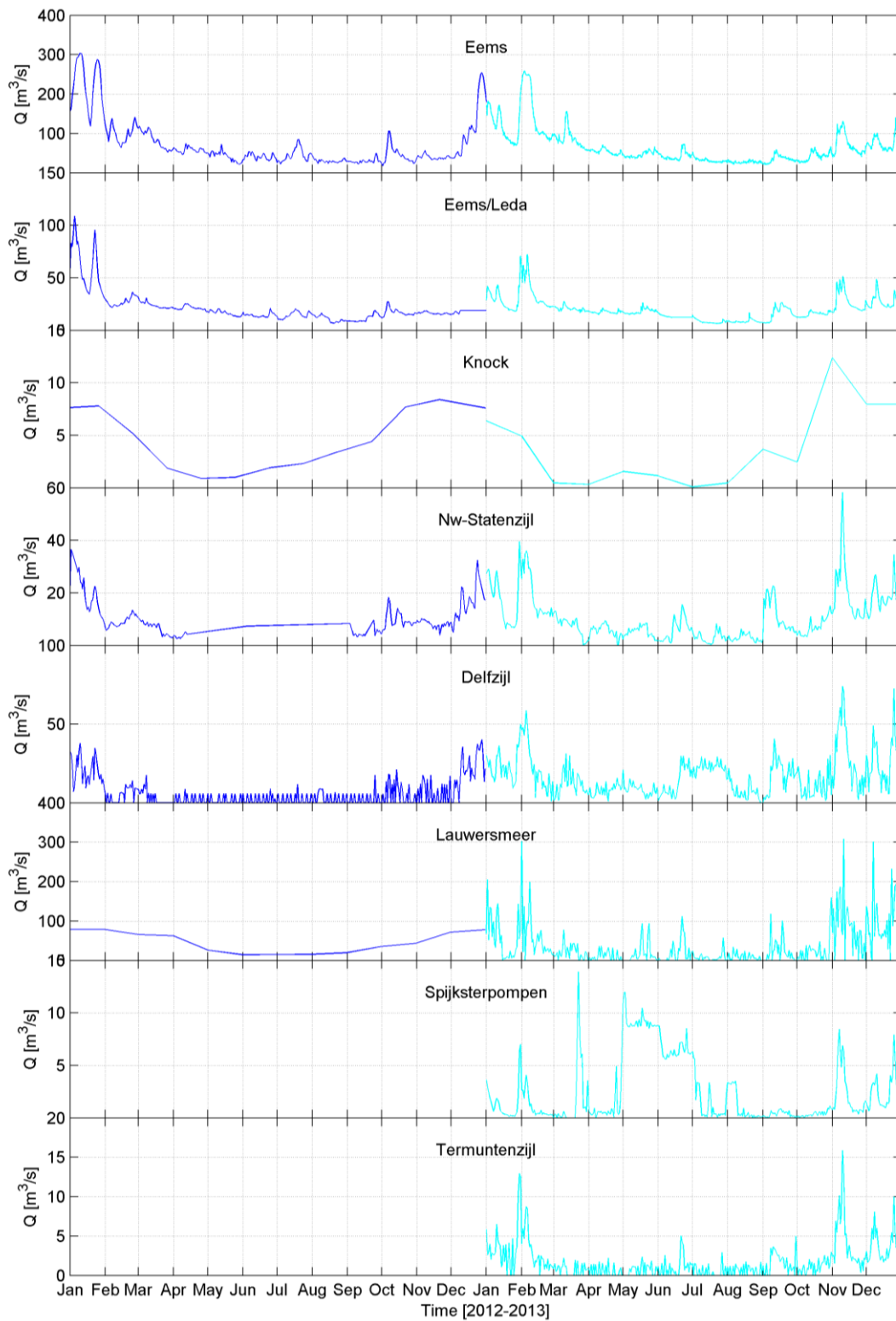


Figure 3.6 Model discharge for the Eems River at Herbrum/Heede (Eems), the Eems River at Leda (Eems /Leda), Knock, Nieuwe Statenzijl, Delfzijl, Lauwersmeer, Spijksterpompen and Termuntenzijl in 2012 (blue) and 2013 (cyan).

The model was initialised with values for salinity, velocity, and waterlevel that were computed for 31 december 2005 (using the TO-KPP model), and used as input for 1 january 2011. The model is subsequently run for the year 2011 (which is sufficiently long for the 2005 conditions to adapt to 2011), resulting in initial conditions for the 2012 model. The results of the 2012 model are subsequently used as input for 2013.

### 3.3.2 Discharges

River discharges are prescribed as single point discharges (Figure 3.6, previous page). For the Ems River at Herbrum, measurements from the German station Heede are used. Other discharge points are the Ems River at Leda, Knock, Nieuwe Statenzijl, Delfzijl and Lauwersmeer. German discharge data were obtained from the NLWKN (Niedersächsischer Landesbetrieb für Wasserwirtschaft, Küsten- und Naturschutz), discharges from Dutch discharge sluices were delivered by the Waterschap Hunze en Aa's and Waterschap Noorderzijlvest.

The 2012 and 2013 discharges differ in several respects. For the Lauwersmeer discharge the long-term averaged discharges used for 2012 have been replaced with actual observations in 2013. The effect of this more variable discharge is probably limited on the Ems estuary, because the discharge peaks have flattened out by the time the released water reaches the Ems estuary. The discharge for Delfzijl in 2012 was partly unavailable, resulting in higher discharge at Delfzijl in 2013 compared to 2012. Finally, two smaller discharges (Spijksterpompen and Termuntenzijl) were added in 2013. Their combined discharge is 2 times smaller than the individual contributions of the nearby stations of Nieuw-Statenzijl and Delfzijl, and therefore their effect is probably limited.

All discharges have constant salinity, with a value of 0 or near-zero. Salinity at Herbrum and Leer/Leda is set to 0.2 ppt, equal to the salinity in the ERD model and consistent with measurements. All other discharge points release fresh water. The temperature of the discharges is set at 10°C, except for Herbrum and Leer/Leda. At these stations the temperature measurements of 2012 are used.

### 3.3.3 Various

The model bathymetry is based on the bed level measurements obtained from the Wasser- und Schifffahrtsamt Emden (WSA). To compensate for a comparatively coarse model resolution in some of the tidal inlets, this bathymetry was slightly modified by Alkyon (2008) to more accurately reproduce observed waterlevels. This bathymetry is the basis of the model used in this study.

Wind-driven flow is computed with a spatially uniform wind field. The wind speed and direction used in the model are derived from measurements at Nieuw-Beerta<sup>3</sup> (see Figure 3.3 for location). During the model setup, model runs were also executed with spatially varying wind fields (HIRLAM, as used for the wave model; see section 3.6 for details). However, when forced with HIRLAM winds the sediment transport model (see report 5) becomes unstable in shallow areas. For the hydrodynamics, the impact of uniform and variable flow fields appeared to be of little significance. Therefore a spatially uniform wind field is used.

---

<sup>3</sup>Available from Koninklijk Nederlands Meteorologisch Instituut, KNMI: [www.knmi.nl](http://www.knmi.nl).

### 3.4 Validation 2012

For 2012, standard monitoring data is available for validation (waterlevels and salinity), as well as velocity measurements obtained by Groningen Seaports and Rijkswaterstaat. A semi-quantitative comparison is done for residual flow fields.

#### 3.4.1 Waterlevels

The computed and observed waterlevels are compared throughout the model domain, see Figure 3.7, Figure 3.8 and Appendix A. Computed and observed waterlevels are compared in the time domain and in the frequency domain (through tidal analysis using t-tide; Pawlowicz et al., 2002).

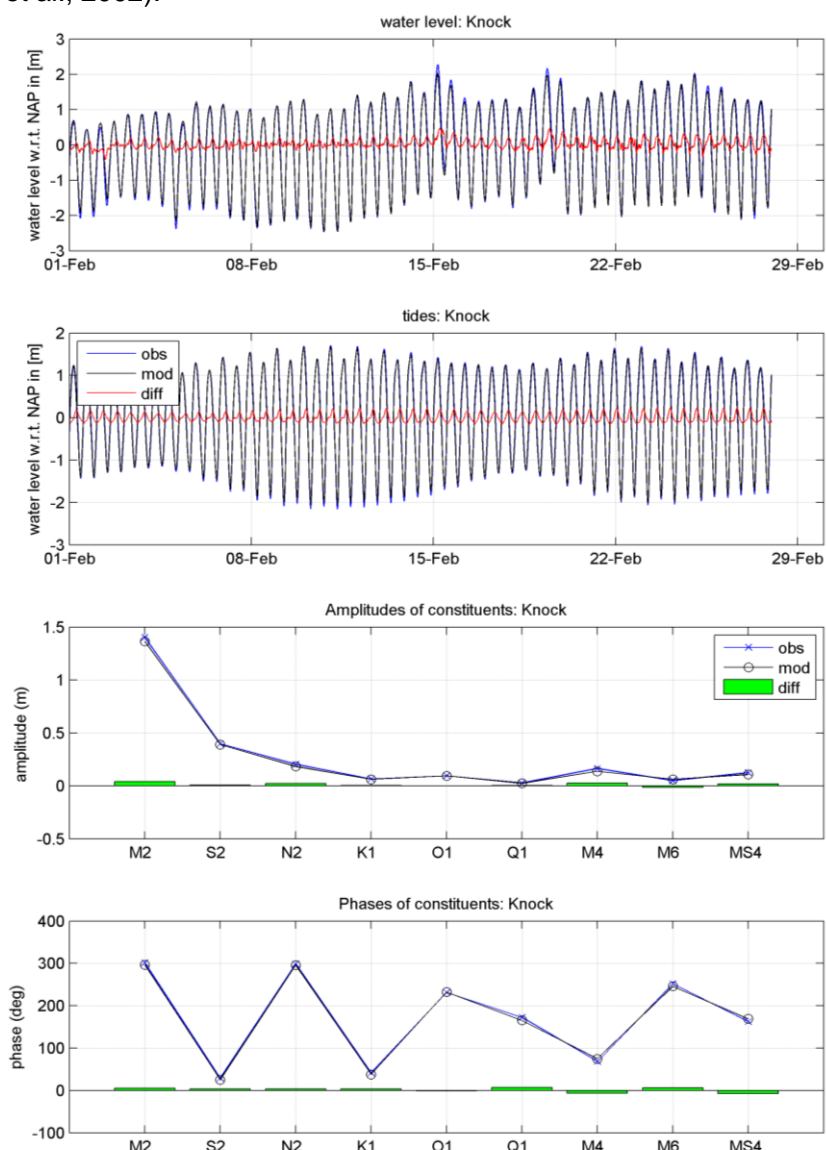


Figure 3.7 Comparison between observed (blue) and computed (black) waterlevels and tidal constituents at Knock: full timeseries (top panel), tidal signal (second panel), tidal amplitudes (third panel) and tidal phases (fourth panel). Time series show the results of February to be able to see some detail; the tidal analysis has been done for the entire year (2012).

Within the Ems Estuary, the error in the computed waterlevel amplitude is several cm or less, and the error in the computed phase less than  $10^\circ$  (see e.g. station Knock in Figure 3.7 and



more stations in Appendix A). An exception is Nieuwe Statenzijl, where a narrow channel conveys water to the observation point. At that location the model grid is too coarse to correctly reproduce the flow dynamics during low water. Deeper into the lower Ems River, starting at Leerort and upstream, the tidal range is slightly overestimated (with the M2 amplitude 10% larger than the observed amplitude; see Figure 3.8). This is probably caused by the lower resolution and a less smooth grid in the lower Ems River (which is one of the reasons to set-up the ERD model, see the next chapter). The phases of the principal diurnal and semi-diurnal tides and the amplitudes of the constituents other than M2 are reproduced better and deviate less than 5-10% of the observations. The focus area of the WED model is the Wadden Sea - Ems estuary region (and not the lower Ems River) waterlevel, making the reproductions sufficient..

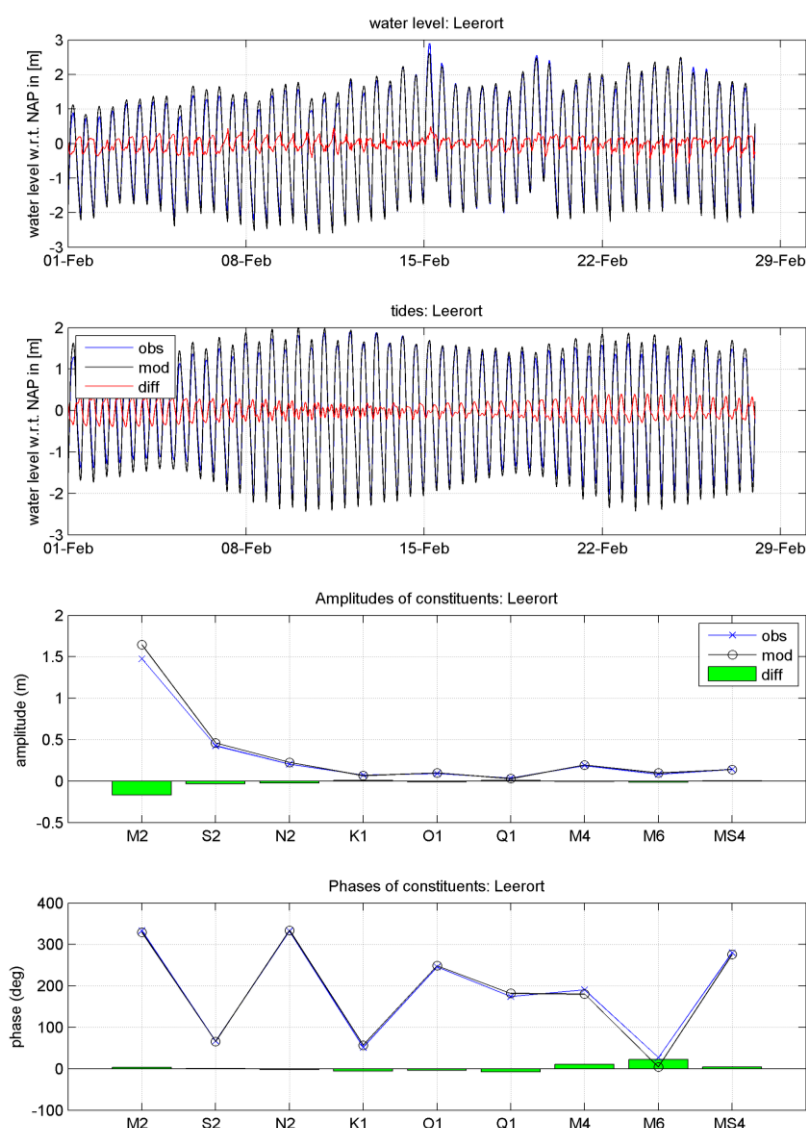


Figure 3.8 Comparison between observed (blue) and computed (black) waterlevels and tidal constituents at Leerort: full timeseries (top panel), tidal signal (second panel), tidal amplitudes (third panel) and tidal phases (fourth panel). Time series show the results of February to be able to see some detail; the tidal analysis has been done for the entire year (2012).

### 3.4.2 Flow velocities

Flow velocities have been observed in 2012 in the main tidal channel of the Ems Estuary<sup>4</sup> (GSP2; and GSP5, each located at a water depth of approximately 12 m); see location in Figure 3.1. The depth-averaged observed and computed eastward and northward velocities at both stations during the entire period (January to June/July) are shown in Figure 3.9 to Figure 3.12. Figure 3.13 and Figure 3.14 display a spring-neap tidal cycle, showing more details. The eastward and northward velocities have been converted to a speed (magnitude) and direction of the flow.

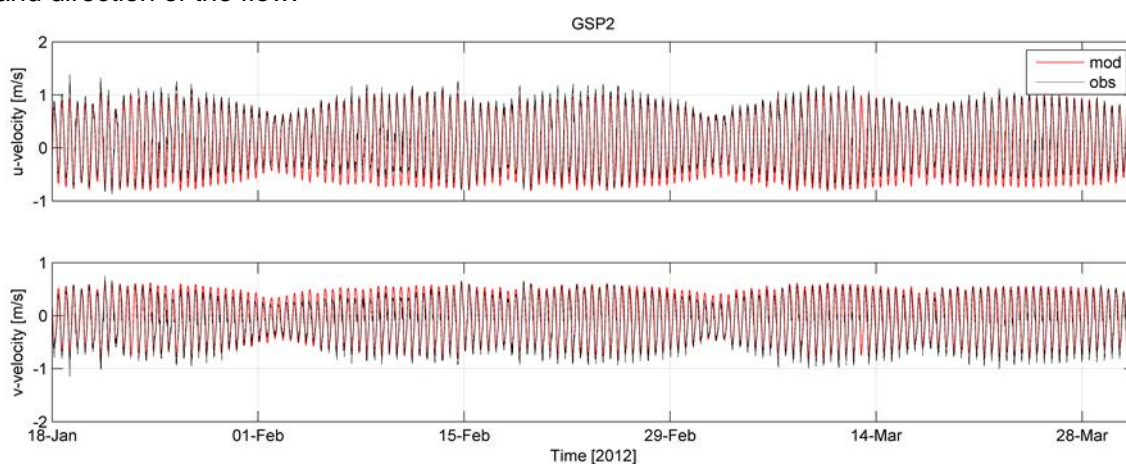


Figure 3.9 Eastward velocity (*u*-velocity) and northward velocity (*v*-velocity) measured and computed at GSP2 during the first quarter of 2012.

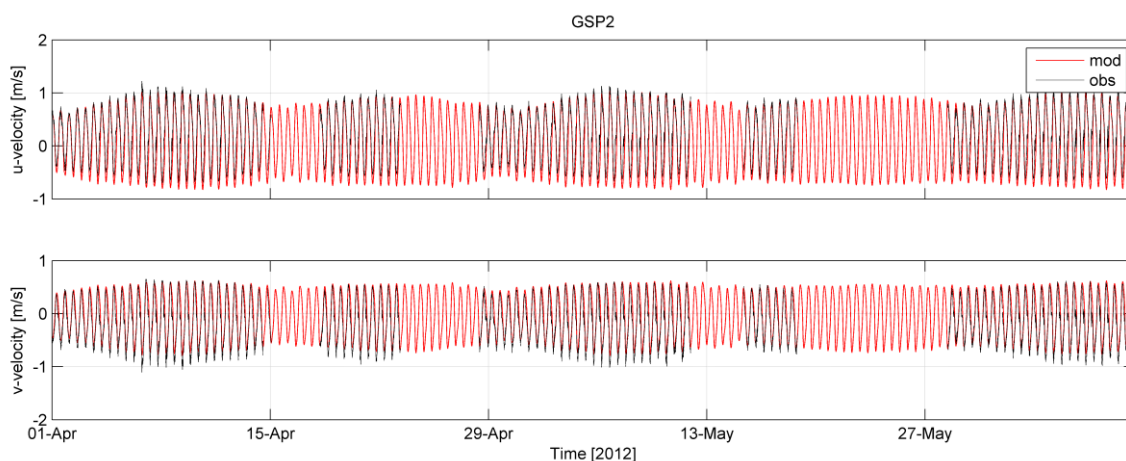


Figure 3.10 Eastward velocity (*u*-velocity) and northward velocity (*v*-velocity) measured and computed at GSP2 during the second quarter of 2012. Data gaps result from malfunctioning of the ADCP.

<sup>4</sup>Data available from Groningen Seaports (GSP) and Rijkswaterstaat.

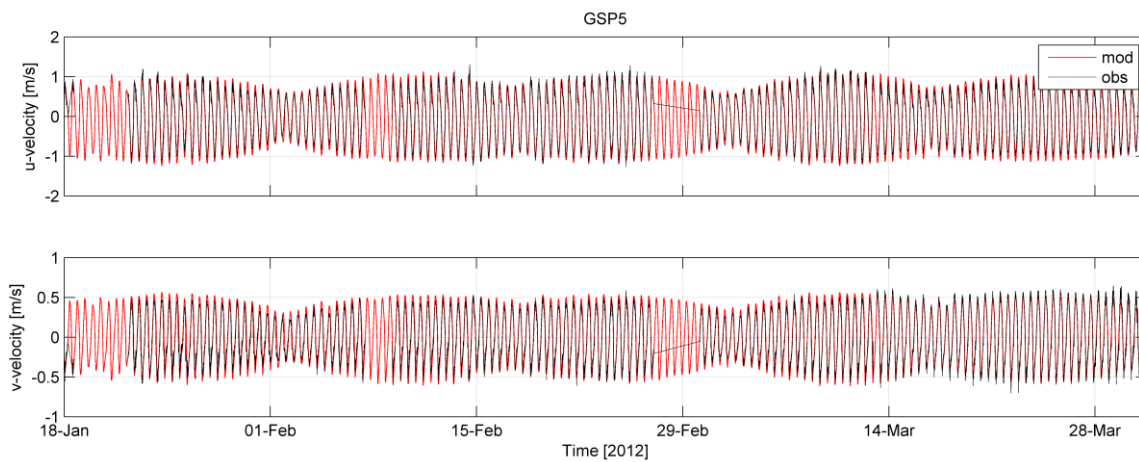


Figure 3.11 Eastward velocity (*u*-velocity) and northward velocity (*v*-velocity) measured and computed at GSP5 during the first quarter of 2012. Data gaps result from malfunctioning of the ADCP.

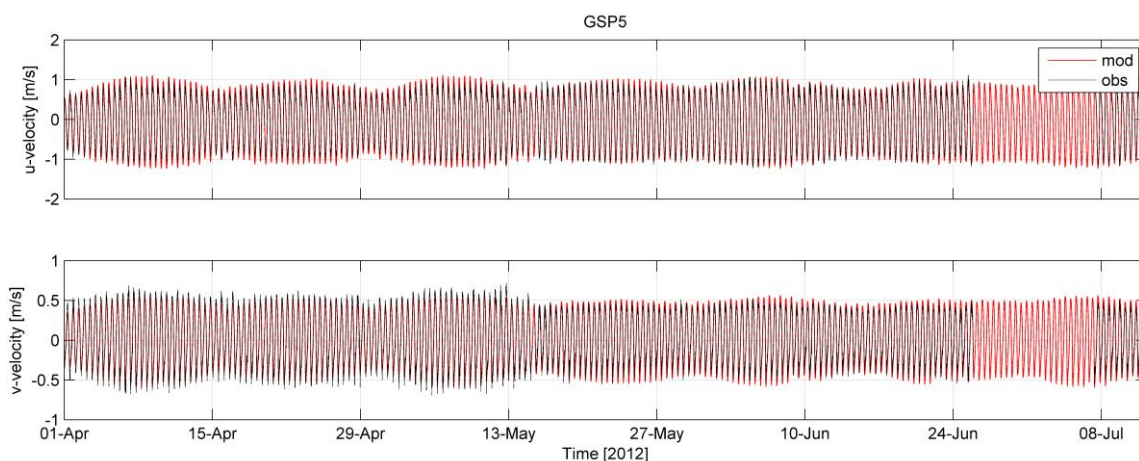


Figure 3.12 Depth-averaged eastward velocity (*u*-velocity) and northward velocity (*v*-velocity) measured and computed at GSP5 during the second quarter of 2012. Data gaps result from malfunctioning of the ADCP.

Observed flow velocities are strongly determined by the local topography, which has a much greater spatial detail than the model can resolve. Therefore modelled and computed flow velocities will always differ. A comparison of long time series of flow velocity components reveals that at GSP2 the computed westward velocity amplitude is slightly underestimated (*u*-component in Figure 3.9 and Figure 3.10). Both the computed flow velocity at GSP2 and GSP5 have a typical spring-neap variation and current velocity amplitude in agreement with observations (Figure 3.11 and Figure 3.12).

The flow velocity has a pronounced intra-tidal asymmetry, which varies spatially. At GSP2, the flood flow velocity is larger than the ebb flow velocity. This pattern is opposite at GSP5 (Figure 3.14, with slightly larger ebb flow velocities). An important observation is that the duration of the flood currents at GSP2 is longer than the duration of ebb currents. A longer duration of the tidal phase in which the velocities are also larger, implies that the flow asymmetry is caused by residual flow (this contrasts with tidal asymmetry, where the tidal phase with maximum flow velocity is shorter than the tidal phase with smaller flow velocity). The type and degree of tidal asymmetry can be more quantitatively addressed through tidal analysis. At the most seaward station (GSP2) the observed  $M_4$  amplitude (the first overtide of the main constituent,  $M_2$ ) is only 2 cm/s (compared to 0.8 m/s for  $M_2$ ), see Table 3.2. The

degree of tidal asymmetry is therefore low at GSP2, and the observed (and modelled) flow asymmetry is caused by residual flow. At GSP5, tidal asymmetry is more pronounced with an  $M_4$  amplitude of 11 cm/s. The type of asymmetry is then more determined by the phase inclination of  $M_4$  with  $M_2$ , given by  $\theta_u = 2\phi_{u_{M_2}} - \phi_{u_{M_4}}$ . The value for  $\theta_u$  is  $298 / 279^\circ$  for observations / model results (see Table 3.2). For  $\theta_u = 225 - 315^\circ$ , tidal asymmetry is characterised by equal ebb and flood flow velocities, but a longer duration of high water (HW) slack tide than of low water (LW) slack tide. High water slack tide asymmetry is typically responsible for import of fine sediments, see report 6 for details. Even though the observed and modelled asymmetry differs  $19^\circ$ , they both lead to HW slack tide asymmetry.

An asymmetry in the flow velocity  $\theta_u = 270^\circ$  corresponds to an asymmetry in the waterlevels of  $\theta_h = 2\phi_{h_{M_2}} - \phi_{h_{M_4}} = 180^\circ$ . Using the values in Appendix A,  $\theta_h$  evolves from  $\sim 170^\circ$  at Huibertgat (in agreement with the flow velocities) to  $\sim 150^\circ$  at Knock to  $\sim 90^\circ$  at Papenburg.  $\theta_h = 90^\circ$  represents a flood-dominant tide with larger flood flow velocities than ebb flow velocities. Apparently, the tide evolves from HW slack-tide dominant at the estuary mouth to maximum flood flow asymmetry deeper into the lower Ems River. Both asymmetries generally lead to sediment import.

Even though tidal asymmetry suggests that the ebb and flood flow velocity should be nearly equal at GSP5, the observed and computed flow velocities are larger in the ebb direction (Figure 3.14). Apparently, an additional ebb-dominant flow asymmetry, probably residual flow, is superimposed on the tidal flow. This will be further elaborated in the next section.

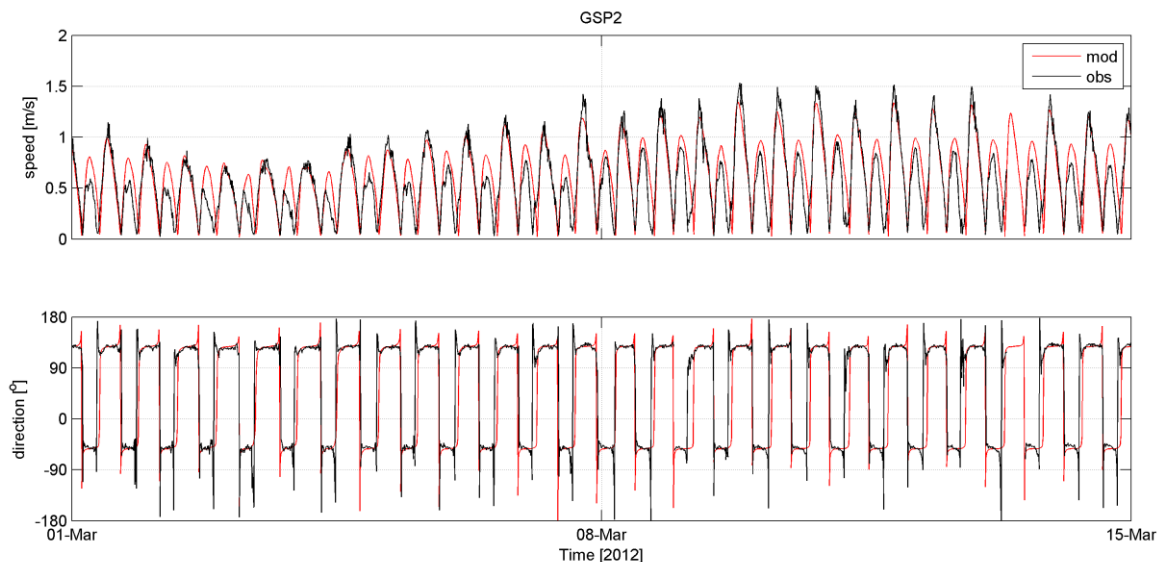


Figure 3.13 Depth-averaged flow speed and direction measured and computed at GSP2 during the first two weeks of March, 2012. The smaller observed flow velocity is in the ebb direction (flow direction  $-50^\circ$ ).

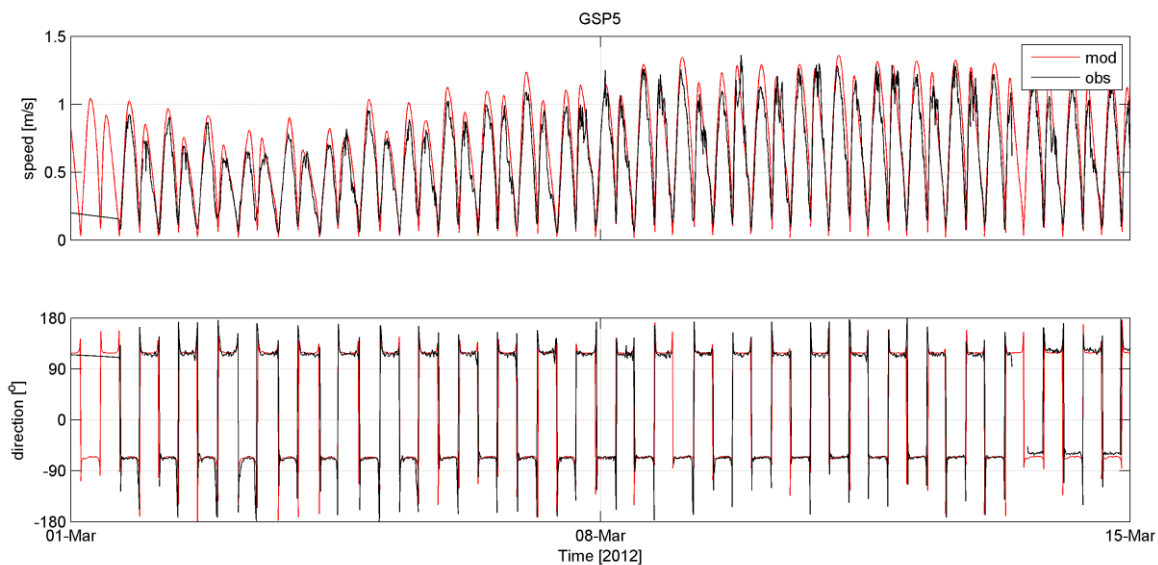


Figure 3.14 Depth-averaged flow speed and direction measured and computed at GSP5 during the first two weeks of March, 2012.

Table 3.2 Observed and modelled amplitudes and phases of the major component of the flow velocity at GSP 2 and GSP5. Observed flow velocity amplitudes of 5 cm/s or less are shaded light grey (including model results for that constituent/location), because small amplitude oscillations are relatively inaccurate to determine from a time-limited set of observations.

Constituent	GSP2				GSP5			
	Amplitude [m/s]		Phase $\phi_u$ [°]		Amplitude [m/s]		Phase $\phi_u$ [°]	
	Obs	Mod	Obs	Mod	Obs	Mod	Obs	Mod
M2	0.80	0.96	13	23	0.87	0.99	32	32
S2	0.22	0.26	85	96	0.22	0.26	103	103
N2	0.17	0.17	351	6	0.17	0.18	10	14
K1	0.02	0.03	136	107	0.02	0.03	122	106
O1	0.03	0.04	326	324	0.04	0.04	331	323
Q1	0.01	0.01	277	259	0.01	0.01	277	257
M4	0.02	0.06	324	137	0.11	0.13	126	145
M6	0.05	0.07	360	327	0.06	0.08	346	343
MS4	0.01	0.05	339	223	0.06	0.08	204	224
$2\phi_{u_{M2}} - \phi_{u_{M4}}$					-	-	298	279

### 3.4.3 Residual flow

Large-scale horizontal flow patterns computed with the model (Figure 3.15) are semi-quantitatively compared with observations by de Jonge (1992). The observed residual flow patterns (Figure 3.16) are based on a large number of transect observations collected from 1971 to 1978. Residual flow patterns are influenced by density-driven flows (and hence discharge), wind-driven flow, and the tidal cycle. Since observations were obtained during varying meteorological conditions, a full quantitative comparison is not possible.



Given these limitations of the data-model comparison, the model reasonably reproduces observations. The observed and computed residual flow velocities are discussed from the sea, heading inland; see Figure 1.1 for names of the tidal channels. South of Borkum, observed and computed (Figure 3.16) residual flow is directed seaward through the Westereems while the residual flow is directed landward through Huibertgat. Near the Meeuwestaart, the net flow direction reverses, directed inland in the Randzelgat and seaward in the Oude Westereems (in both the model and the observations). Near Emshorngat, the direction of residual flow reverses again according to observations, but not in the model. Deeper in the estuary, the computed and observed residual flow in the Bocht van Watum and the Emden navigation channel is seaward. The residual circulation in the Dollard is also reproduced with the model, showing a clockwise residual flow entering the main channel (Groote Gat). In line with the analyses in section 3.4.2, the residual flow is in the flood direction at the location of GSP2, and in the ebb direction at location GSP5.

The computed vertical variation in residual flow has not been compared to observations. In chapter 5 (of this report) and in report 7, the changes in near-bed residual flows will be analysed in more detail.

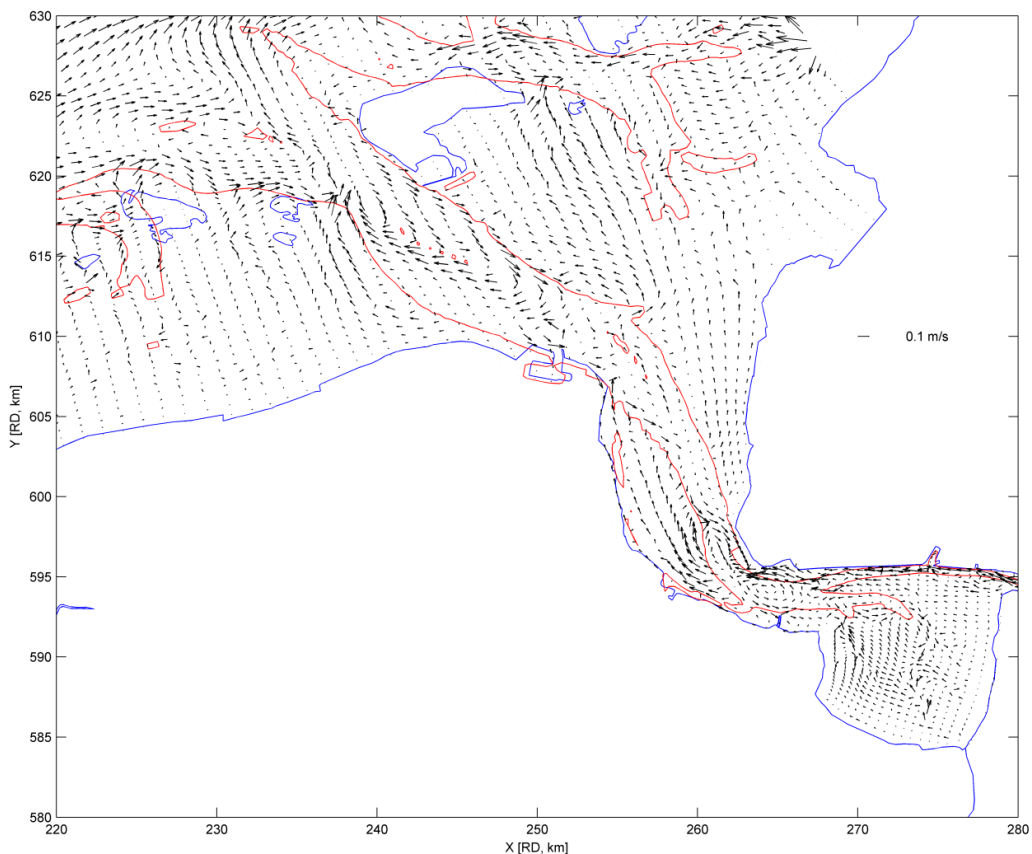


Figure 3.15 Computed depth-averaged residual flow velocity in January 2012, with the -6 m depth contour in red.

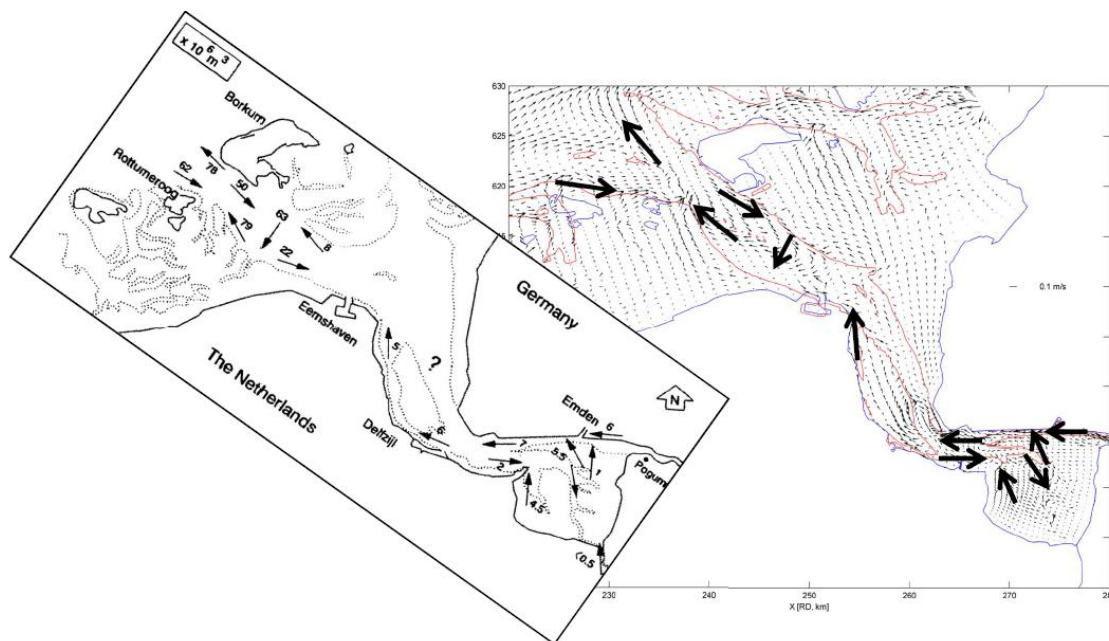


Figure 3.16 Residual water transport per channel per tide, based on averages of several through-tide transect observations carried out between 1971-1978 (de Jonge, 1992), combined with an interpretation of the residual flow field in Figure 3.15.

#### 3.4.4 Salinity

In May and June 2012, unrealistically high salinity was measured at MWTL stations compared to the salinity in (1) the remainder of the year, (2) previous years, and (3) continuous measurement stations in the Ems Estuary (Knock, GSP2, GSP5): see Figure 3.17, Figure 3.18 and Appendix B. Comparing the 2012 salinity observed at Huibertgat (Figure 3.17) with long-term observations (Figure 3.19) reveals that the salinity was exceptionally high (> 33 ppt). Additionally, GSP2 and Huibertgat are spaced several km apart, but the high salinity observed in the Huibertgat is not observed at GSP2 (difference of 5 ppt). It is therefore likely that the MWTL stations are at least part of 2012 unreliable, and MWTL results in May and June are not used for model comparisons. The MWTL measurements are taken near the surface and compared with the surface layer of the model. The NLWKN data are compared with the average of model layers 3 to 6, because the NLWKN measurements are taken lower in the water column. Exceptions are the stations Gandersum, Leer/Leda and Herbrum, for which floating instruments are used. Consequently, these stations are compared to the salinity in the surface layer of the model.

In the outer estuary (see also appendix B), the model seems to slightly overestimate the salinity. The computed salinity in the outer area is strongly dependent on the offshore boundary conditions, for which limited information is available. The modelled intratidal salinity variation is a bit larger (typically 1-2 ppt) compared to the measured intra-tidal variation at GSP5, whereas the computed intra-tidal variation at GSP2 is slightly less than observations (see the GSP measurements in Appendix B). Both the intratidal amplitude and the absolute salinity level at Knock are reproduced, whereas in the station slightly up-estuary (Emden) the computed average salinity is too high and the intra-tidal amplitude too low. Both the computed intra-tidal variation and the absolute salinity levels improve again in the lower Ems River (Gandersum and further up-estuary; see Appendix B). This can be caused by (errors in) (1)



the horizontal gradient (with the computed largest horizontal salinity gradient several km too much up-estuary), or (2) vertical stratification (with the model incorrectly reproducing vertical salinity gradients).

Despite these differences, the salinity is better reproduced by the adapted WED model than by the TO-KPP model, probably because fresh water discharges are more realistically prescribed. Especially the discharge prescribed at Leda is more accurate than in the TO-KPP model, while additionally the discharge at Knock was not accounted for in the TO-KPP model. Other parameters influencing salinity (such as vertical and horizontal mixing) have remained unchanged (compared to the 2005 model).

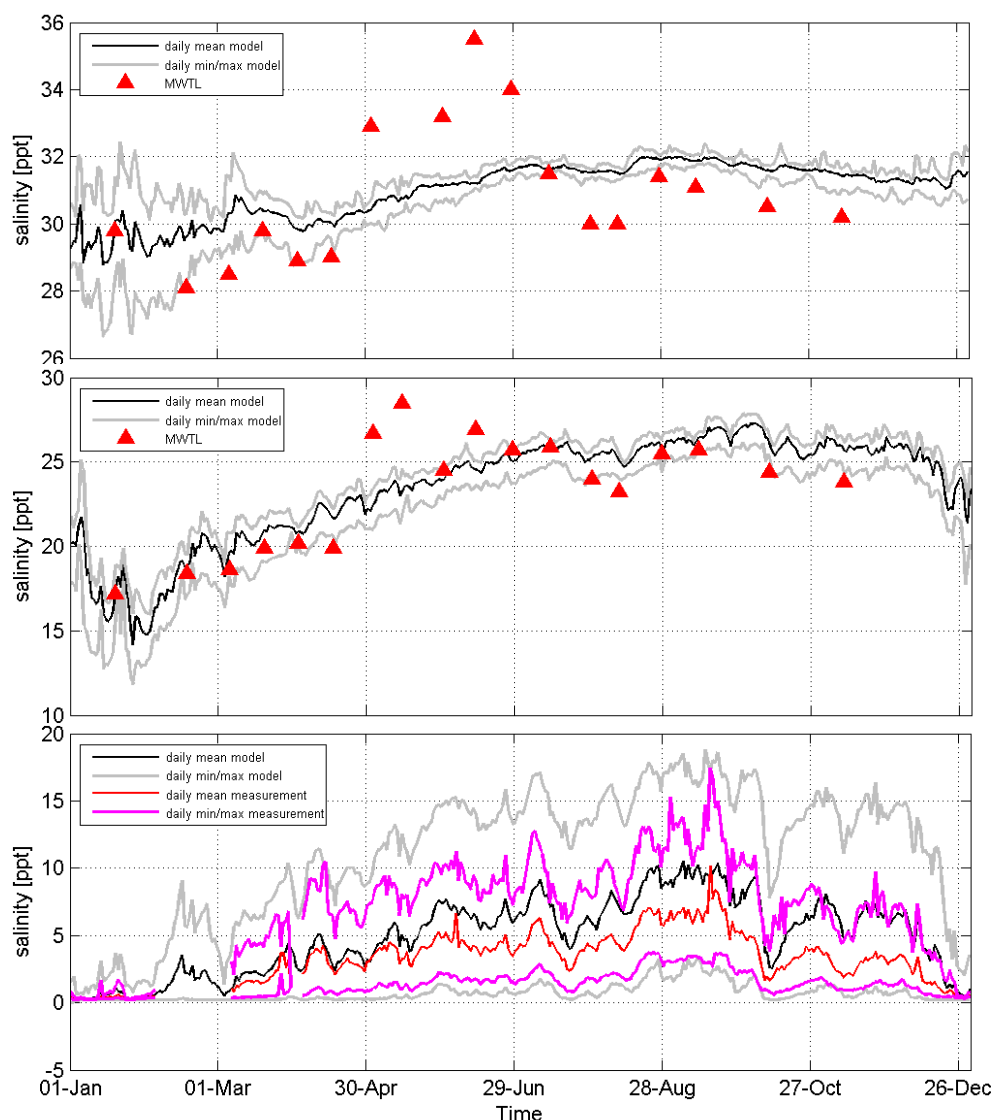


Figure 3.17 Daily averaged (black) and daily extremes (grey) salinity computed with the model for 2012. MWTL observations are indicated with red triangles (top panel is Huibertgat, second panel is Bocht van Watum)). For continues measurements at Terborg (lower panel) the daily average (red) and extremes (magenta) are given.

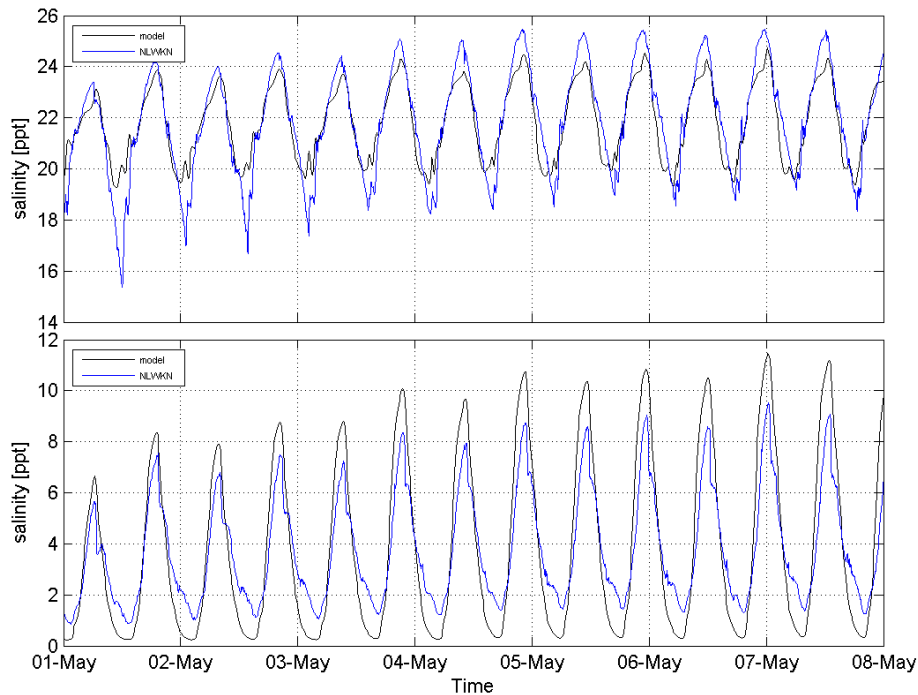


Figure 3.18 Salinity reproduced by the model (black) and measured (blue) in May 2012 for Knock (top) and Terborg (bottom). Data from NLWKN.

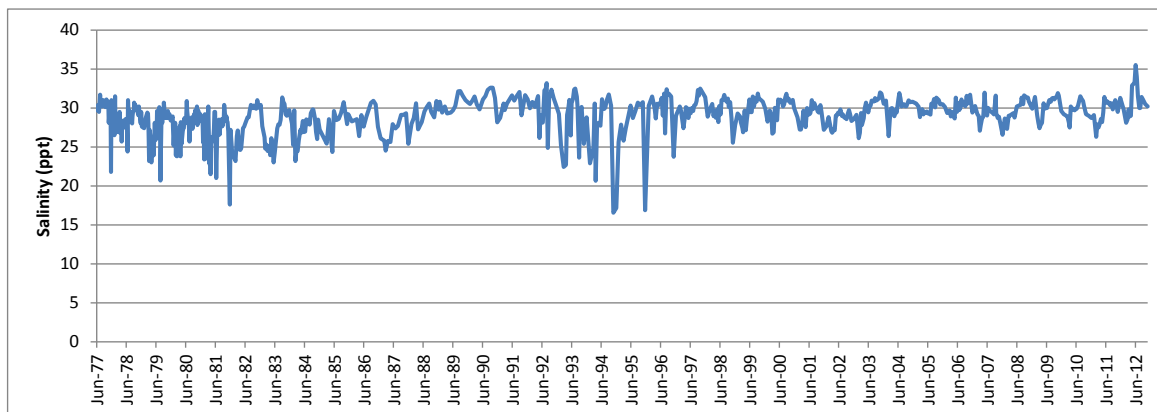


Figure 3.19 Observed salinity at Huibertgat since 1977.

## 3.5 Validation 2013

### 3.5.1 Waterlevels

The hydrodynamic forcing of the model for 2013 is derived in the same way as for 2012. There are some small changes in the discharge points (as described in 3.3.2), but this will not influence the waterlevel prediction of the model. Comparison of the waterlevel signal, the tidal signal and the phases and amplitudes of the main tidal constituents, reveal that the model reproduces the waterlevels similar as for 2012 (compare Figure 3.20 with Figure 3.7 and Figure 3.21 with Figure 3.8). The amplification of the tide in the lower Ems River is, also in 2013, about 10% too large.

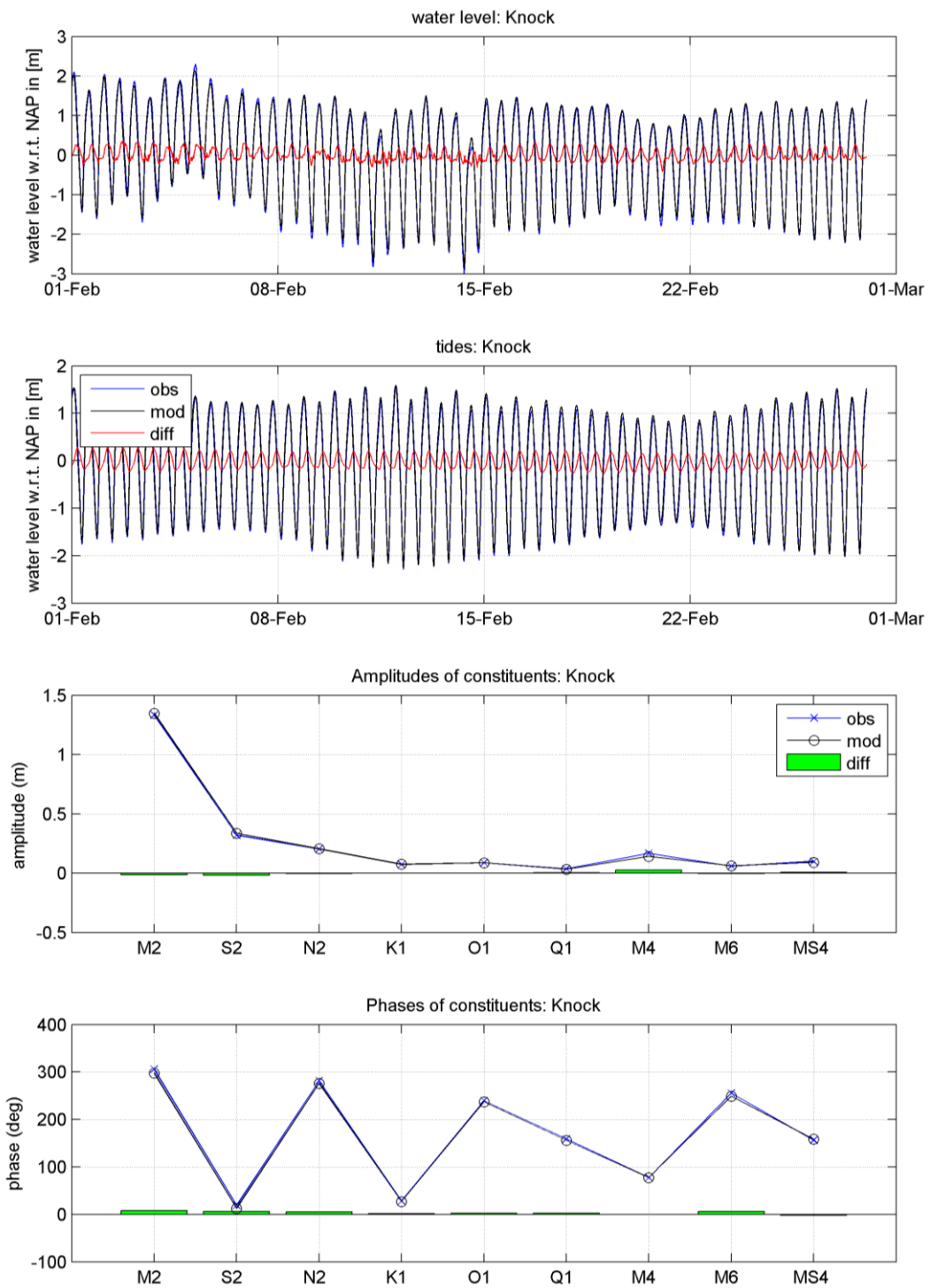


Figure 3.20 Comparison between observed (blue) and computed (black) waterlevels and tidal constituents at Knock for 2013. Time series show the results of February to be able to see some detail; the tidal analysis has been done for the entire year (2013).

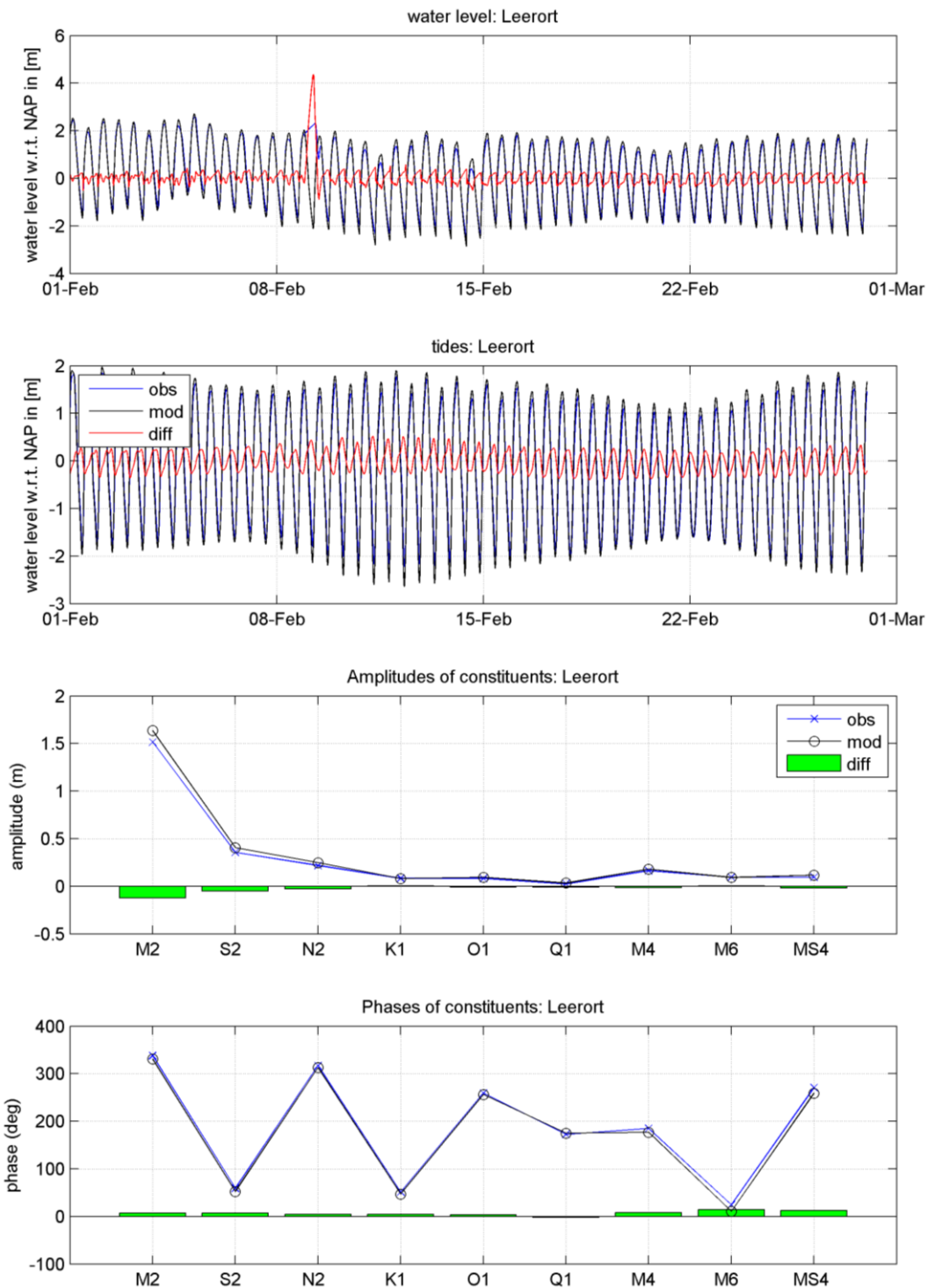


Figure 3.21 Comparison between observed (blue) and computed (black) waterlevels and tidal constituents at Leerort for 2013. Time series show the results of February to be able to see some detail; the tidal analysis has been done for the entire year (2013). The high observed waterlevel on 9 February is probably caused by closure of the storm surge barrier at Gandersum (the setup is observed at all stations in the lower Ems River). This closure is not included in the model.

### 3.5.2 Salinity

Comparison of the salinity between observations and modelling results, show the same pattern as in 2012. In the North Sea and Wadden Sea region, the computed salinity is a bit too high (compared to the MWTL stations: see Huibertgat in the top panel of Figure 3.22 and Appendix B.2 for more stations). The poorest reproduction of the intratidal variation of salinity is again near Emden, where the minimum salinity is overestimated by the model (Appendix B.2). Also at Terborg, comparable results are obtained in 2012 (Figure 3.17) and 2013 (Figure 3.22): the variation in the model is larger than in the measurements. At Knock and Gandersum, the modelled average daily salinity and daily extremes are within several ppt of the observed salinity in summer, but the salinity is overestimated in winter (Appendix B.2).

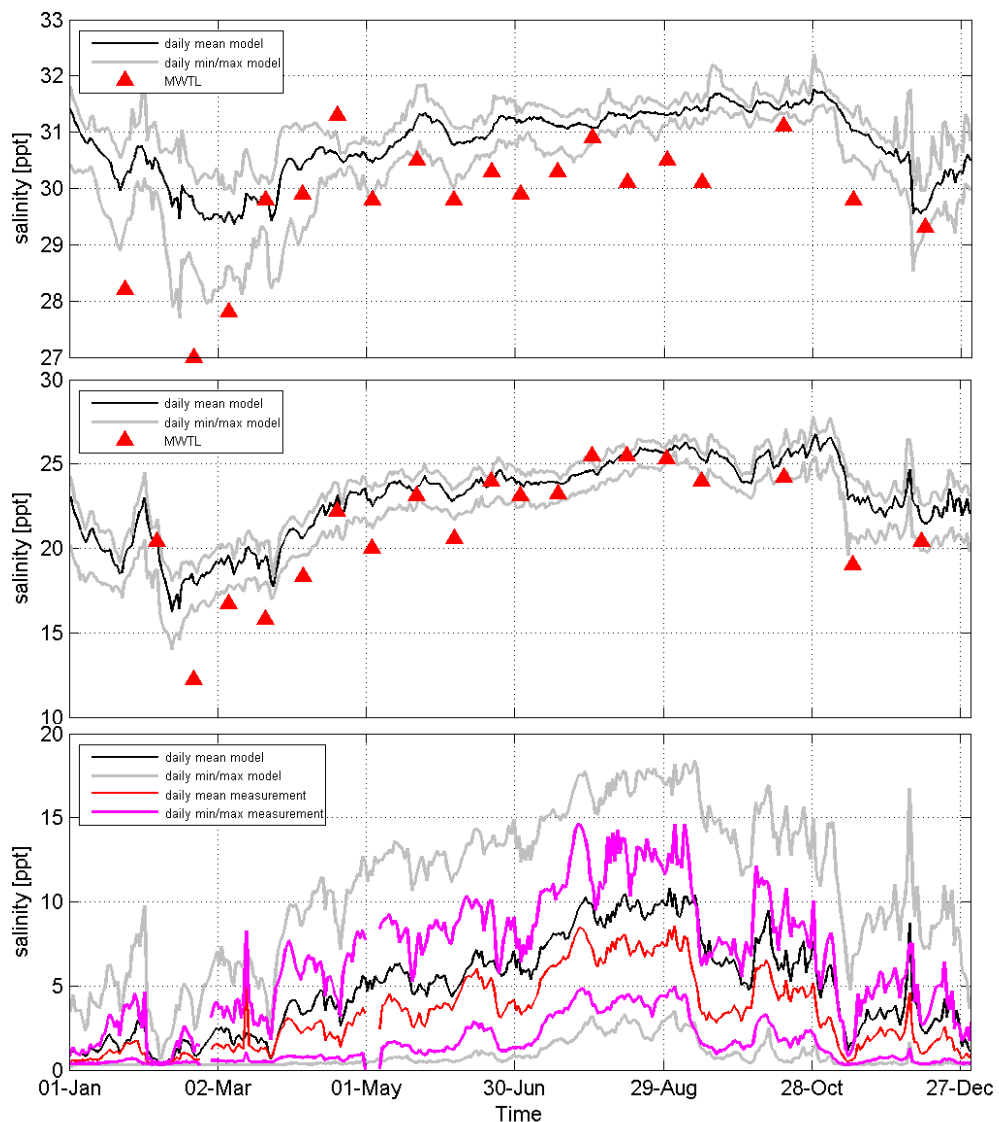


Figure 3.22 Daily averaged (black) and daily extremes (grey) salinity computed with the model for 2013. MWTL observations are indicated with red triangles (top panel is Huibertgat, second panel is Bocht van Watum)). For continues measurements at Terborg (lower panel) the daily average (red) and extremes (magenta) are given.

### 3.6 Wave modelling

#### 3.6.1 Objectives and approach

The main objective of the wave modelling is to compute the additional bed shear stresses caused by the presence of (breaking) waves in the North Sea, Wadden Sea, and within the Ems-Dollard estuary itself. In the previous WED model, a simple fetch-length approach was used, which underestimates waves (and therefore bed shear stresses) in the North Sea relative to wave-induced bed shear stresses within the sheltered Ems estuary. Using a model like SWAN to compute the wave-induced bed shear stress will result in a steeper energy gradient from the sea to the tidal flats, which enhances the landward transport of sediment.

The wave model is set up within the Delft3D modelling suite using the numerical model SWAN. SWAN (acronym for Simulating Waves Nearshore) is an energy balance based frequency domain model developed by Delft University of Technology (Booij et al., 1999; Holthuijsen, 2007). It is a state-of-the-art shallow water phase-averaging wave model, and takes into account (a.o.) the following processes:

- wave propagation in time and space, including shoaling and refraction,
- frequency shifting due to currents and non-stationary depth;
- wave generation by wind;
- white-capping and depth-induced breaking;
- bottom friction and dissipation due to vegetation or fluid mud;
- wave-induced set-up;

The wave model is coupled to a 2DH version of the 3D flow model described in previous sections, thereby including the effects of waterlevel variations on the wave propagation. It is forced using measured wave data from an offshore buoy, and wind data obtained from the European meteorological forecast system HIRLAM. The model is set up for 2012 and 2013, providing wave-induced bed shear stresses for both years. The sensitivity of wave height and computed bed shear stress is only evaluated for 2012.

In the sediment model (report 6), the hydrodynamics computed with the 3D model is used to compute advection of sediment. Resuspension is computed with bed shear stress fields from the 2D FLOW/WAVE model. The bed shear stress is therefore composed of a flow component, a wave-component, but also the wave-current interaction.

#### 3.6.2 Model set up

The wave model is set up in combination with a two-dimensional (depth-averaged) version of the flow model described in section 3.3 and 3.4 (online coupled). The hydrodynamics of the wave model are computed in depth-averaged mode for practical reasons: in 2D mode the computation already takes 2 weeks on a fast computer to simulate a full year. In the sediment transport model and the water quality model, the bed shear stress computed with the 2D wave model is combined with the 3D hydrodynamics (waterlevels, flow velocity). This method does not account for wave-induced flows in under breaking waves, but in the Ems Estuary such currents are probably not important because of the relatively low wave height and smooth bed topography.

The coupling interval is 1 hour (meaning there is exchange of information between both models every hour), and the computational grid is identical to the hydrodynamic grid (Figure 3.23). The wave model bathymetry is identical to the FLOW model (see section 3.3). The wave model is forced with

- Wave conditions prescribed at offshore model boundary
- Spatially and temporarily varying wind field
- Waterlevels computed by the hydrodynamic 2DH model

#### *Boundary conditions*

The wave boundary condition is applied along the western, northern and eastern model boundaries assuming a JONSWAP-spectrum (Hasselmann et al., 1973), consisting of significant wave height, maximum wave period and mean wave direction measured at a buoy located just north of the island of Schiermonnikoog (SON, see Figure 3.23). Note that this station is located within the model domain (and not at the model boundary), but the local water is considered sufficiently deep (~25 m) for SON to represent the boundary conditions. The observed time series and corresponding wave rose (Figure 3.24) reveal wave heights generally below 2 m, and sometimes up to 5 m. The maximum wave periods vary between 8 and 15 seconds. The dominant wave direction is between north and west. For about 68% of time the waves are from the north-western quadrant. A significantly smaller portion of the waves originates from the south-western or north-eastern quadrant (respectively 14 and 16%). Waves only rarely originate from the south-eastern quadrant (2% of time), which can be explained by the coastal geometry and the sheltering effect of the Wadden Island and Dutch mainland. Note that the higher wave events ( $H_s > 2$  m) only occur during north-westerly waves.

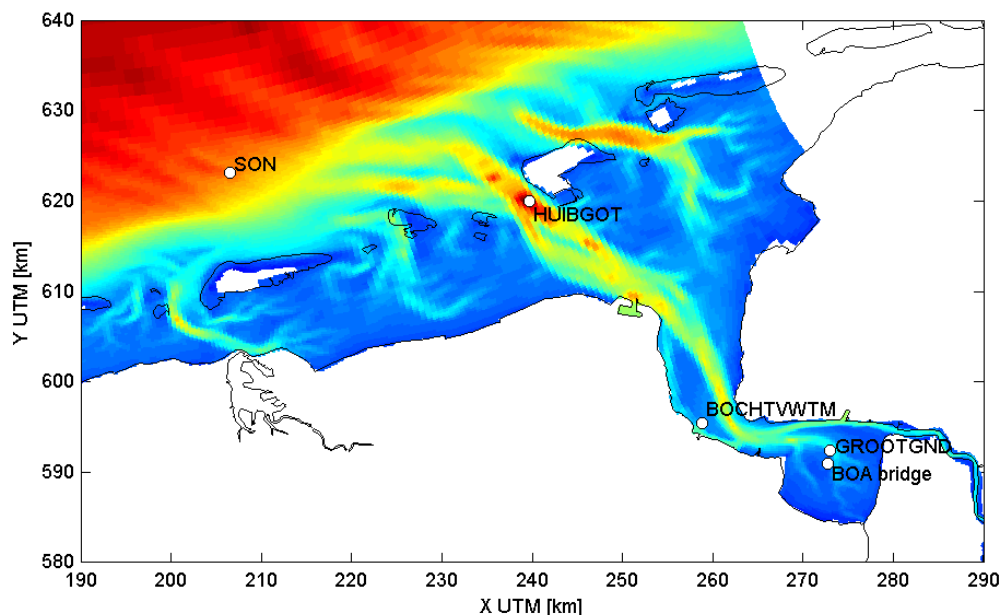


Figure 3.23 Model bathymetry and locations of model timeseries output

#### *Wind*

Locally wind-generated waves are expected to be relevant within the estuary. For the hydrodynamic model, the wind data used was measured at an inland weather station (see section 3.3). However, this data is probably not representative for wind conditions offshore,



which are important for wave modelling. Therefore, results from the numerical weather prediction forecast system HIRLAM are used. HIRLAM is an acronym for High-Resolution Limited Area Model, and is developed in cooperation between meteorological institutes from various European countries (e.g. The Netherlands, Denmark, Finland, Sweden, Spain).

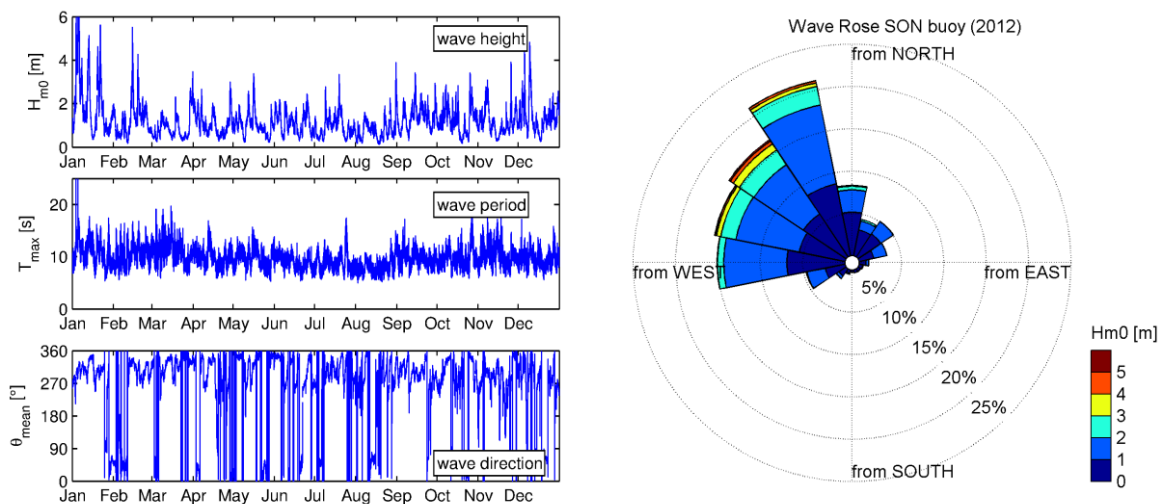


Figure 3.24 Time series of wave height, wave period and wave direction (left panel), and the corresponding wave rose (right panel) based on the measurements at the Schiermonnikoog-Noord buoy for 2012.

HIRLAM uses a computational grid with a horizontal resolution of 5 to 15 km, and includes several meteorological processes. The model is used for weather prediction, and utilizes data assimilation to optimize the model results. The results used in the wave model consist of spatially varying air pressure, and horizontal components of the wind-velocity ( $u$  and  $v$ ). Two examples of wind field snapshots applied in the wave model are given in Figure 3.25. For more detailed information about HIRLAM, reference is made to <http://www.hirlam.org>.

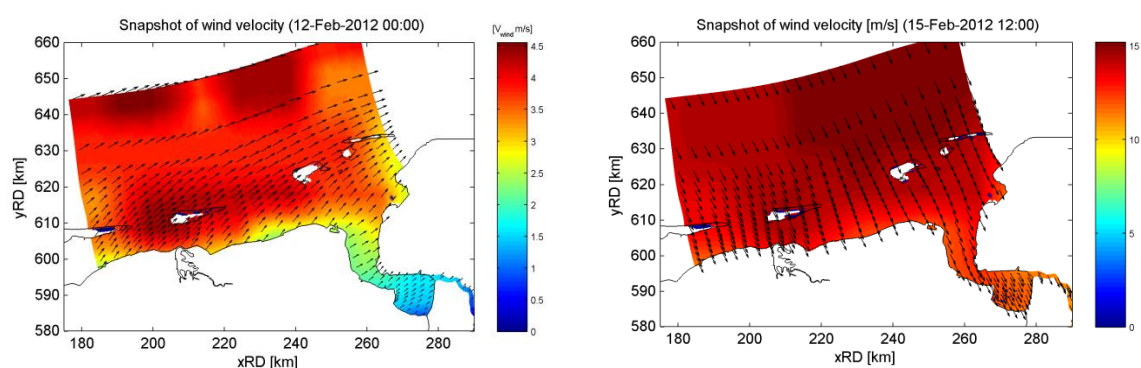


Figure 3.25 Example snapshots of a low-energy (left) and high-energy (right) wind field used in the wave model (based on the results of the meteorological model HIRLAM).



### Settings

SWAN computes the stationary wave field in an iterative manner. For this a number of numerical settings have been done. Since the focus is on waves in the Ems-Dollard estuary, which are expected to be rather short and small, some test simulations were carried out with the frequency-space settings to obtain a higher accuracy for shorter waves. Comparison with the model results for default numeric settings, however, revealed that the effect is negligible. Therefore, the most of the default SWAN model settings are used (Table 3.3), reducing the computation time significantly.

Table 3.3 Main numerical settings of the SWAN model adapted in this study (default SWAN and used in the Ems model).

Process	Parameter	unit	Default SWAN	Applied
Depth-induced breaking	Battjes - Jansen $\alpha$	-	1	1
	Battjes - Jansen $\gamma$	-	0.73	0.6
Bottom friction	JONSWAP	m <sup>2</sup> /s <sup>3</sup>	0.038	0.067
Iterations				
Frequency space	Lowest frequency	Hz	0.03	0.03
	Highest frequency	Hz	2.5	1
	Frequency bins	-	50	50
Wave-current interaction	-	-	Yes	No
Accuracy criteria	Change per iteration	%	2	2

### 3.6.3 Model verification

The flow-wave model is run for the entire year 2012. However, for clarity only results for February 2012 are shown (Figure 3.26), including both low-energy wave conditions (around February 12<sup>th</sup>,  $H_{m0} \sim 0.3$  m) and high-energy wave conditions (around February 15<sup>th</sup>,  $H_{m0} \sim 5.5$  m; largest wave heights of 2012). The wave period is rather constant throughout time (between 8 and 15 s). High energy wave conditions are dominantly from the NW, whereas low-energy waves are mainly from the NE.

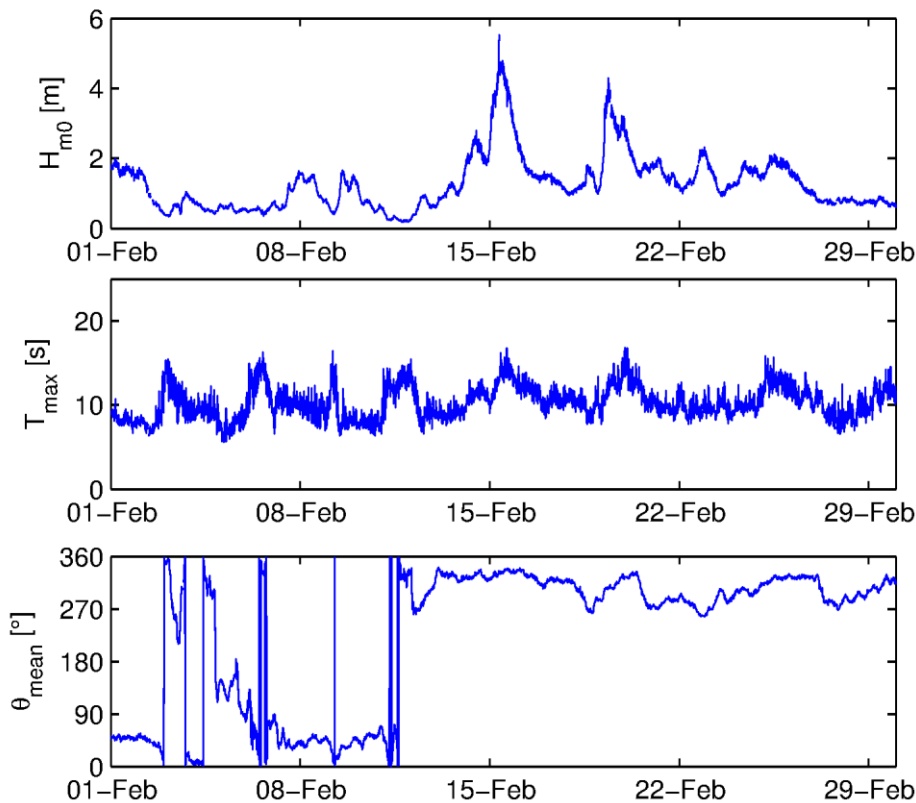


Figure 3.26 Time series of significant wave height (top), maximum wave period (middle), and mean wave direction (bottom panel) measured at the SON-buoy for February 2012. Note that this is a zoom of Figure 3.24.

The model is first run with default SWAN wave settings, which have been assessed to give accurate results in many coastal areas. Comparing the computed wave height at SON buoy with observations reveals (Figure 3.27) that the computed wave height is slightly larger than observations. As a sensitivity analysis, the wave height imposed at the model boundary was decreased with 10 and 20% (Figure 3.27). The results suggest that the computed wave height is relatively insensitive to the wave height provided at the boundary: the computed wave height is apparently mainly determined by local wind-generated waves and the user-defined uniform bottom friction coefficient.

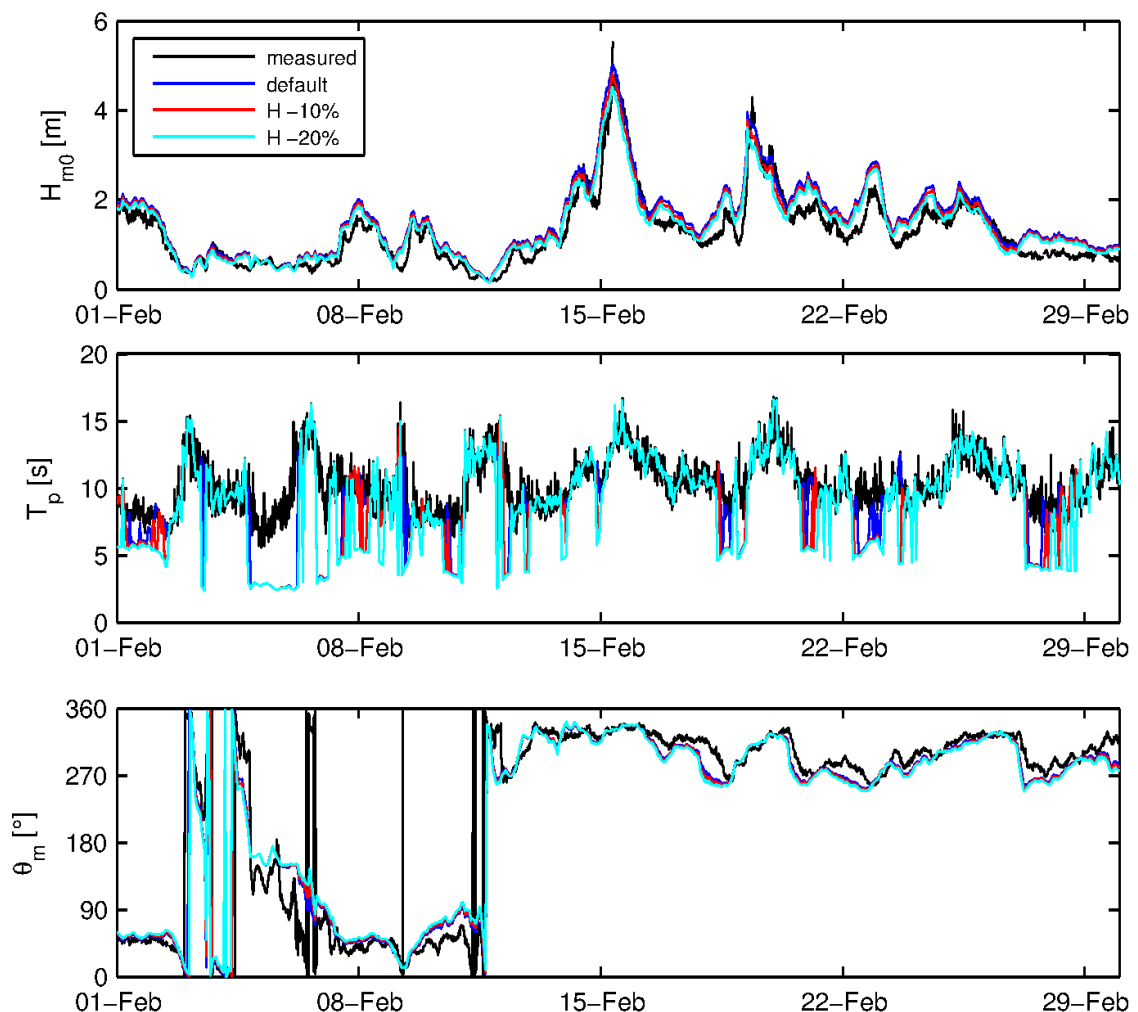


Figure 3.27 Comparison with the measured (black) and the simulated wave characteristics at the SON-buoy location. The simulations contain different boundary conditions: time series measured by the buoy (blue) at the offshore boundaries, and with 10 (red) and 20% (magenta) lowered wave height applied as offshore boundary condition.

During the calibration of the sediment transport model (report 5), the wave-induced bed shear stress seems to be overestimated in muddy areas. This may be related to the bed friction formulations in SWAN, which have been derived for sand-dominated environments, which may not be accurate in mud-dominated environments. Therefore the effect of additional numerical parameters on wave dissipation within the Ems Estuary is evaluated. First, the depth at which breaking occurs was modified. By default, the depth-induced wave dissipation is computed using the Battjes – Jansen (1978) model (see the Delft3D wave manual for details). In this model, depth-induced breaking is determined by the ratio of wave height  $H_m$  over water depth  $d$  ( $\gamma_{BJ} = H_m / d$ ). Decreasing  $\gamma_{BJ}$  from 0.73 to 0.6 leads to lower wave heights in shallow areas. Secondly, the bottom friction coefficient was varied. Within the default friction model in SWAN (JONSWAP, Hasselman et al. 1973) the friction parameter should be  $0.038 \text{ m}^2/\text{s}^3$  (Van Vledder et al., 2010), a setting typical for swell waves. Increasing the friction factor to  $0.067 \text{ m}^2/\text{s}^3$  (a value frequently used as well) leads to more energy dissipation.

The up-estuary decrease in wave height shown in Figure 3.28 is further illustrated by Figure 3.29 and Figure 3.30. The snapshots reveal a strong decrease in wave height landward of the Wadden Sea islands. Largest wave heights occur in the main tidal channels ( $H_s < 2$  m). At the Port of Delfzijl the maximum significant wave height  $H_s$  is  $\sim 1$  m, at the mouth of the Dollard 0.5 m (although occasionally 0.6-0.7 m, see Figure 3.28). The wave period is typically between 1 and 3 seconds, and the wave direction is rather variable with a dominant north-westerly component. The wave model using  $\gamma_{BJ} = 0.6$  and a JONSWAP coefficient of  $0.067 \text{ m}^2/\text{s}^3$  is only slightly more dissipative, leading to marginally lower wave height at the four locations (Figure 3.28).

Overall, the wave model seems to be insensitive to input parameters (boundary conditions, the friction factor and breaking parameter). However, these latter two may influence the computed wave-induced bed shear stress, which will be evaluated in the next section.

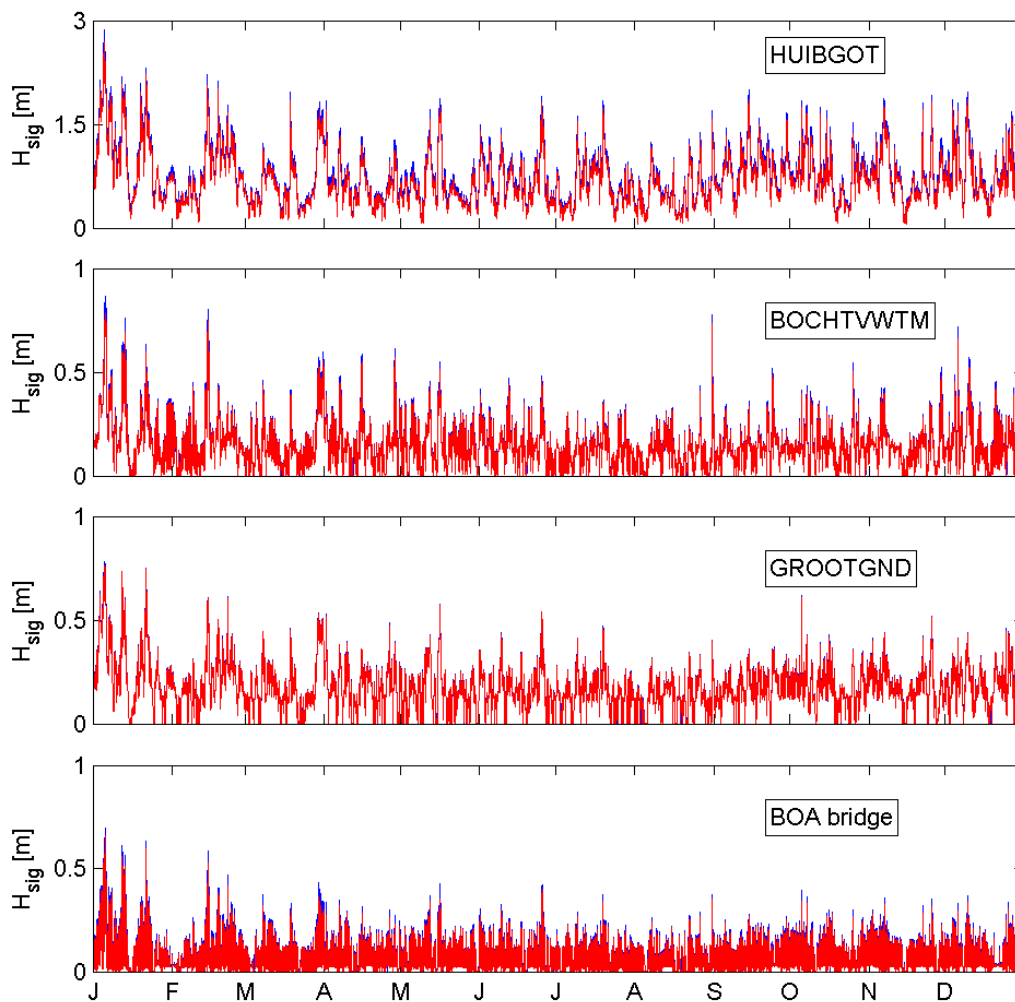


Figure 3.28 Computed wave height at Huibergat, Bocht van Watum, Grootte Gat Noord, and BOA bridge using the default settings (blue) and using  $\gamma_{BJ} = 0.6$  and a JONSWAP coefficient of  $0.067 \text{ m}^2/\text{s}^3$  (red), for 2012. Both simulations largely overlap; only at the most seaward station (HUIBGOT) the default wave height is slightly larger. See Figure 3.23 for locations.

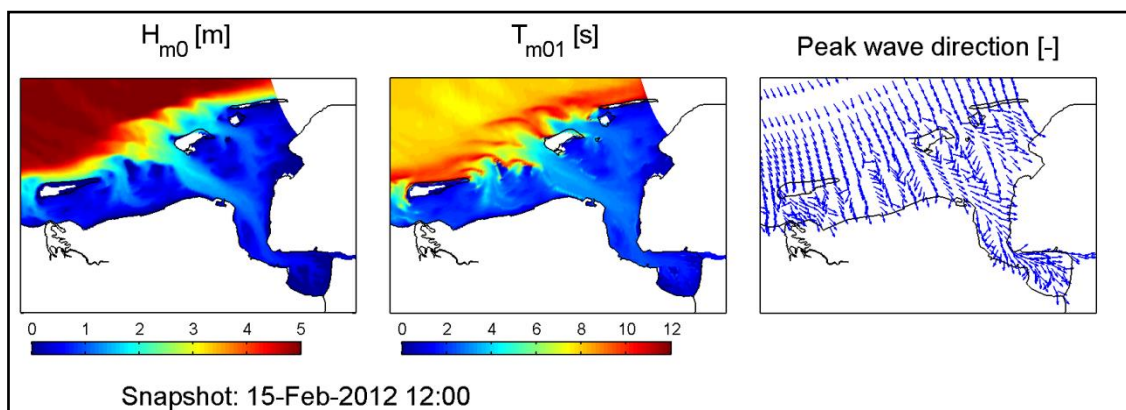


Figure 3.29 Snapshots of the wave characteristics for a high-energy wave condition computed by the model: wave height (left), wave period (middle) and peak direction (right).

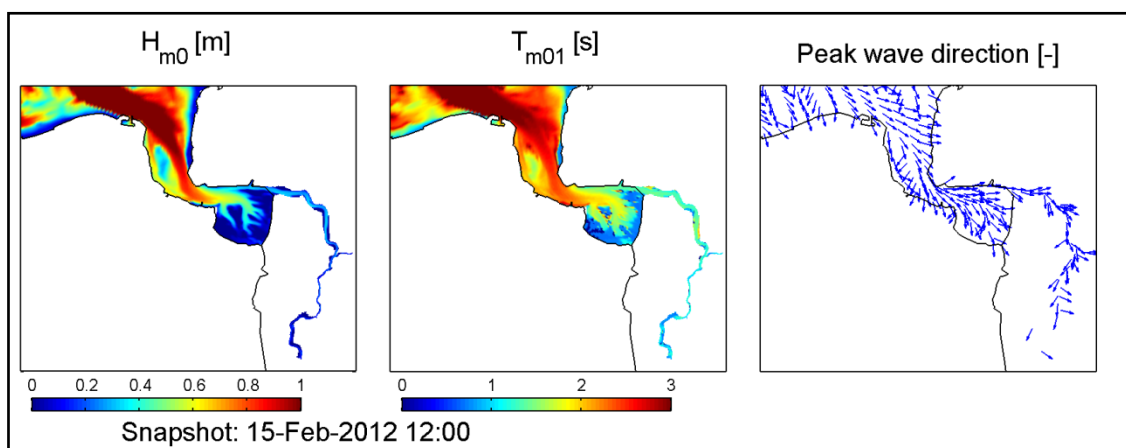


Figure 3.30 Snapshot of wave characteristics within the Ems-Dollard estuary for a high-energy wave condition (zoom of Figure 3.29).

#### 3.6.4 Bed shear stress

The main purpose of the SWAN model is to use the computed bed shear stress for sediment resuspension. Therefore the computed bed shear stress is evaluated for two successive conditions in February, where the largest storm of 2012 (February 15) was preceded by calm conditions.

In the North Sea and the shallow parts of the Wadden Sea, the bed shear stress sharply increases during high energy events (Figure 3.31). For low wave conditions the flow-only and the combined bed shear stresses are similar, but for high-energy wave conditions the combined bed shear stresses are much larger. This is mainly the case in the North Sea and Wadden Sea, but also within the estuary significantly larger bed shear stresses are computed, mainly near the entrance of the estuary.

The effects of the Battjes-Jansen breaking parameter and the JONSWAP coefficient have a minor impact on the computed bed shear stress distribution (compare Figure 3.31 with Figure 3.32). The bed shear stress is slightly lower, especially in the Wadden Sea, using the modified breaking and friction parameter.

In Figure 3.33 time series of the bed shear stress computed by the 2DH flow and the coupled flow-wave model are plotted for four observation locations (for the locations see Figure 3.23). The figure gives an indication of the relative contribution of waves to the local bed shear stress. At the most offshore location (HUIBGOT) and one of the locations in the estuary (GROOTGND) the time series are nearly identical. This implies that at these locations the bed shear stress is only a function of the currents. For the other two locations, however, the bed shear stresses are regularly significantly higher when including waves in the model, especially during higher energetic wave events (such as around February 15<sup>th</sup>).

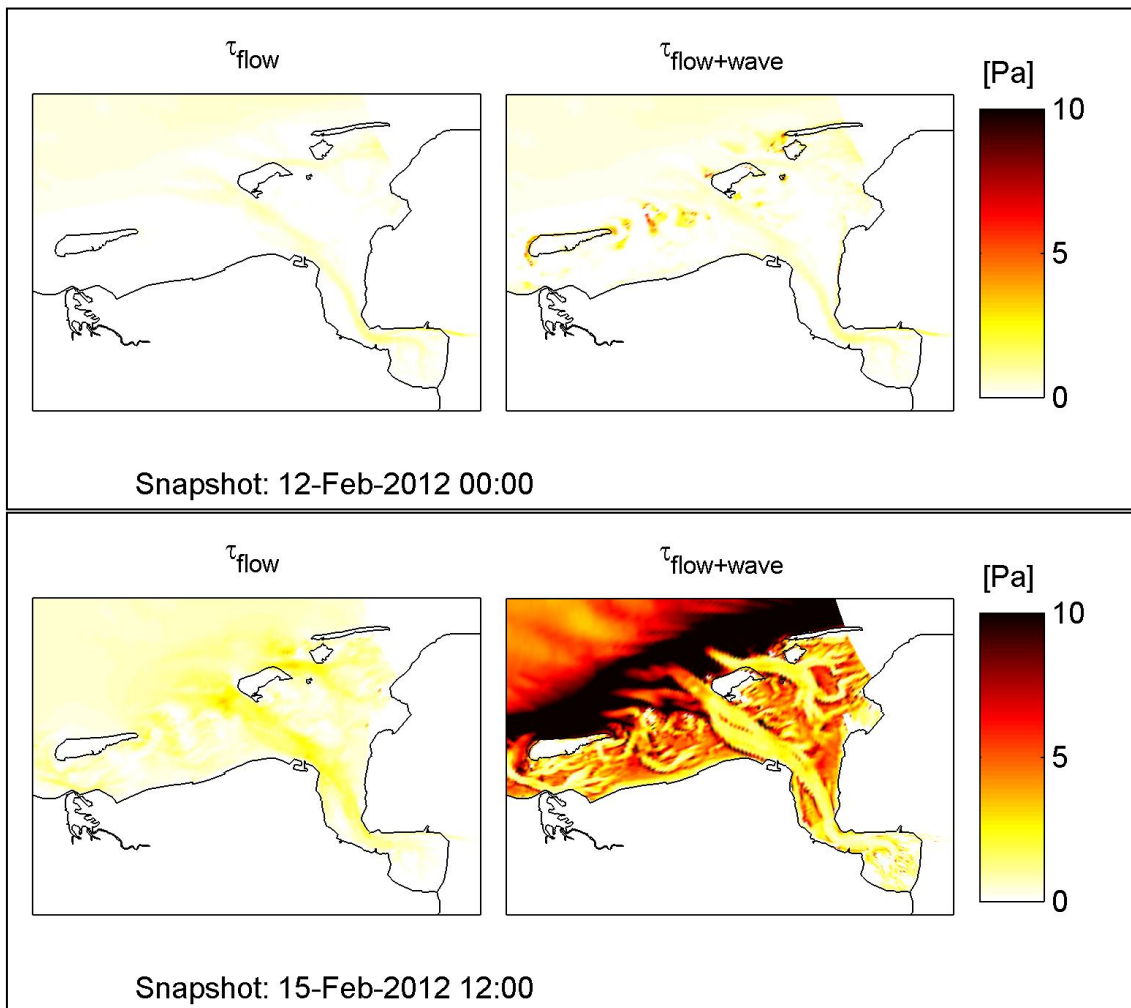
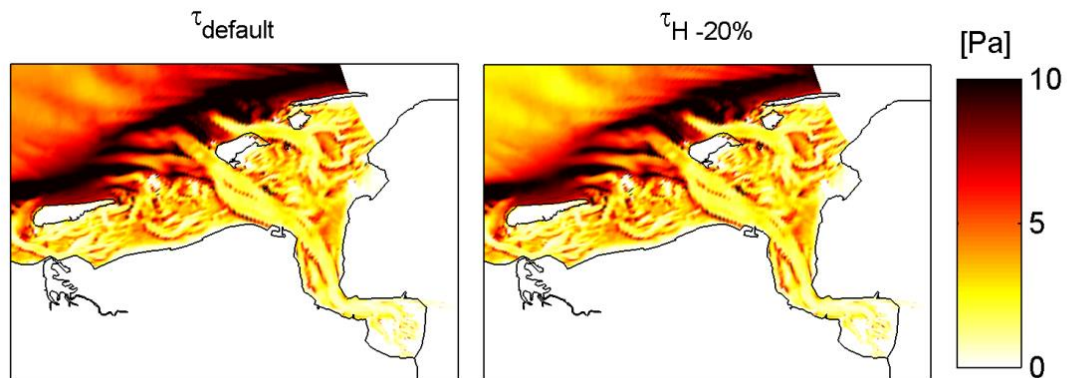


Figure 3.31 Snapshots of the bed shear stress without (left) and with waves (right) included for a low-wave conditions during spring tide (top) and high-wave conditions shortly after spring tide (bottom).



Snapshot: 15-Feb-2012 12:00

Figure 3.32 Snapshots of the bed shear stress using  $\gamma_{BL} = 0.6$  and a JONSWAP coefficient of  $0.067 \text{ m}^2/\text{s}^3$ , standard wave boundary conditions (left) and with 20% reduction in offshore wave height (right).

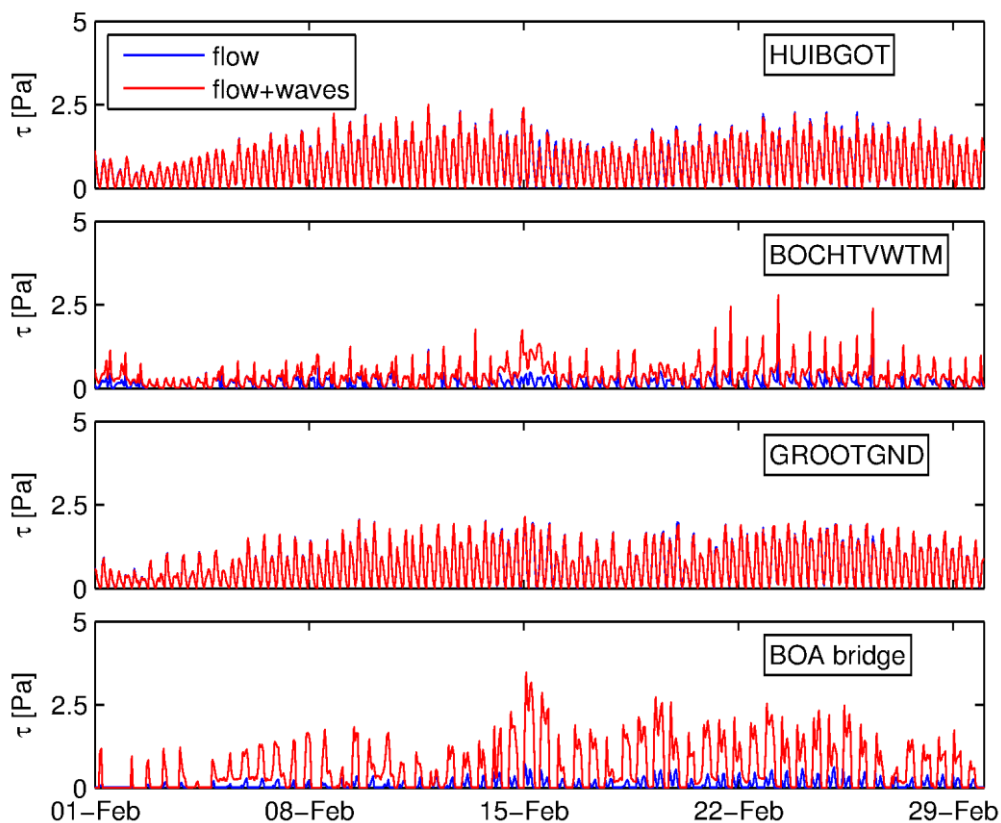


Figure 3.33 Time series of maximum bed shear stress (February 2012) computed by the 2DH flow (blue) and the coupled flow-wave model (red) for 4 observation stations in and around the Ems-Dollard estuary. In deep water (HUIBGOT and GROOTGND) the blue and red lines overlap.

### 3.6.5 2013 wave conditions

Using the model settings derived for the year 2012 (lower depth-induced breaking parameter and larger friction parameter), the model was run for 2013 as well. In Figure 3.34 time series of wave height, period and direction measured at the SON buoy and the corresponding wave rose are shown for 2013. Overall, the wave conditions were similar to 2012 (compare Figure



3.34 with Figure 3.24), although there are less high-wave events. Comparing the wave roses it can be seen that the dominant direction is again northwest, while the rose also shows the relatively low contribution of high energy wave events. Based on these observations, the offshore wave conditions in 2013 are less energetic compared to 2012.

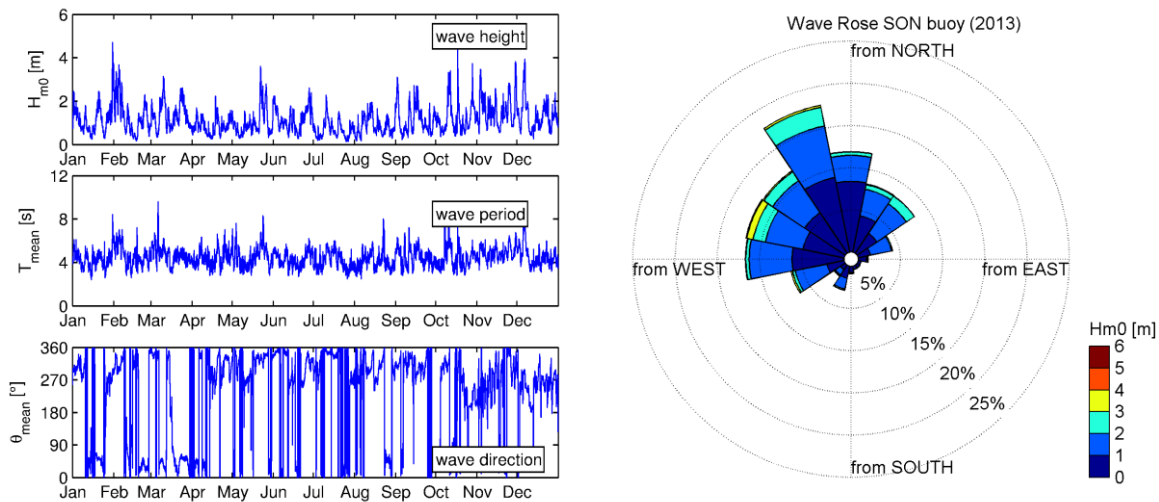


Figure 3.34 Time series of wave height, wave period and wave direction (left panel), and the corresponding wave rose (right panel) based on the measurements at the Schiermonnikoog-Noord buoy for 2013.

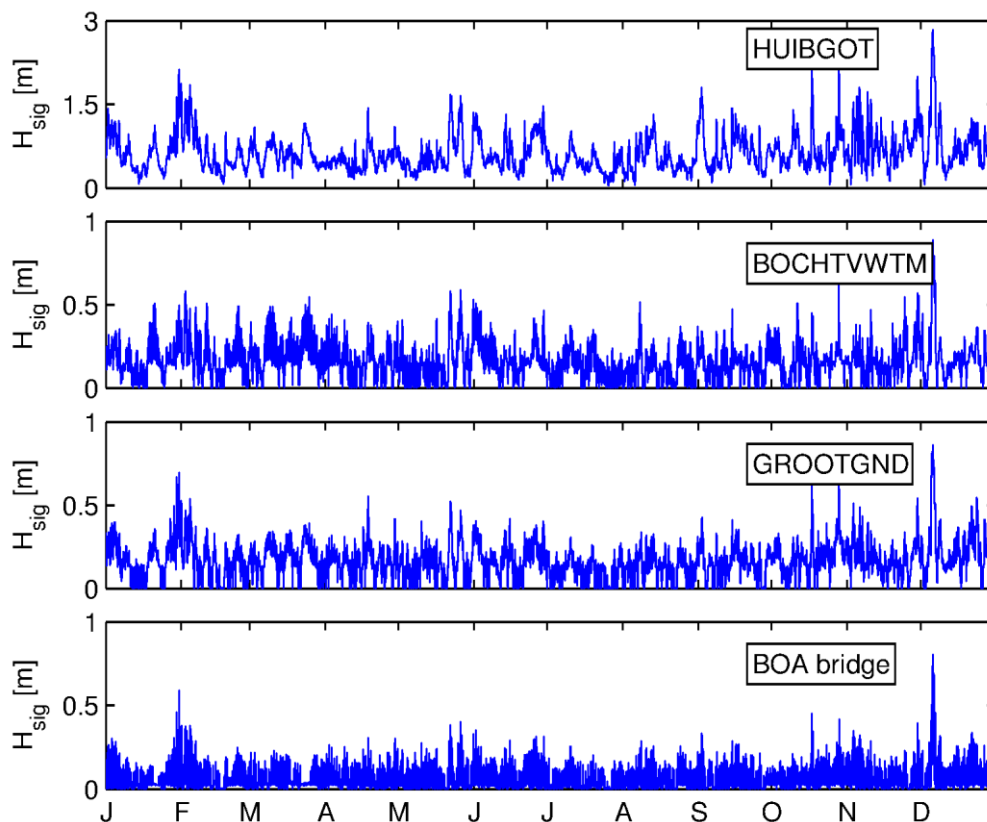


Figure 3.35 Wave height at Huibertgat, Bocht van Watum, Groote Gat Noord, and BOA bridge using the default settings for 2013.



The difference in wave height seems less pronounced within the estuary (compare Figure 3.28 with Figure 3.35). At the most offshore located station (Huibertgat) the wave height varies between 0.5 and 2.5-3 m, but is most of the time between 0.5 and 1 m (as in 2012). A difference within the estuary is that the highest waves in 2012 occur in January-February (Figure 3.26), but more towards the end of the year in 2013 (Figure 3.35).

### 3.7 Model accuracy

A method to quantitatively address model uncertainty was developed in the framework of 'KPP B&O Waterkwaliteitsmodelschematisaties' (Harezlak et al., 2014). This method provides a framework with steps to be taken to determine the accuracy of numerical models, including

- Definition of the model aim: which questions does the model have to address?
- Definition of target variables / indicators: which model parameter will be quantitatively compared with observations? And over which period / space should which sort of statistical parameter (mean, exceedance interval) be computed with what accuracy?
- Which techniques should be used to (1) analyse the observations and model, and (2) quantify the relation between observations and model results?
- How sensitive is the model to (uncertainties in) the model input?
- And based on the previous steps: what is the uncertainty in the model to address the research questions?

Quantifying model uncertainties is not part of the present report; this will be done in the framework of a separate study (the long-term research project 'KPP B&O Waterkwaliteitsmodelschematisaties'). Although these results are not part of the present report, this more quantitative approach will be part of the overall final project report (report 12). In this section, we relate the aim for the hydrodynamic model to target variables, and qualitatively discuss the accuracy of the available data and the degree to which the model reproduces these observations.

The aim of the effect-chain model (hydrodynamics, sediment transport, and water quality) is to determine changes in suspended sediment concentration and resulting changes in primary production, resulting from human impacts in the past and future (scenarios for improvement, phase 3 of the project), within the Ems Estuary. The main aim of the hydrodynamic model is to provide the hydrodynamic input for the effect-chain model. The most important hydrodynamic processes (see chapter 2) are

- Tidal propagation and changes in tidal propagation in the Ems Estuary and lower Ems River as a result of deepening
- Residual flows resulting from river discharge, wind and salinity, and changes therein as a result of deepening

For water quality, these processes can be translated into two hydrodynamic target variables, determining the suspended sediment and nutrient dynamics (and hence primary production):

- *Flow velocity*. The tidal dynamics determine the tide-induced resuspension of sediments and nutrients, which is most closely approximated by the current velocity.
- *Residual flow*. Advection of nutrients, algae, and slow-setting sediment particles is strongly influenced by residual flow patterns.

These variables are not measured directly. Waterlevels and salinity are available for a large number of stations, and flow velocity for two stations. Waterlevels are a good indicator for the tidal dynamics and therefore tide-induced flow velocity. The focus on waterlevel data-model

comparison was on tidal constituents, providing a quantitative comparison but also yielding physical understanding of the tidal dynamics. Within the estuary, the error in amplitude and phase of the tidal waterlevel constituents was typically within several percent; the error in the modelled flow velocity is typically 10%. Equilibrium sediment transport scales with the cubed flow velocity, and therefore an error of 10% in the flow velocity leads to an error of 33% in the sediment transport. However, in many estuaries, transport of fine sediment is not in local equilibrium with the flow velocity but often more strongly determined by sediment supply than by local flow velocities. The residual transport of fine sediment is then the result of horizontal and temporal asymmetries in the flow, and sinks and sources in the sea and estuary. An error in the flow velocity can therefore not be directly translated into an error estimate in the absolute sediment transport, even less for the residual sediment transport.

The asymmetry of the flow is evaluated for  $M_2$  and its main overtide  $M_4$ . The modelled asymmetry of the computed  $M_2/M_4$  constituents (defined as  $\theta_u = 2\phi_{u_{M_2}} - \phi_{u_{M_4}}$ ) differs  $19^\circ$  from the observed  $M_2/M_4$  asymmetry (equivalent to 5%). For residual transport, spatial variations in asymmetry may be more important than local asymmetries, but deeper into the estuary only waterlevel observations are available. The data-model comparison (Appendix A) indicates that within the Ems Estuary, the observed spatial variation in the main source of waterlevel asymmetry (determined by the phases of  $M_2$  and  $M_4$ ) is reproduced by the model. In the lower Ems River, the tidal propagation becomes less accurate, with errors of 10% of the observed waterlevel amplitude and phase. However, the WED model specially aims to reproduce hydrodynamics in the Ems Estuary, and less in the lower Ems River.

Residual flow is difficult to measure because it is strongly influenced by local conditions, and requires long and accurate observation periods. The long-term dispersion of tracers affected by residual flow, such as salt, can be a good indicator for evaluating the accuracy of the computed residual flow field. A complication with using the salinity to determine model accuracy is that some of the observations are probably erroneous (section 3.4.4). Some of the observations have unrealistically large values and differ strongly from nearby salinity observations. Throughout the estuary and the lower Ems River the computed intra-tidal variation corresponds qualitatively to observations, except near Emden. Salinity-driven residual flows will be elaborated in more detail in section 5.2 and in report 7.

### 3.8 Recommendations

The hydrodynamic model can be improved by increasing the resolution. An increase in the horizontal resolution will increase the accuracy of depth-uniform flows, especially in areas of variable topography. More vertical resolution will improve vertical circulation processes and more accurately resolve stratification. Such improvements lead to an increase in computational time, which makes them unpractical for long-term simulations (months-years) such as the current study.

The modelled salinity can be improved without modifying the resolution. The base of the current project was the KPP Ems-Dollard model, which was adapted for 2012 and 2013 and fresh water sources are more realistically implemented. As a result of better freshwater sources, the computed salinity better matches salinity observations compared to these previous studies. The remaining deviations between observed and computed salinity may be the result of

- Erroneous observations: especially MWTL observations have yielded suspicious results.
- Fresh water sources and seaward boundary conditions. Not all smaller fresh water sources, especially on the German side, are included in the model. However, given their

- small magnitude, these are probably insignificant. The fresh water source at Leda may be improved. In the model, the net discharge is prescribed as a fresh water source, instead of a tidally varying discharge with a tidally varying salinity. The largest uncertainty arises from the seaward side of the model. The salinity gradient from the Wadden Sea to the North Sea is large, and has a strong influence on the salinity in the outer estuary and probably also the inner estuary. This can only be improved by nesting salinity in a 3D North Sea model in which the salinity is better resolved. With MWTL measurements as boundary conditions, the modelled salinity cannot be substantially improved.
- Errors in horizontal and / or vertical mixing. The salinity gradients are determined by the salinity sources (above) in combination with vertical and horizontal mixing. Both horizontal and vertical mixing parameters may be improved if sufficient observational data is available. This requires complete timeseries of salinity covering the full year, at several locations in the estuary, and at multiple depths.

### 3.9 Summary

The TO-KPP hydrodynamic model for the Ems Estuary was modified, run for 2012 and 2013, and validated against a large number of salinity and waterlevel observations, and a limited number of flow velocity observations. For both years, the errors in tidal constituent water level amplitudes and phases of several percent. The error in the flow velocity is typically 10% (amplitude) or less (phase). Both the model and observations suggest that the dominant type of tidal asymmetry is High Water slack tide asymmetry (with a longer duration of HW slack compared to LW slack), generally leading to import of fine sediment. The absolute value and the intra-tidal variation in salinity typically differs 1-2 ppt from observations. The greatest mismatch is at Emden, where the computed salinity range is about half the observed range. Qualitatively, the spatial residual flow patterns are in line with observations. With the available data, the model seems sufficiently able to capture the essential flow dynamics (the (changes in) tidal dynamics and residual flow) in the Ems Estuary. The tidal propagation in the lower Ems River is not accurate, with errors in tidal amplitudes in excess of 10%.

A wave model has been set up using SWAN to compute the wave-induced bed shear stress (necessary for the sediment transport model developed in report 5). The model itself has not been calibrated, but a sensitivity analysis suggests limited effect of key input parameters on computed wave height and period.



## 4 Set up and calibration of the ER and ERD models

### 4.1 Introduction

The exchange of water and sediment between the Ems estuary and the Emden navigation channel (the approach channel to the port of Emden), as well as sediment dynamics within the navigation channel and the lower Ems River, are very complex. The sediment concentration in these areas is high, leading to complex and poorly understood sediment transport processes (e.g. Talke et al., 2009; Winterwerp, 2011). Important consequences of these high sediment concentrations are that (1) the apparent bed roughness is low, and (2) sediment contributes to the density of the water-sediment mixture, influencing turbulent mixing and thereby hydrodynamics and (3) non-Newtonian effects may play a role. The effect of sediment on turbulent mixing can be simulated with Delft3D sediment-online, but not with Delft3D WAQ, which is applied in the WED model. Moreover, the resolution of the WED model is too coarse to simulate the hydrodynamics and sediment dynamics in the Emden navigation channel and lower Ems River in great detail. Therefore a second model is set up, which is smaller compared to the WED model, but better aligned and more refined in the navigation channel and Ems River, the Ems River Dollard model (ERD). The set up and calibration of this model is described in section 4.2.

During the calibration of the sediment transport model, it proved difficult to model the sediment dynamics in the Ems River with the ERD model, because the long morphological time scales (required for the Dollard area) conflicted with the long simulation times needed for Delft3D sediment-online. Therefore a variant of the ERD was developed, from which the Ems estuary and the Dollard basin was stripped (the Ems River or ER model). The set up and calibration of this model is described in section 4.3.

### 4.2 Set up and calibration of the ERD model

#### 4.2.1 Numerical grid and bathymetry

The numerical grid of the resulting ERD model has a higher resolution in the lower Ems River and near Knock than the WED model (down to 20 m instead of 200 m). Also, the grid is better aligned with the depth contours, especially within the lower Ems River. To compensate for the higher resolution, while maintaining reasonable computational times, the model domain has been made smaller. The sea-side boundary is now located in the Wadden Sea near the Eemshaven (Figure 4.1), for the following reasons:

- The boundary needs to be seaward of the Hond-Paap Island to simulate the distribution of flow through the two adjacent tidal channels (the Bocht van Watum west of Hond-Paap island and the Friesche Gaatje east of Hond-Paap island).
- Waterlevel observations at Eemshaven can be used to directly force the model.
- The boundary is sufficiently far away from the entrance of the lower Ems River and the Dollard basin.

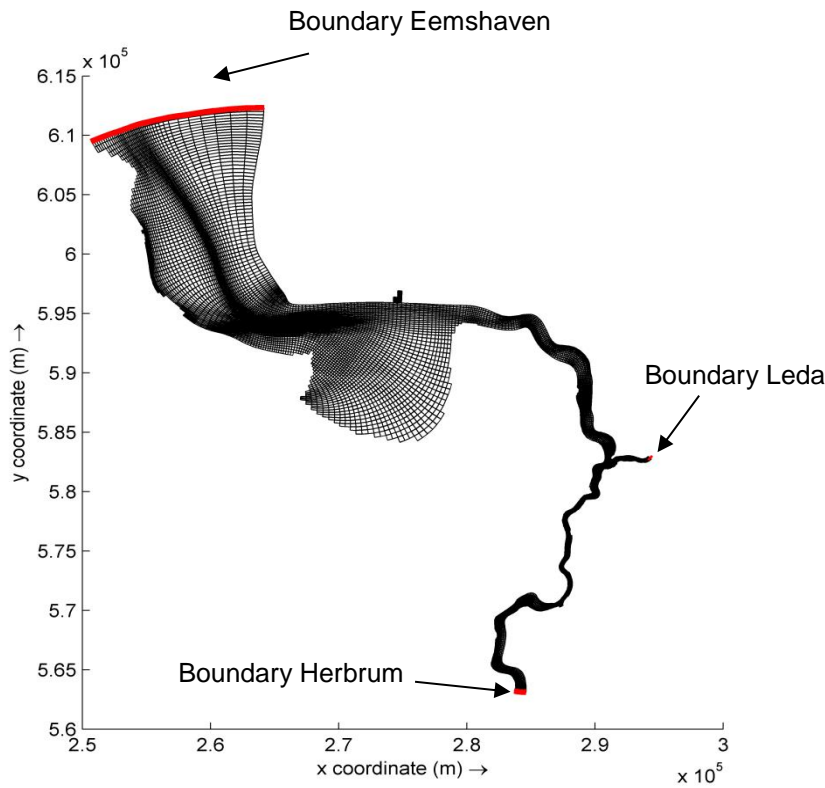


Figure 4.1 Overview of the computational domain of the ERD model, the model grid and the location of the boundaries.

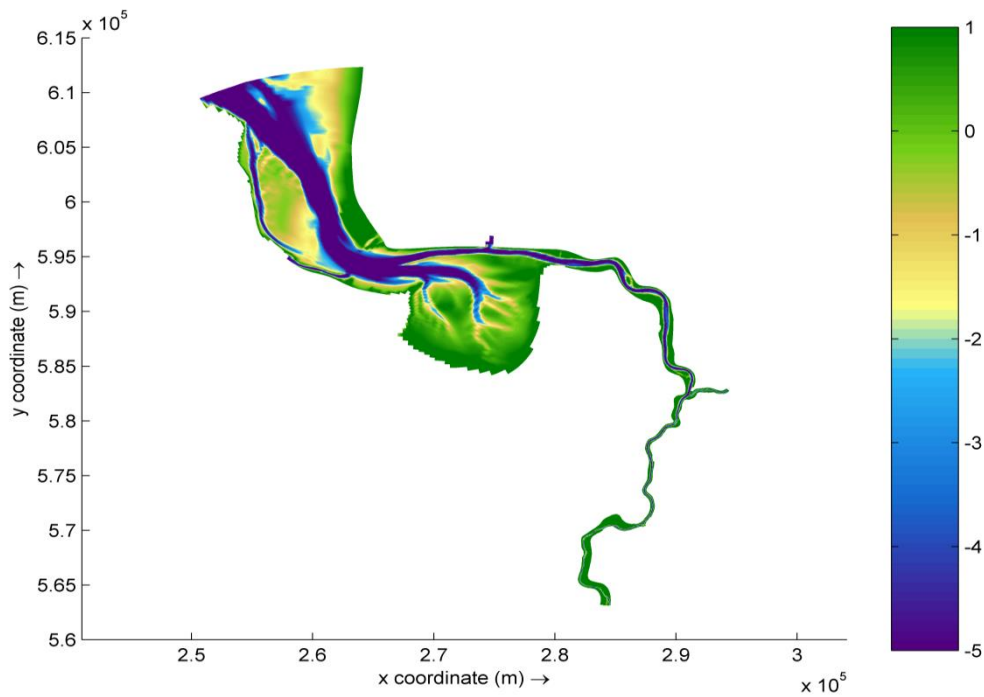


Figure 4.2 Initial bed level of the ERD model, based on 2005 soundings. Data from Rijkswaterstaat vaklodingen and WSA Emden (Ems River).

The upstream boundaries are set at the same locations of the WED model: Leer/Leda and Weir Herbrum. The total number of computational grid cells is about half (13553 cells) of the WED model grid (26246 cells). In the Dollard Estuary, the computational grid was extended to allow simulation of the situation before the large-scale land reclamations in the past centuries (see report 3). For the calibration of the present situation, the area landward of the dikes has been filled up with dry points. The bathymetry of the model is taken from 2005 high resolution soundings<sup>5</sup> from Rijkswaterstaat and Wasser- und Schifffahrtsamt (WSA) Emden. All data was interpolated to the computational grid with Delft3D Quickin software, see Figure 4.2. The model is used in depth-averaged (2D) mode to calibrate the tidal propagation, and in 3D mode (using 10 vertical equidistant sigma layers) to simulate salinity-driven flows.

#### 4.2.2 Boundary conditions

The model is set up and run for the year 2005, because for this year a bathymetry was available, flow velocities were measured (at Knock), and high-resolution sediment concentration data was available. The model is forced at the seaward boundary with waterlevels observed at Eemshaven (taken from the Waterbase database<sup>6</sup>) to calibrate against observed waterlevels and flow velocities at various locations throughout the time domain (see Table 4.2).

Table 4.1 Main processes and parameter settings of the adapted hydrodynamic ER and ERD model.

Parameter	
Timestep (s)	30 seconds
Vertical layers	10 vertical $\sigma$ -layers (equidistant).
Horizontal viscosity	Uniform ( $1 \text{ m}^2/\text{s}$ )
Vertical mixing	k- $\epsilon$ turbulence model (with background viscosity of $1 \cdot 10^{-5} \text{ m}^2/\text{s}$ )
Bed roughness	Manning's $n$ , spatially varying (ERD, Figure 4.7) or constant (ER, 0.01 – see calibration figures Figure 4.14 to Figure 4.17)
Offshore Boundary conditions	Waterlevels (observed) and salinity (modified continues timeseries)
Discharges	Discharges (from NLWKN) with 0.2 ppt.
Wind	no

At the two upstream boundaries (Leer/Leda and Weir Herbrum), freshwater discharges ( $\text{m}^3/\text{s}$ ) are prescribed (see Figure 4.3 and Figure 4.4). Discharge data have been obtained from the German Niedersächsischer Landesbetrieb für Wasserwirtschaft, Küsten- und Naturschutz (NLWKN). At Weir Herbrum, daily discharge data from Verssen is used, whereas at Leer/Leda 15 min data is used. The discharge at Verssen is typically 2 to 5 times higher than at Leer/Leda, and also more seasonally varying. Additionally, discharges were added in Delfzijl and in Nieuwe Statenzijl using discharge points.

<sup>5</sup>Available on Open Earth: <http://opendap.deltares.nl/opendap/rijkswaterstaat/vaklodingen/contents.html>.

<sup>6</sup>Accessible via Open Earth: [http://opendap.deltares.nl/opendap/rijkswaterstaat/waterbase/sea\\_surface\\_height/id1-EEMSHVN.nc.html](http://opendap.deltares.nl/opendap/rijkswaterstaat/waterbase/sea_surface_height/id1-EEMSHVN.nc.html) and Waterbase: [live.waterbase.nl](http://live.waterbase.nl).



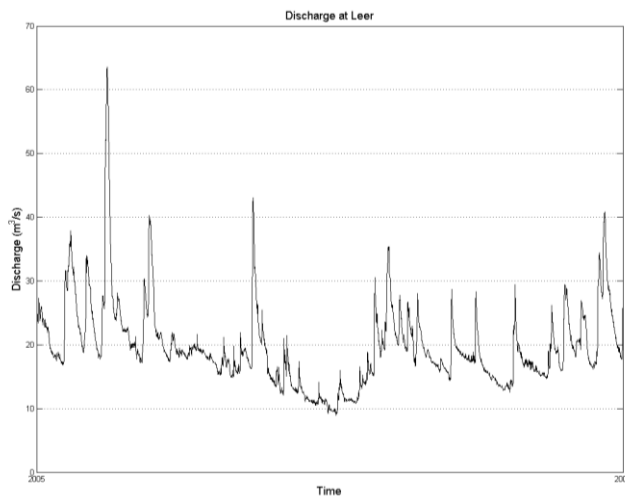


Figure 4.3 Discharge ( $m^3/s$ ) at the model boundary Leer Leda, obtained from NLWKN.

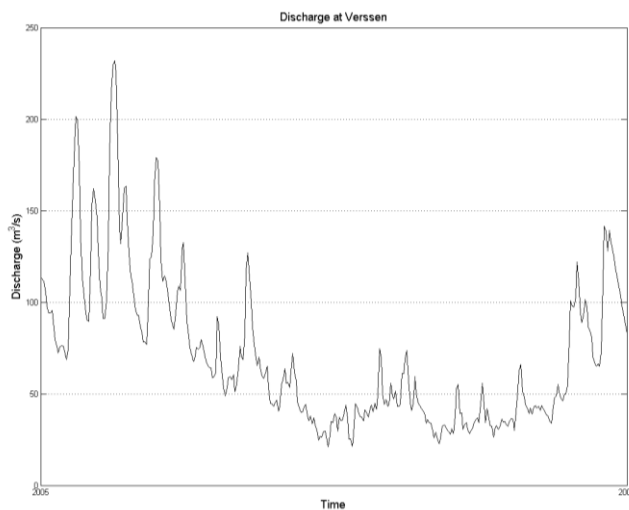


Figure 4.4 Discharge ( $m^3/s$ ) at the model boundary Weir Herbrum, obtained from NLWKN.

The salinity is specified at the model boundary near Eemshaven. There is no time series available of the salinity at that location, and therefore we use the salinity observed at Knock (data obtained from NLWKN). Since this station is located further landward, the salinity is lower, and needs to be corrected. For this purpose the salinity gradient computed with the WED model is used (not the absolute values from the WED model). The computed salinity difference between the ERD boundary and Knock is linearly related to the absolute salinity value at Knock, see Figure 4.5. This relation is used to convert observed salinity values at Knock to estimated salinities at the location of the ERD model, as in:

$$S_{bound} = 0.2422 S_{Knock} + 23.415$$

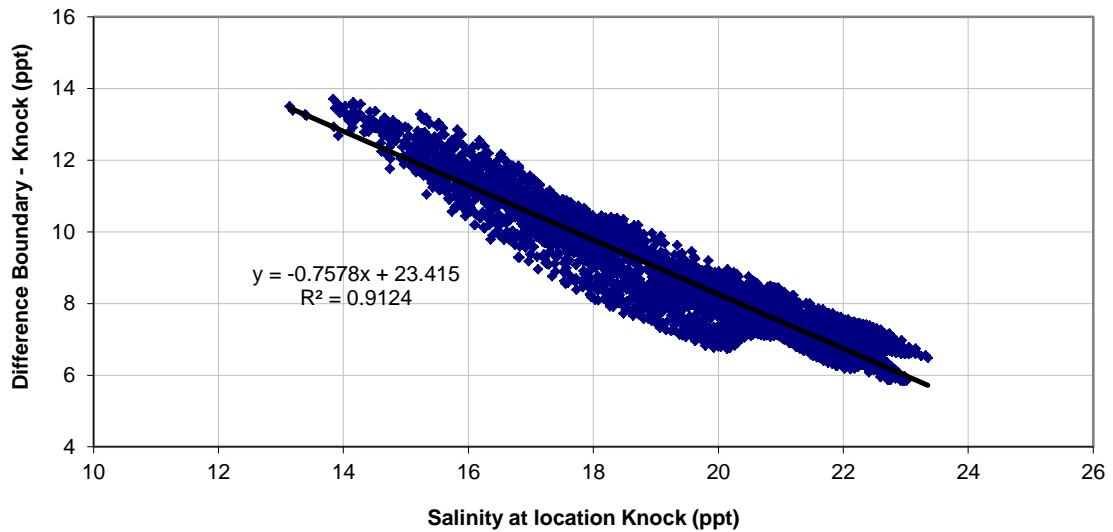


Figure 4.5 Computed salinity difference ERD model boundary – Knock (from the WED model), as a function of the observed salinity at Knock.

The salinity at all discharge boundaries (Herbrum and Leer/Leda) was initially set at 0 ppt (during calibration changed to 0.2 ppt).

#### 4.2.3 Miscellaneous

The model includes several other features such as:

##### Thin dams

Thin dams are located around the port of Delfzijl and near the Ems Sperrwerk at Gandersum. During the first model runs, the Geisedam was also included as a thin dam, which means it cannot be flooded. During the model set up, data of the crest level of the Geisedam were received from dr. Weilbeer (Bundesanstalt für Wasserbau, BAW). With this information, the dam was included as a 2D weir with crest levels of about 0.4 – 1.1 m above reference level. In the 3D models, the Geisedam was included as a local weir, requiring a slightly different numerical implementation.

##### Observation points

Several observation points were included in the model. Names and locations correspond to the original points from the WED model. Figure 4.6 shows all observation locations. At those stations, model results were stored with a time interval of 10 min.

##### Numerical parameters

The values for horizontal viscosity ( $1 \text{ m}^2/\text{s}$  in the 2D and 3D) and diffusivity ( $10 \text{ m}^2/\text{s}$  in the 2D model,  $1 \text{ m}^2/\text{s}$  in the 3D model) are typical for a Delft3D hydrodynamic model with grid dimensions as the ERD model. Vertical mixing is computed using the k- $\epsilon$  model, for which a background viscosity is prescribed which is varied in the sensitivity analyses.

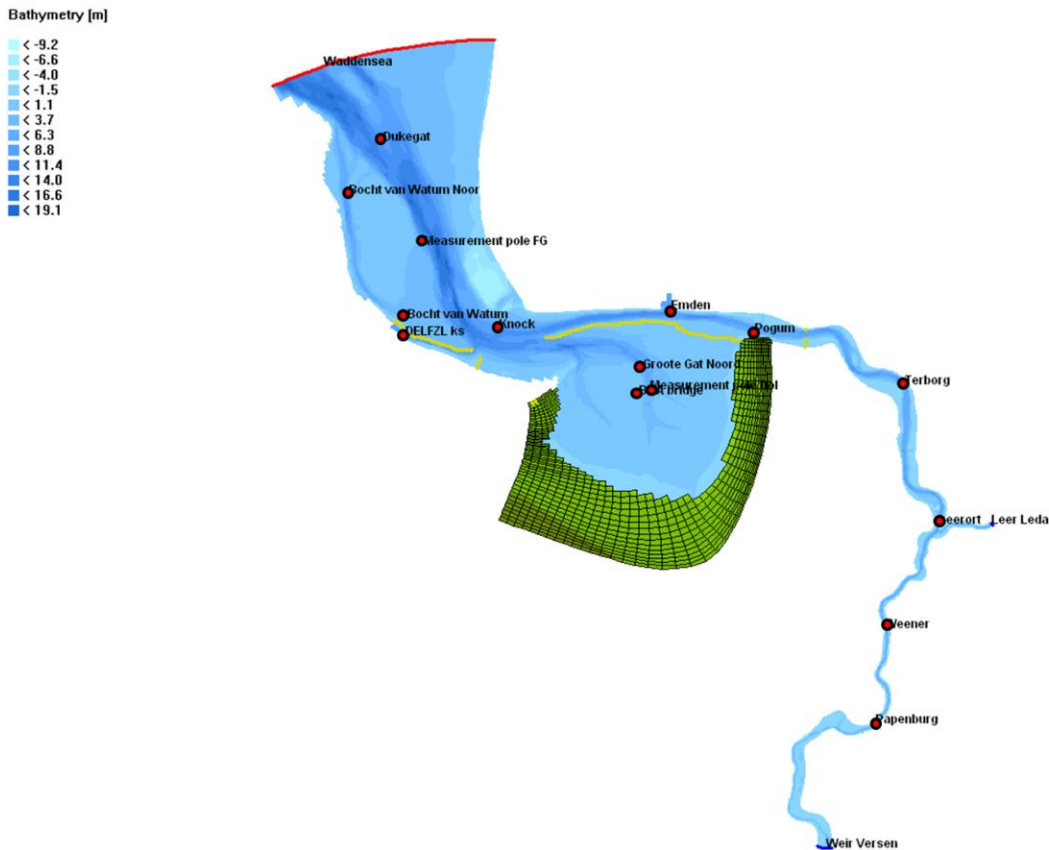


Figure 4.6 Location of the observation points (red points), dry points (green cells) and thin dams (yellow lines) in the model.

#### 4.2.4 Calibration

The model is calibrated in two steps. First, the model is calibrated in depth-averaged (2D) mode against waterlevels. Waterlevels are marginally influenced by 3D hydrodynamic processes, and therefore 2D modelling is a fast and flexible method for calibration. Simulating salinity and a vertically varying flow velocity requires a 3D model. Therefore in a second step, the model is switched to 3D, and calibrated against salinity and flow velocity.

##### 4.2.4.1 Waterlevels (2D)

The first step in the model calibration was to run the model in 2D mode. The aim of this part of the calibration is to check the model performance against waterlevel measurements at all available waterlevel stations (see Table 4.2), by changing parameters as listed in Table 4.3. After the 2D calibration, the model was extended to 3D, using 10 equidistant  $\sigma$ -layers. Although ten  $\sigma$ -layers may be sufficient for the hydrodynamic model, it is a low resolution in the lower Ems River where consolidation processes and resulting fluid mud deposits are important. This will be elaborated in Report 5. The model performance in the 3D mode was validated with available data: one flow velocity measurement at station Knock and salinity measurements at the stations given in Table 4.2.

The main calibration parameter for the 2D model is the bed roughness. The roughness is modelled with a Manning - Chézy relation, in which the Chézy roughness value is computed from a user-defined Manning's  $n$  value. A typical value for sand-bed dominated systems is a Manning's  $n = 0.02$ , and therefore this value was uniformly applied for the initial run (Cal01).

Although model results are reasonable in the Ems estuary, waterlevels in the lower Ems River are poorly reproduced: see Appendix C. This is in line with expectations: in 2005 extensive fluid mud deposits are present in the lower Ems River, resulting in low hydraulic drag, and therefore requiring lower Manning's  $n$  values typical for mud-dominated, smooth systems:  $n = 0.01 - 0.012$ .

Table 4.2 Calibration and validation stations

Station	Waterlevel	Salinity	Velocity
Dukegat	X		
Knock	X	X	X
Pogum	X	X	
Terborg	X	X	
Leerort	X	X	
Weener	X		
Papenburg	X		

Table 4.3 Model calibration runs

Run id	dt	Roughness	Depth	Geisedam	Other options
Cal01	1 min	uniform $n = 0.02$	2005	Thin Dam	
Cal09*	1 min	From WED model	2005	Weir	Including salinity
Cal14*	1 min	From WED model	smoothed	Weir	Including salinity
Cal16	1 min	Ems $n = 0.01$	smoothed	Corrected weir*	Including salinity

\* in Cal09-Cal14 the weir was incorrectly implemented

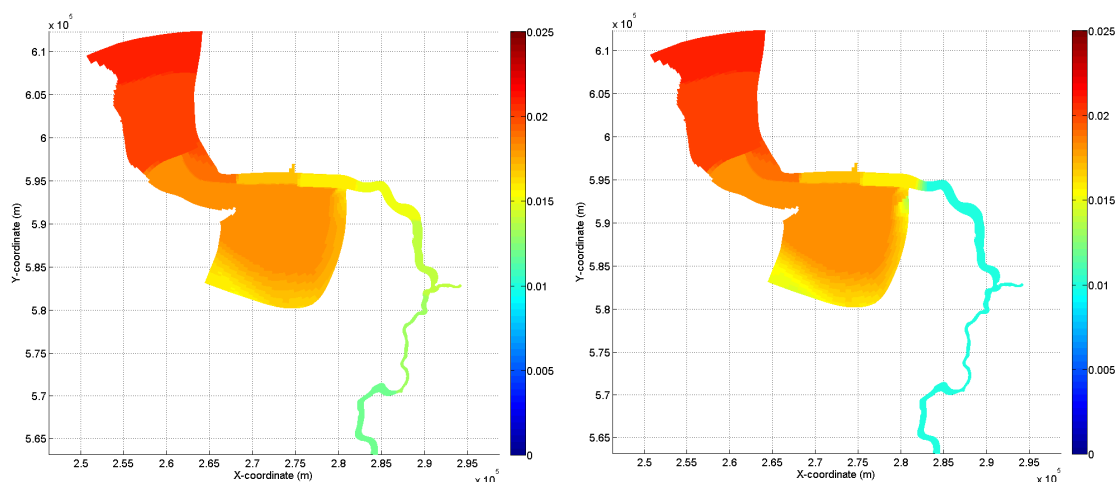


Figure 4.7 Manning's roughness in the original WED model copied to the ERD model (left) and modified roughness in the ERD model (right)

For a uniform bed roughness the  $M_2$  tidal constituent is 30% too low at the most upstream station (Papenburg); see cal01 in Appendix C.7. In order to represent the effects of fluid mud in the lower Ems River through a low bed roughness, a spatially varying Manning's  $n$  was used. Initially the spatially varying Manning's  $n$  from the original WED model (left panel in Figure 4.7) was used. This greatly improves the computed waterlevels in the upstream stations (compare Cal09 with Cal01), especially for the amplitude of  $M_2$  (Appendix C.5 – C.7) and the high waterlevels (Appendix D). Low waterlevels are still poorly reproduced (Appendix D) because the channel became too shallow using triangular interpolation techniques. The

channel depth was therefore corrected for these interpolation errors (Cal14 in Appendix D). A further reduction of the roughness in the Ems estuary (Cal 16; with a spatially roughness as given in the right panel of Figure 4.7) improved the predicted waterlevels in the lower Ems River and the Ems Estuary (see also Figure 4.8 and Figure 4.9), especially downstream of Weener. The phase and amplitude of M2 are well reproduced, but the higher harmonics at Weener and at Papenburg (M4, M6) can still be improved. However, the tidal propagation in these areas is probably strongly influenced by sediment-induced friction effects which vary seasonally, fortnightly and tidally, which cannot be captured with a 2D hydrodynamic model. Therefore the model is subsequently switched to 3D mode.

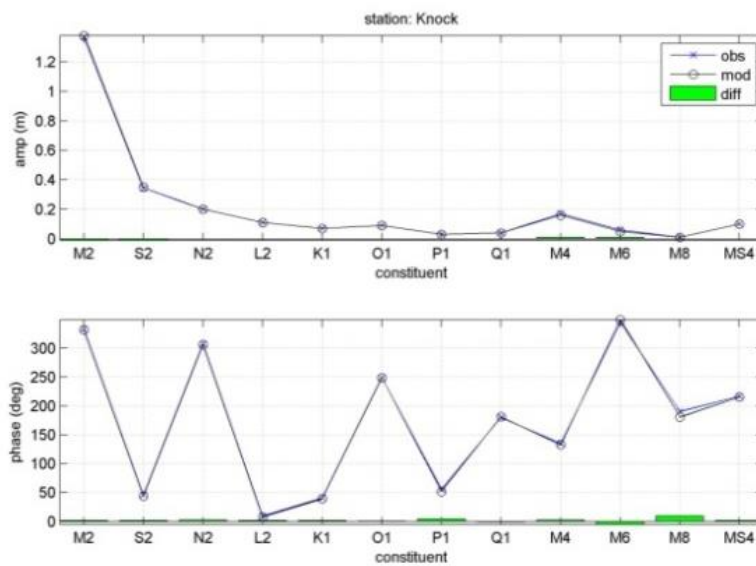


Figure 4.8 Observed and computed main tidal constituents at Knock (near the entrance of the lower Ems River), final calibration settings of the 2D model

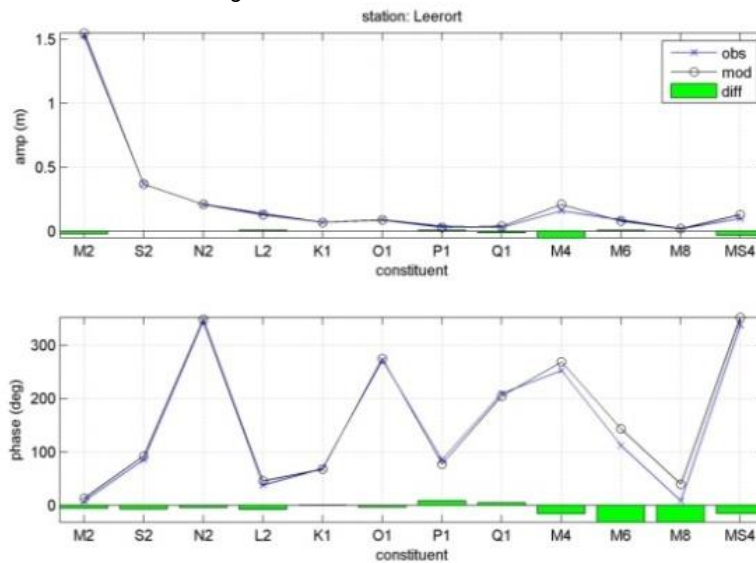


Figure 4.9 Observed and computed main tidal constituents at Leerort, final calibration settings of the 2D model

Table 4.4 Calibration parameters of the 3D ERD model

Run id	dt	salinity	Eddy diffusivity [m <sup>2</sup> /s]
Cal163D	1 min	From 2D model	Horizontal: 10 Vertical: 0
Cal193D	0.5 min	Eemshaven -2ppt, discharge 0.2ppt	Horizontal: 1 Vertical: 1 10 <sup>-4</sup>
Cal203D	0.5 min	Eemshaven -2ppt, discharge 0.2ppt	Horizontal: 1 Vertical: 1 10 <sup>-5</sup>
Cal213D	0.5 min	Eemshaven -2ppt, discharge 0.2ppt	Horizontal: 1 Vertical: 0

#### 4.2.4.2 Flow velocity and salinity (3D)

The tidal intrusion computed with the 3D model was too low using the default eddy diffusion (10 m<sup>2</sup>/s; Cal163d). This was greatly improved using an eddy diffusion of 1 m<sup>2</sup>/s (a typical value for 3D models, see simulation Cal193d in Appendix E). In Cal193D, the salinity was also modified. Since the overall salinity in the model is too large, the salinity at the seaward boundary at Eemshaven was reduced with 2 ppt. In the lower Ems River, the lowest measured salinity was 0.2 ppt, and therefore the salinity of the lower Ems River and Leda River was also set to 0.2 ppt. Both the lower eddy diffusivity and the modified salinity significantly improved the computed salinity (compare simulation Cal163d with Cal193d in Figure 4.10). Modifications to vertical mixing parameters (the vertical eddy diffusivity) do not significantly influence the computed salinity (see Figure 4.10 and Appendix E; simulations cal193d, cal203d, and cal213d mostly overlap). At locations Knock and Terborg, the computed salinity differs less than 2 ppt (see appendix E): differences mainly occur at the end of flood. In-between, at station Pogum the salinity is 2-5 ppt overestimated by the model, it is not clear why this station is so poorly reproduced. At Leerort, the computed intra-tidal variation in salinity is larger than in the observations.

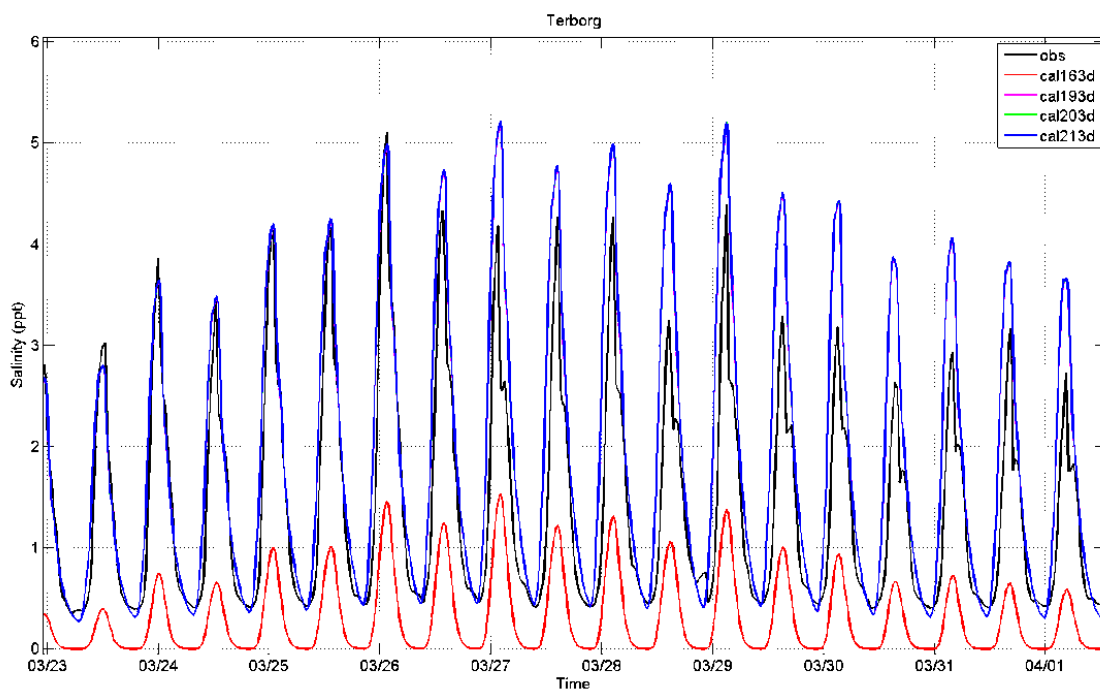


Figure 4.10 Measured (black) and computed salinity at Terborg, March 2005. Salinity of cal193d and cal203d are poorly visibly since they overlap with cal213d.

The results of the 3D model were also calibrated against flow velocity measured 1.60 m below the water surface at Knock (point measurement only). The largest differences between the 2D and the 3D simulation occur during ebb flow (flow direction around 280 degrees). The peak flow velocities are larger in the 3D model than in the 2D model and the 3D results are in better agreement with observations (Figure 4.12). Velocity peaks are also higher during flood flow, but this is less pronounced. During flood flow, with lower flow velocities and directions around 105 degrees, the model simulates the current velocities better than during ebb tide (for both spring tide, Figure 4.11 and neap tide, Figure 4.12). The ebb tide currents are substantially underestimated during spring tide ebb conditions (underestimating the flow velocity with 0.2 to 0.4 m/s).

Maximum flow asymmetry can be generated by residual flow or by tidal asymmetry. Residual flow generates flow asymmetry where velocities are high during the longest tidal phase (ebb or flood). In case of tidal asymmetry, the period (ebb or flood) during which the flow velocity is largest, is shorter than the period with smaller flow velocity. An important observation is that the period with maximum flow velocity (ebb) is longer in duration than the period with lower flow velocity (flood). This means that the flow asymmetry is generated by residual flow. An asymmetry as pronounced as in Figure 4.11 cannot be caused by river flow because the river discharge is much smaller than the tidal discharge. Therefore the residual flow in the ebb direction must be caused by topographic effects (e.g. blockage of the flood current, large-scale eddies). Such topographic effects are local and are therefore (1) not modelled with sufficient detail but (2) also not representative for the whole cross-section.

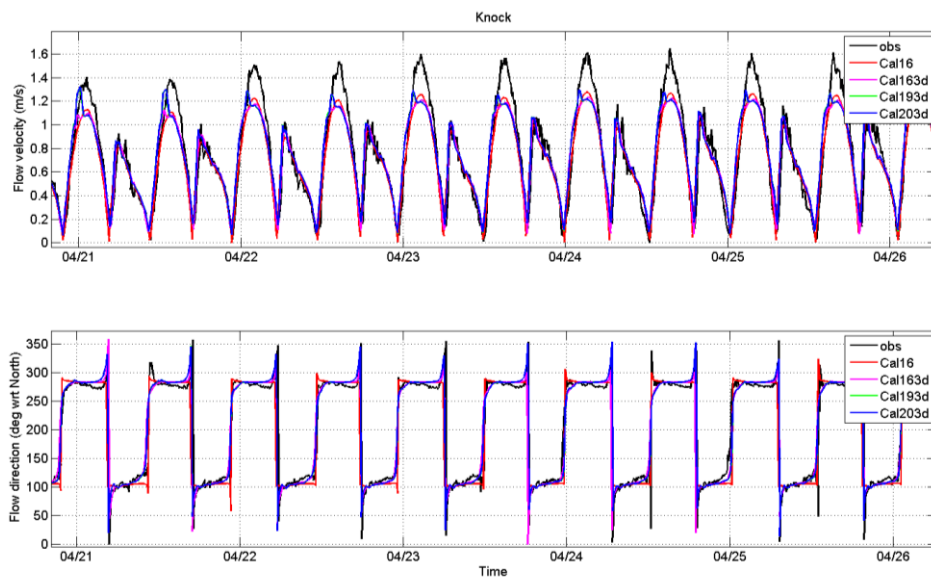


Figure 4.11 Measured and computed flow velocity at Knock, spring tide. Results of Cal193D (green) are nearly identical to Cal203d (blue) and therefore cannot be distinguished.



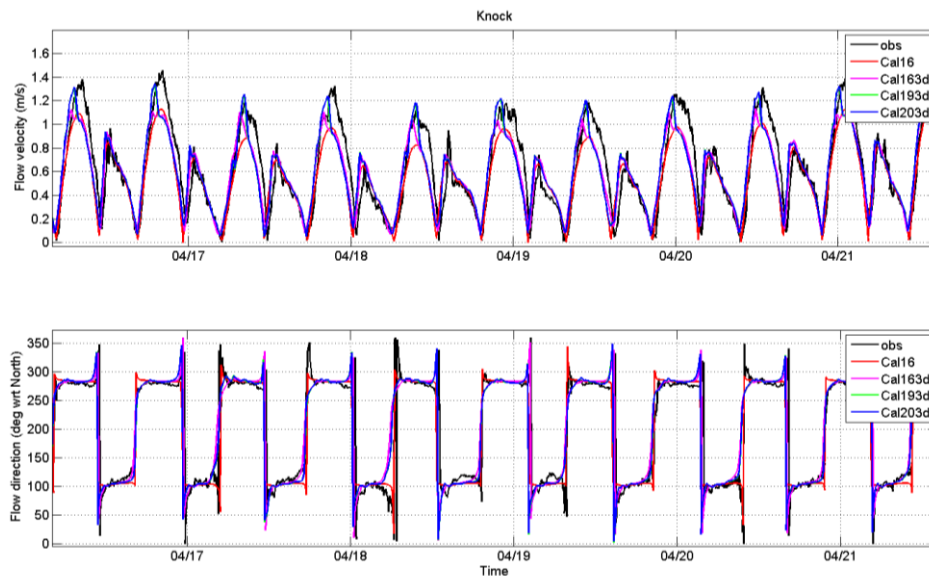


Figure 4.12 Measured and computed flow velocity at Knock, neap tide. Results of Cal193D (green) are nearly identical to Cal203d (blue) and therefore cannot be distinguished.

The background value for the vertical eddy viscosity (see Table 4.4) has no significant effect on computed flow velocity (Figure 4.11 and Figure 4.12) and salinity (Figure 4.10). As a result, there is no obvious preferred best-performing model simulation. The background eddy viscosity used in Cal203d ( $1 \cdot 10^{-5} \text{ m}^2/\text{s}$ ) is most frequently used in Delft3D applications, and therefore used as default value here as well.

### 4.3 Set up and calibration of the ER model

The ER model covers the lower Ems River (up to Herbrum) and the Emden navigation channel (Figure 4.13). This model domain has several advantages (each of similar importance) compared to the ERD model, especially for the additional set up of a sediment transport module:

- The seaward boundary of the ER model is located at Knock, where long-term monitoring of waterlevel, salinity and suspended sediment is available. This allows an easier and more realistic model forcing, especially for suspended sediment, compared to the ERD model.
- The ER model domain is smaller, and therefore computationally faster compared to the ERD model.
- The morphologic timescales involved for the Dollard are large (multiple years to attain dynamic equilibrium). The ER model, without the Dollard, is faster but therefore also reaches equilibrium earlier. Even more, different sediment transport processes are responsible for the dynamic equilibrium in the Dollard than in the Ems River. Excluding the Dollard allows a better focus on the processes relevant for the Ems River.

The model is forced at the open boundary by waterlevels and salinity observed at Knock, and at the landward boundary by discharges at the weir Herbrum and at Leer-Leda (Figure 4.3 and Figure 4.4). The bed roughness is low, because the model covers dominantly the high-concentration (and therefore hydraulically smooth) reaches of the estuary. Since almost the whole model domain is probably hydraulically smooth, a uniform bed roughness is applied. Numerical settings are the same as the 3D version of the ERD model (see section 4.2, Table 4.2).



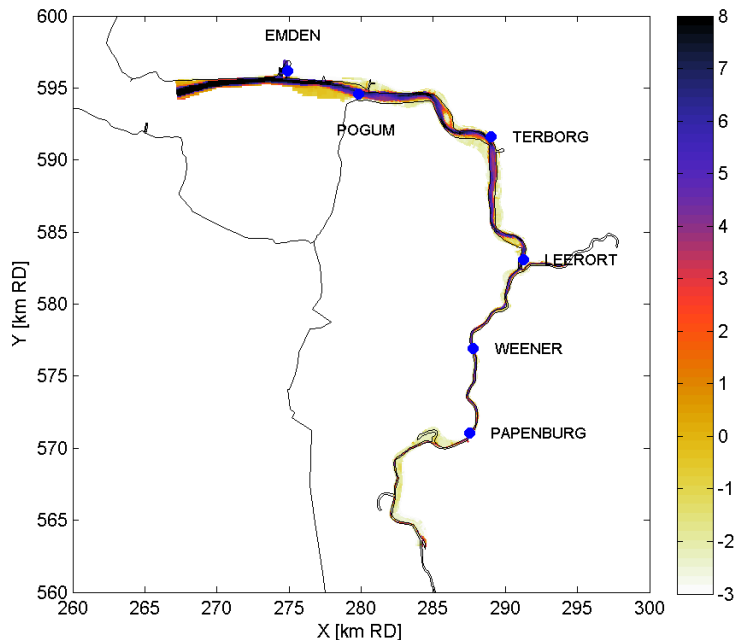


Figure 4.13 Initial bed level of the model, based on 2005 soundings, and observation stations.

The model is calibrated against waterlevels in a similar way as the ERD model, by varying the hydraulic roughness and comparing computed and observed tidally analysed waterlevels. The hydraulic roughness is varied by varying the Manning's  $n$  between 0.01 and 0.02. A value of 0.02 is a value typical for sand-dominated systems, whereas a value of 0.01 indicates a very smooth bed (typically the lower limit of Manning's  $n$  values observed in nature). The performance of the ER model is similar to the ERD model: the computed waterlevel amplitude and phase of the main tidal constituents is close to the observations (Figure 4.14 and Figure 4.15). Deeper into the lower Ems River the accuracy decreases, notably of the shallow water constituents (M4, M6, MS6).

Of particular importance for estuarine sediment dynamics is the behaviour of the main astronomical tide  $M_2$  and its overtide  $M_4$ . The propagation speed of the tidal wave is accurately reproduced throughout the lower Ems River using a Manning's roughness of  $0.01 \text{ m/s}^{1/3}$ , demonstrated by the phase angle  $\phi$  of  $M_2$  (Figure 4.16) and  $M_4$  (Figure 4.17). The computed amplitude of  $M_2$  peaks at Leerort, decreasing up-estuary, whereas the observed  $M_2$  amplitude peaks at Papenburg. This suggests that the friction is still too large, especially deeper into the lower Ems River. Decreasing the friction throughout the river would overestimate the  $M_2$  amplitudes everywhere in the model domain. Moreover, with  $n = 0.01 \text{ m/s}^{1/3}$ ,  $M_4$  is already overestimated;  $n = 0.015 \text{ m/s}^{1/3}$  would be more appropriate for the  $M_4$  amplitude. However, the overall tidal dynamics seem to be best reproduced using  $n = 0.01 \text{ m/s}^{1/3}$ .

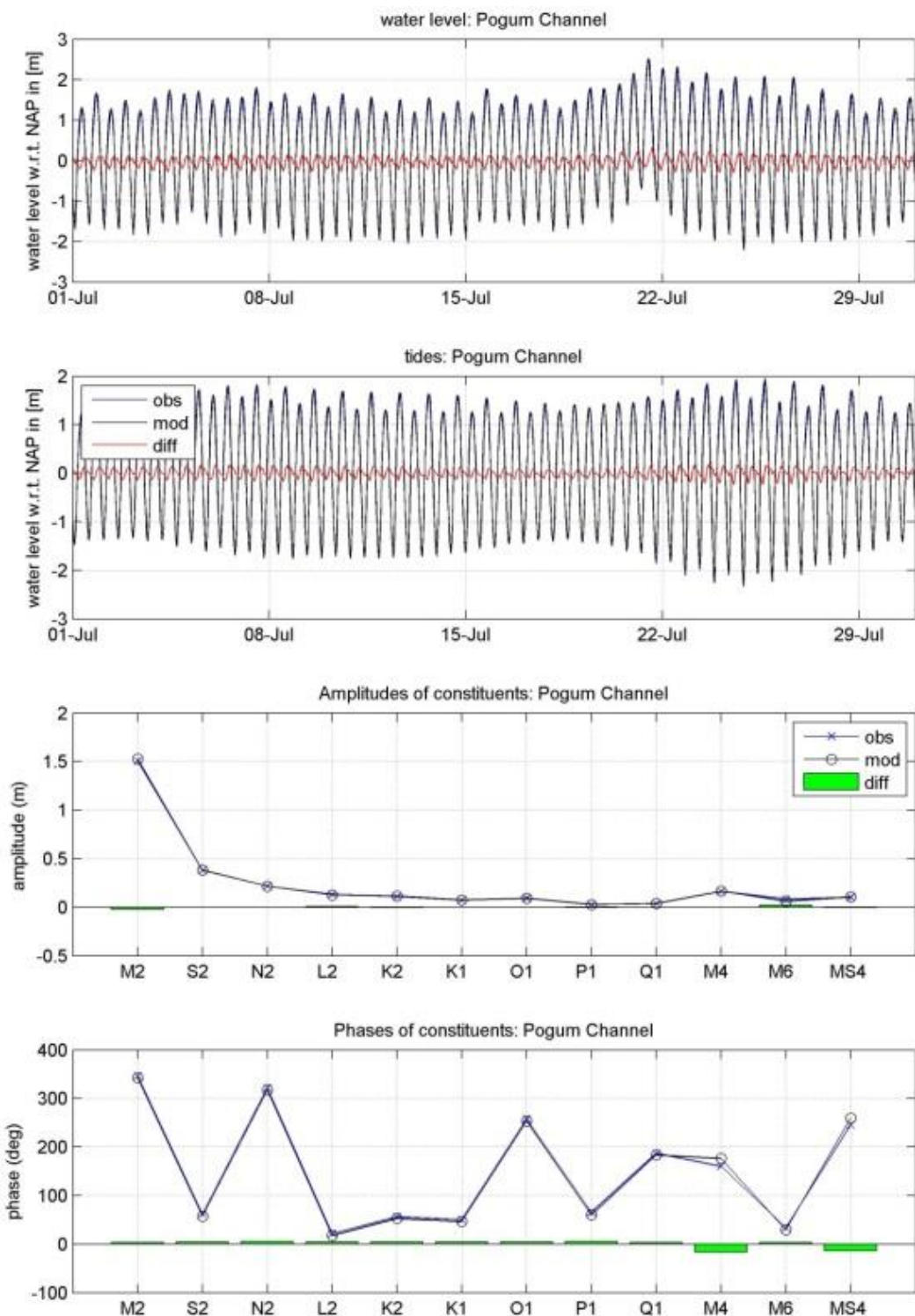


Figure 4.14 Computed (blue) and observed (black) waterlevel (top panel: total, second panel, tide-only; both in July during a low river discharge), harmonic amplitudes (third panel) and phases for Pogum;  $n = 0.01 \text{ m/s}^{1/3}$ . The observed and computed values are difficult to distinguish because of overlap.

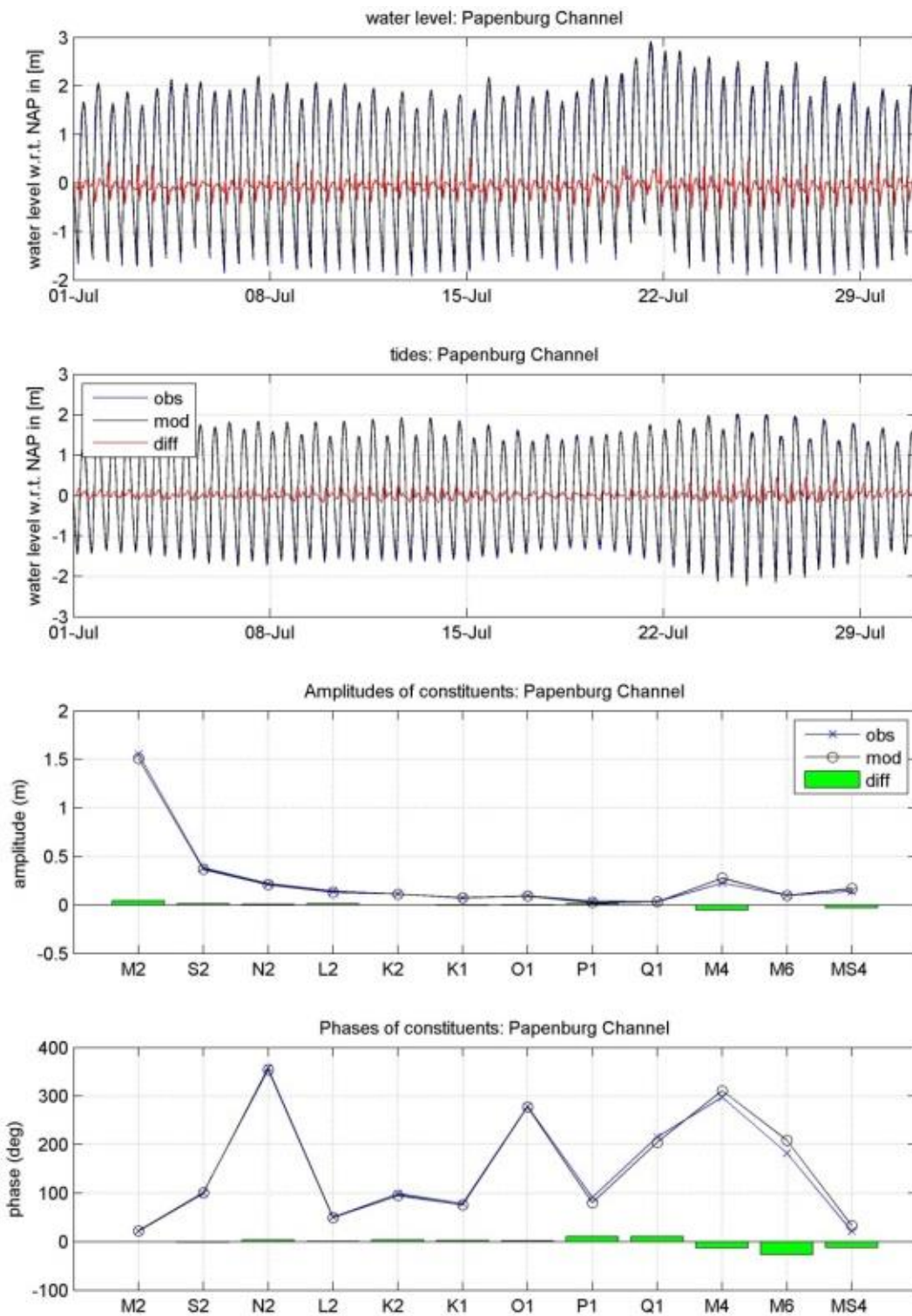


Figure 4.15 Computed (blue) and observed (black) waterlevel (top panel: total, second panel, tide-only; both in July during a low river discharge), harmonic amplitudes (third panel) and phases for Papenburg;  $n = 0.01 \text{ m/s}^{1/3}$ . The observed and computed values are difficult to distinguish because of overlap.

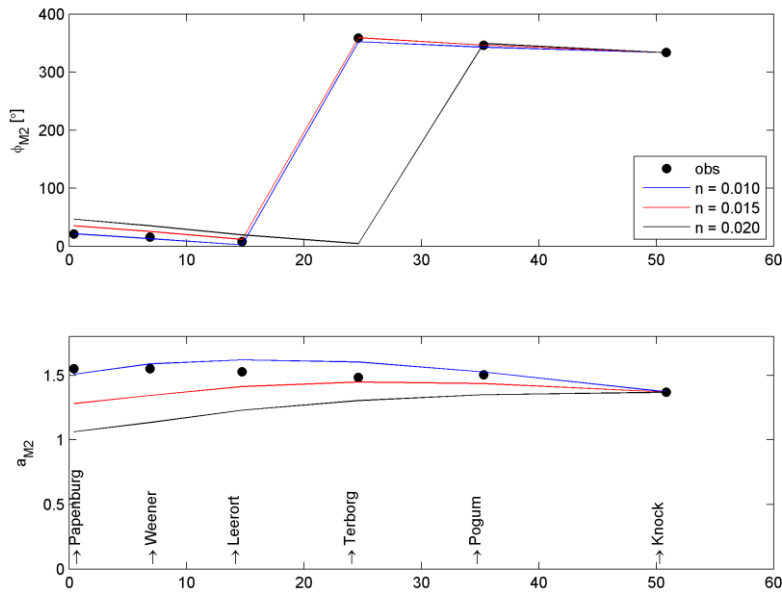


Figure 4.16 Observed (black dots) phase (top panel) and amplitude (lower panel) of  $M_2$  throughout the lower Ems River using Manning coefficient of 0.01, 0.015, and 0.02  $m/s^{1/3}$

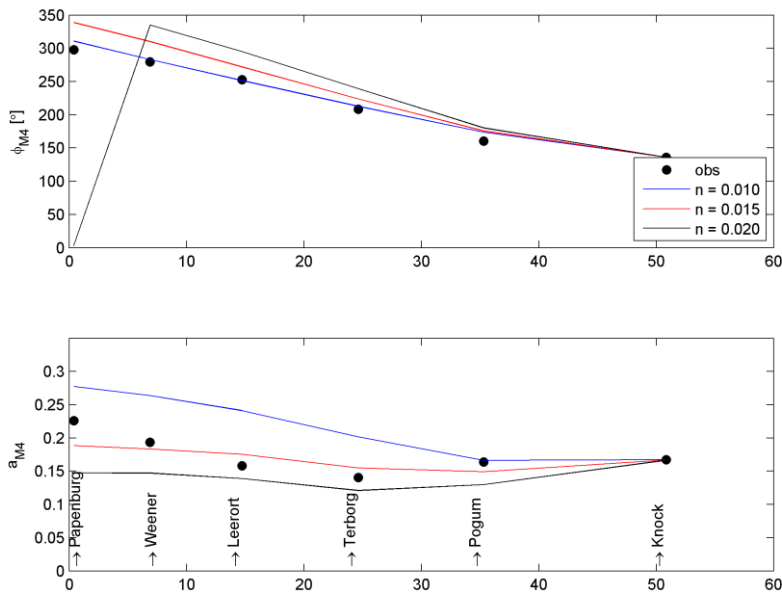


Figure 4.17 Observed (black dots) phase (top panel) and amplitude (lower panel) of  $M_4$  throughout the lower Ems River using Manning coefficient of 0.01, 0.015, and 0.02  $m/s^{1/3}$

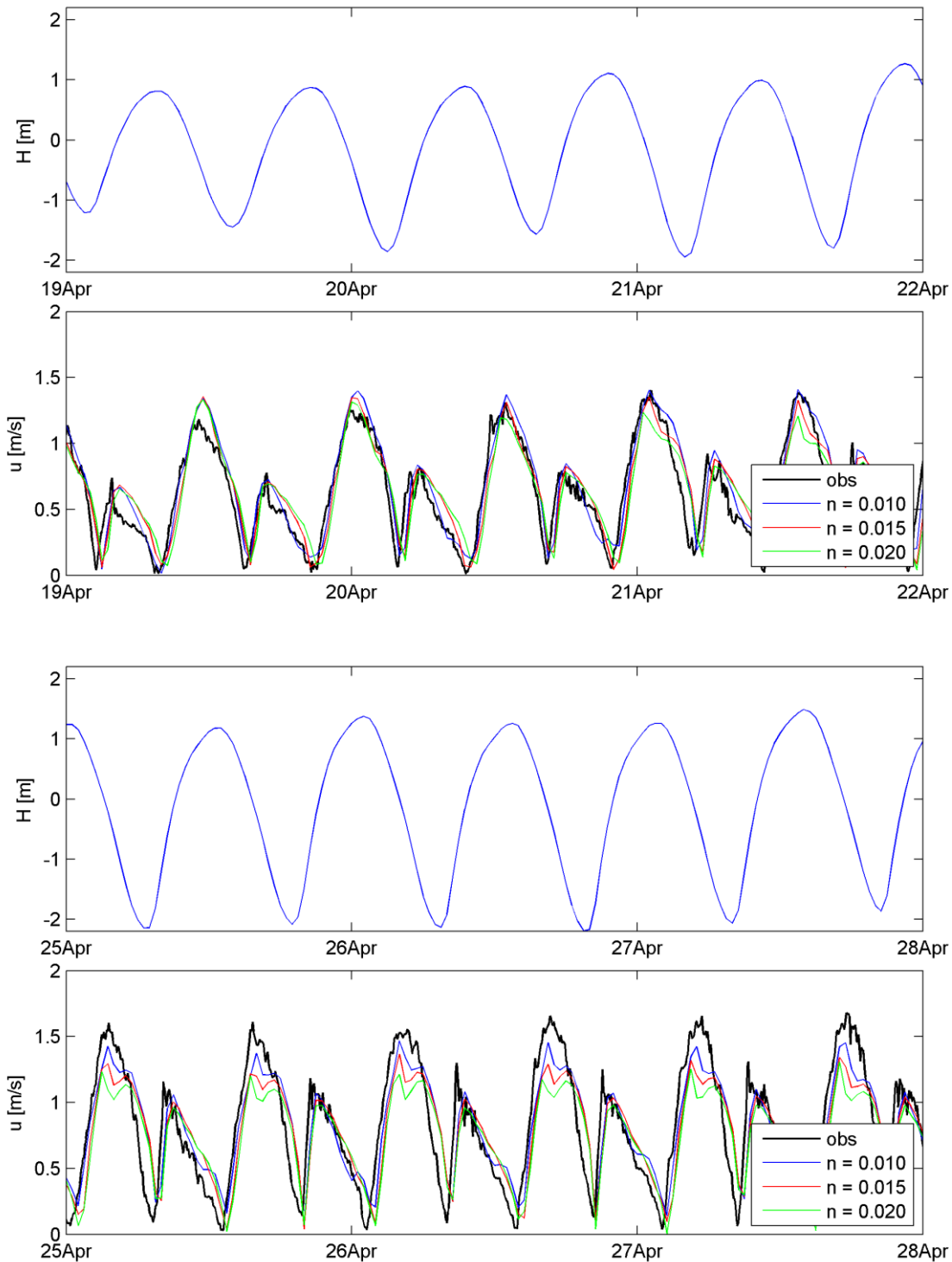


Figure 4.18 Waterlevel and flow velocity at Knock during neap tide (19-22 April) and spring tide (25-28 April). The flow velocity is given for observations (black) and model results using a Manning coefficient of 0.01 (blue), 0.015 (red), and 0.02 (green)  $m/s^{1/3}$ .

Computed flow velocities are compared with flow velocities observed at Knock (Figure 4.18). At this station, the flow seems ebb-dominant, probably resulting from a residual flow

component (resulting in a tidal phase with both a longer duration and flow velocity magnitude, see the previous section on the ERD model). This flow asymmetry is well reproduced by the model during neap; during spring tide the ebb flow velocity is underestimated. This is probably the result of topographic effects on a smaller scale than resolved by the model, and the observation is not representative for the whole cross-section. The underestimation of the ebb currents is lowest with  $n = 0.01 \text{ m/s}^{1/3}$ . Also the neap tide currents are better reproduced using  $n = 0.01 \text{ m/s}^{1/3}$ .

Conclusively, the observed waterlevels in the Ems River are best reproduced using a bed roughness corresponding to hydraulically smooth conditions, in line with expectations. The phases and amplitudes of most individual harmonic constituents are reproduced within 5% from observations as far upstream as Papenburg, with along-river patterns in corresponding to observations. Only the M4 tide is overestimated using a hydraulic roughness as low as  $n = 0.01 \text{ m/s}^{1/3}$ : for M4  $n = 0.015 \text{ m/s}^{1/3}$  would give more realistic results. Also flow velocities are better resolved with a low Manning's n bed roughness.

#### 4.4 Model accuracy

The methodology to quantify model uncertainty (Harezlak et al., 2014) is briefly described in section 3.7 and will therefore not be repeated here. In Chapter 2, the dominant hydrodynamic processes were summarised as

- Tidal propagation and changes in tidal propagation in the Ems Estuary and lower Ems River as a result of deepening
- Residual flows resulting from river discharge, wind and salinity, and changes therein as a result of deepening

In the lower Ems River, wind-driven flows and salinity-driven flows are probably comparatively less important than tidal dynamics and residual flows by river discharge.

The aim of the ER and ERD models is to reproduce the tidal dynamics (waterlevels and flow velocities) in the lower Ems River (and in the ERD model also in the Dollard). The ER model is also used to simulate suspended sediment transport (and changes therein in the past decades). Tidal dynamics can be quantified with waterlevel data, especially if supported by velocity observations. For suspended sediment dynamics, residual flow (estuarine circulation) and tidal asymmetry (bed shear stress, vertical mixing) is important. The hydrodynamic target variables are therefore

- Tidal phases and amplitudes (absolute values but also the phase angle relationships between  $M_2$  and  $M_4$ )
- The bed shear stress by currents (important for resuspension of sediments from the bed)
- The residual flow (important for advection of sediment particles)

As far upstream as Papenburg, the error in the tidal phase and amplitude of the main tidal constituents is several percent. The computed amplitude of the  $M_4$  overtide is too large, typically 10 to 20%. Since sediment transport is a non-linear function of flow velocity, the error in computed residual transport will be larger than 10 to 20%. The phase of  $M_4$  is better resolved (several per cent error), and therefore the type of tidal asymmetry (determined by  $\theta_\zeta = 2\phi_{\zeta_{M_2}} - \phi_{\zeta_{M_4}}$ ) is reproduced correctly. Also the computed flow velocities are in reasonable agreement with observations. Therefore the ER model and the ERD models are

sufficiently reliable tools to analyse the (changes in) tidal dynamics. The ER model performs slightly better than the ERD model, for both waterlevels and flow velocities. Because of the required computational time of both models, the ER model will be used to develop a sediment transport model as well (report 5).

The salinity forcing of the ERD model (using computed salinity gradients to compute salinity boundaries from salinity timeseries observed elsewhere) is not very accurate. The ERD model should therefore not be used to (changes in) compute density-driven flow.

## 4.5 Summary

Two models (ER and ERD) were developed for the Ems estuary aiming at (1) reproducing the hydrodynamics (tidal dynamics, including tidal asymmetry, and density-driven flows) for present-day conditions and (2) analysing the exchange of the lower Ems River with the Ems Estuary. The model calibration required low roughness values, corresponding to expectations based on the hyper-turbid conditions (resulting in low hydraulic drag), to reproduce the waterlevel variation along the lower Ems River and the flow velocity at the river mouth. For the ER model, historic scenarios will be set up (next chapter) and a sediment transport model developed (report 5). The ERD model is used to simulate scenarios affecting tidal dynamics in the Dollard area (as done by Haskoning, 2013).

## 5 Historic scenarios

### 5.1 Introduction

One of the aims of the project is to understand changes in the turbidity and water quality of the Ems Estuary. These changes will be analysed in report 7, using the hydrodynamic models (see this report) in combination with the sediment transport module (report 5) and the water quality module (report 6). In order to model changes, historic model scenarios need to be developed. In this chapter, historic scenarios are set up for the ER and WED models.

### 5.2 The WED model

#### 5.2.1 Scenario set up

The effect of changes in bathymetry on hydrodynamics (and later on turbidity and water quality, report 7) is evaluated by running the model with the oldest available bathymetry, collected by the Dutch ministry of Public Works in 1985 (Figure 5.1). These soundings cover the majority of the Ems estuary, but not the lower Ems River and the North Sea. In order to differentiate the effect from the changing bathymetry in the Ems estuary from the changes in bathymetry in the lower Ems River, the depth of the lower Ems River was not changed. The impact of the lower Ems River is assessed using the ER model (see section above), whereas morphological changes in the North Sea are probably insignificant (especially for mud dynamics in the Ems Estuary).

As explained in section 3.3, the 2005 bathymetry in the model was slightly adapted to better reproduce the waterlevels in the model to compensate for grid cell size restrictions. Therefore the 1985 bathymetry cannot be interpolated to the grid without a similar modification. The 1985 bathymetry is generated by first computing a difference map between 1985 and 2005 (based on sounding data), which is subsequently interpolated to the numerical grid of the WED model (Figure 5.2). This difference is subtracted from the 2005 interpolated model bathymetry, resulting in the 1985 bathymetry in Figure 5.1.

The bathymetry of the lower Ems River is not adapted to 1985, for 2 reasons:

- The main purpose of the WED model is to explore changes in the Ems Estuary, and not so much changes in the lower Ems River (where the model accuracy is insufficient). Adapting only the Ems Estuary, and not the lower Ems River, allows identification of the effects of bathymetric changes within the Ems Estuary (and not the lower Ems River).
- No accurate and detailed data was available for 1985, only estimates of the bed (as used in the ER model).



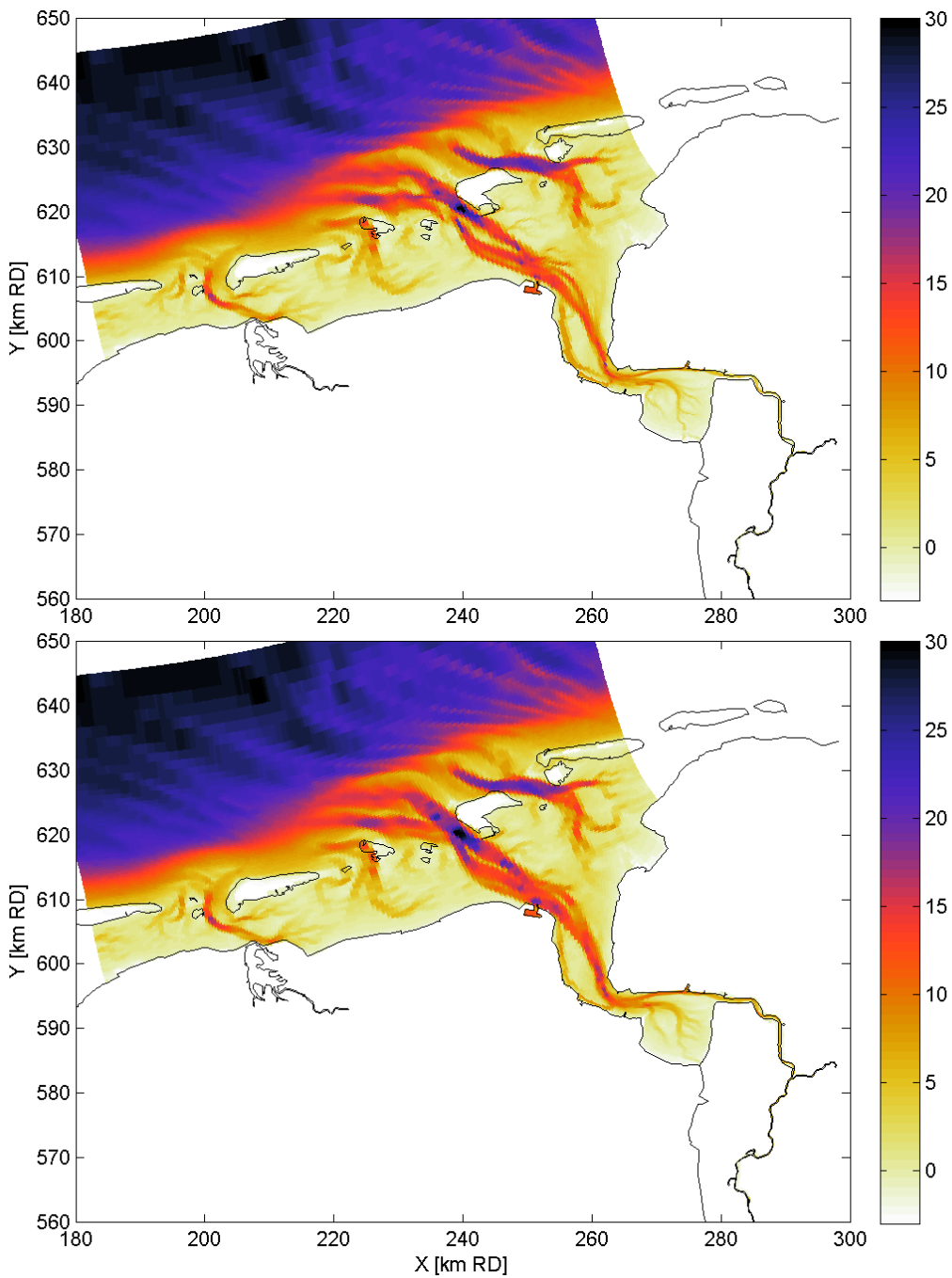


Figure 5.1 Historic model bathymetry (1985, top) and 2005 bathymetry (lower panel). The 1985 bathymetry is based on soundings by the Dutch ministry of Public Works in the Ems estuary. The bathymetry of the North Sea and the lower Ems River is identical to the 2005 bathymetry.

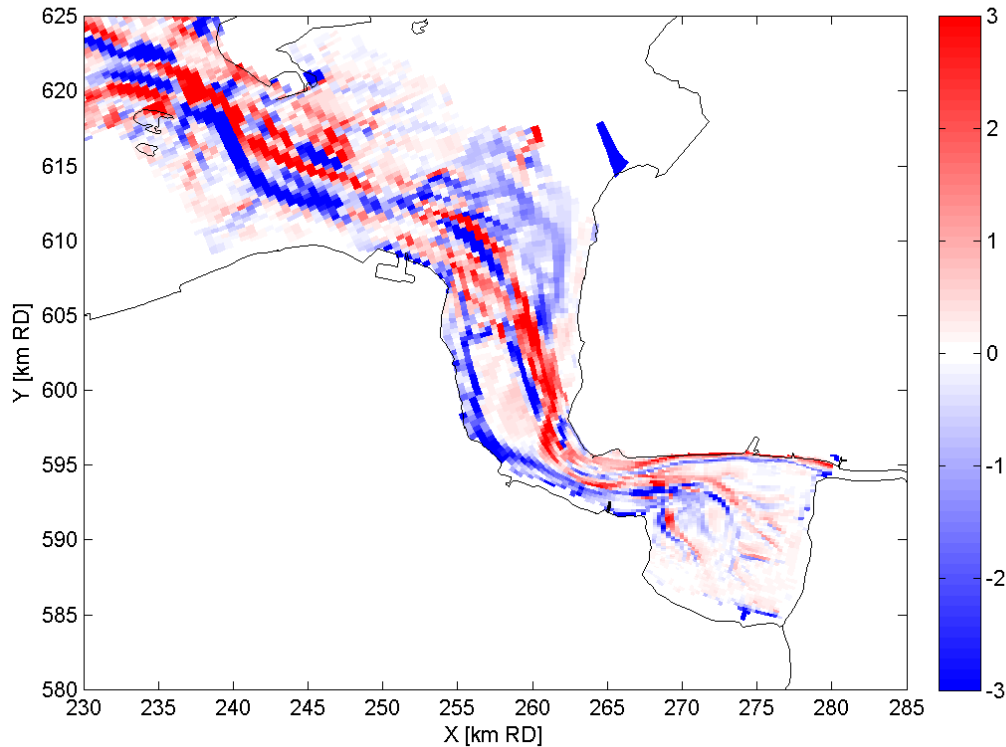


Figure 5.2 Modelled difference [m, deepening in red] between 1985 and 2005.

### 5.2.2 Hydrodynamic comparison

The change in bathymetry potentially influences tidal propagation and estuarine circulation, and thereby the sediment dynamics in the Ems Estuary. The tidal amplitudes and phases computed for both the 1985 and 2005 bathymetry are very similar (Figure 3.7 and Figure 5.3). Apparently, the change in the depth of the tidal channels in the Ems estuary has a negligible effect on the tidal range. This is supported by analysis of long-term waterlevel data (report 3, see Figure 5.4). Both  $M_2$  and  $M_4$  vary with the 18.6 year nodal cycle, and an increase in both their amplitude occurred in the 1960's, but from 1985 to 2005 the change in amplitude is non-existent ( $M_2$ ) or small ( $M_4$ ). It should be noted that the 1985-2005 comparison focuses on bathymetric changes in the Ems Estuary, and therefore the model excludes any bed level changes in the lower Ems River (which were substantial).

The bed level changes do influence residual flow patterns: compare the upper (1985) and lower panel (2005) of Figure 5.5. In 2005, an up-estuary un-interrupted near-bed residual flow connects the Eemshaven with the Dollard, with velocities of 5 to 10 cm/s. In 1985, this up-estuary near bed flow is more irregular, especially in the narrow section of the Friesche Gaatje (see Figure 1.1 for channel names), between Y-km 594 and 600. Such changes in residual circulation may be important for fine sediment dynamics, which will be explored in report 7.

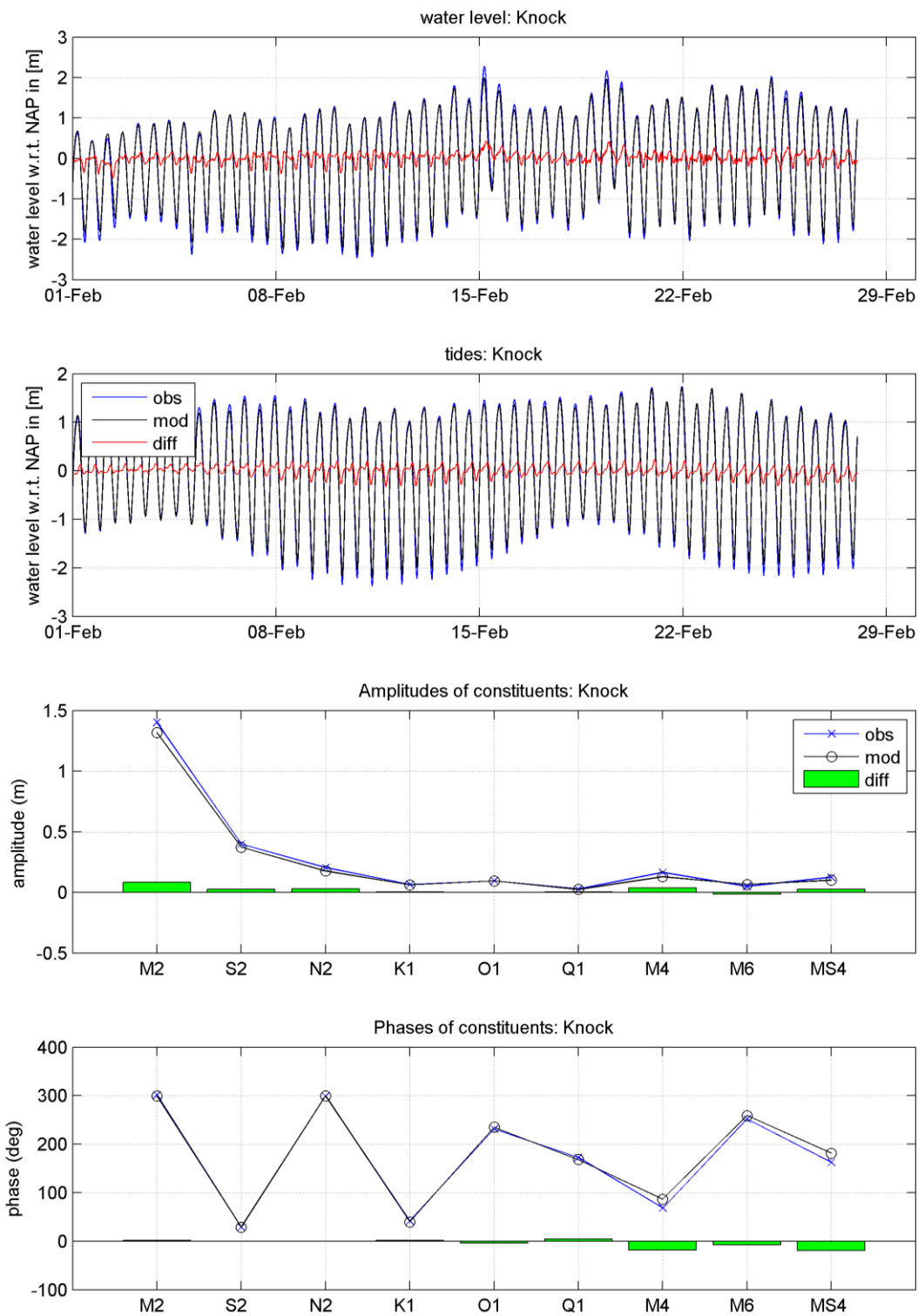


Figure 5.3 Comparison between observed (blue) and computed (black) waterlevels and tidal constituents at Knock: full time series (top panel), tidal signal (second panel), tidal amplitudes (third panel) and tidal phases (fourth panel). Time series show the results of February to be able to see some detail; the tidal analysis has been done for the entire year (2012 hydrodynamics, using 1985 bathymetry).

The model predicts an increase in salinity of 1-2 ppt in both Huibergat and Groote Gat as a result of deepening (Figure 5.6). This may reflect a more up-estuary intrusion of the salt wedge, leading to an overall increase in the salinity in the estuary. The MWTL observations also suggest that the salinity is increasing with ~3 ppt in the past 35 years (Figure 5.7). The comparison with the MWTL data suggests that the modelled increase in salinity is realistic, and results from morphologic changes in the estuary. However, the salinity measurements should be interpreted with some reservations because they are influenced by observational methodologies.

Conclusively, the deepening of the tidal channels of the Ems Estuary had little effect on tidal dynamics, but did influence the estuarine circulation and the salinity distribution.

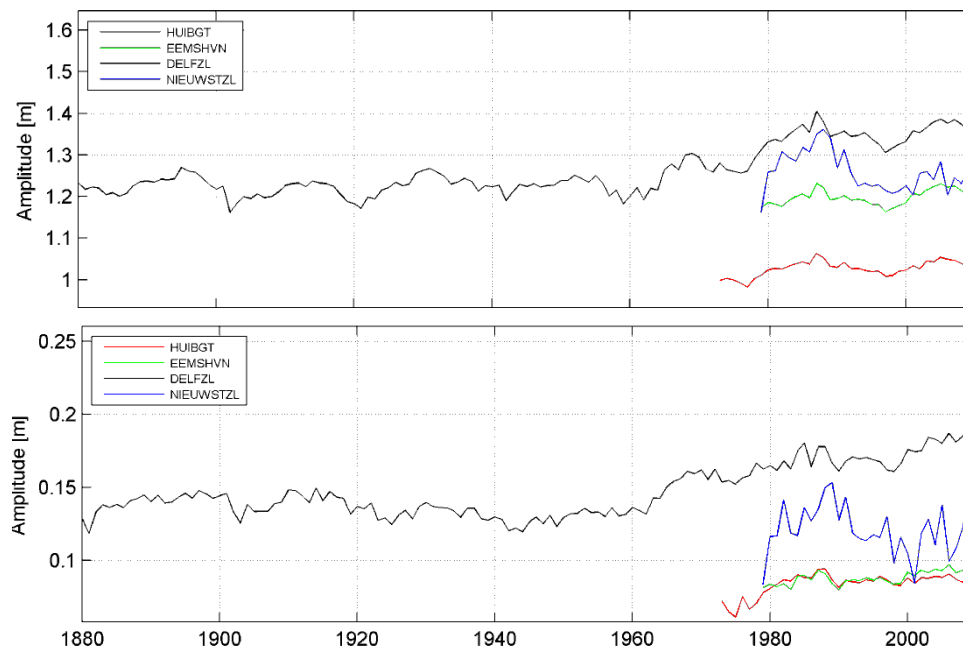


Figure 5.4 Amplitude of  $M_2$  (top) and  $M_4$  (below) for Huibergat, Eemshaven, Delfzijl, and Nieuw Statenzijl, for the period for which data is available.

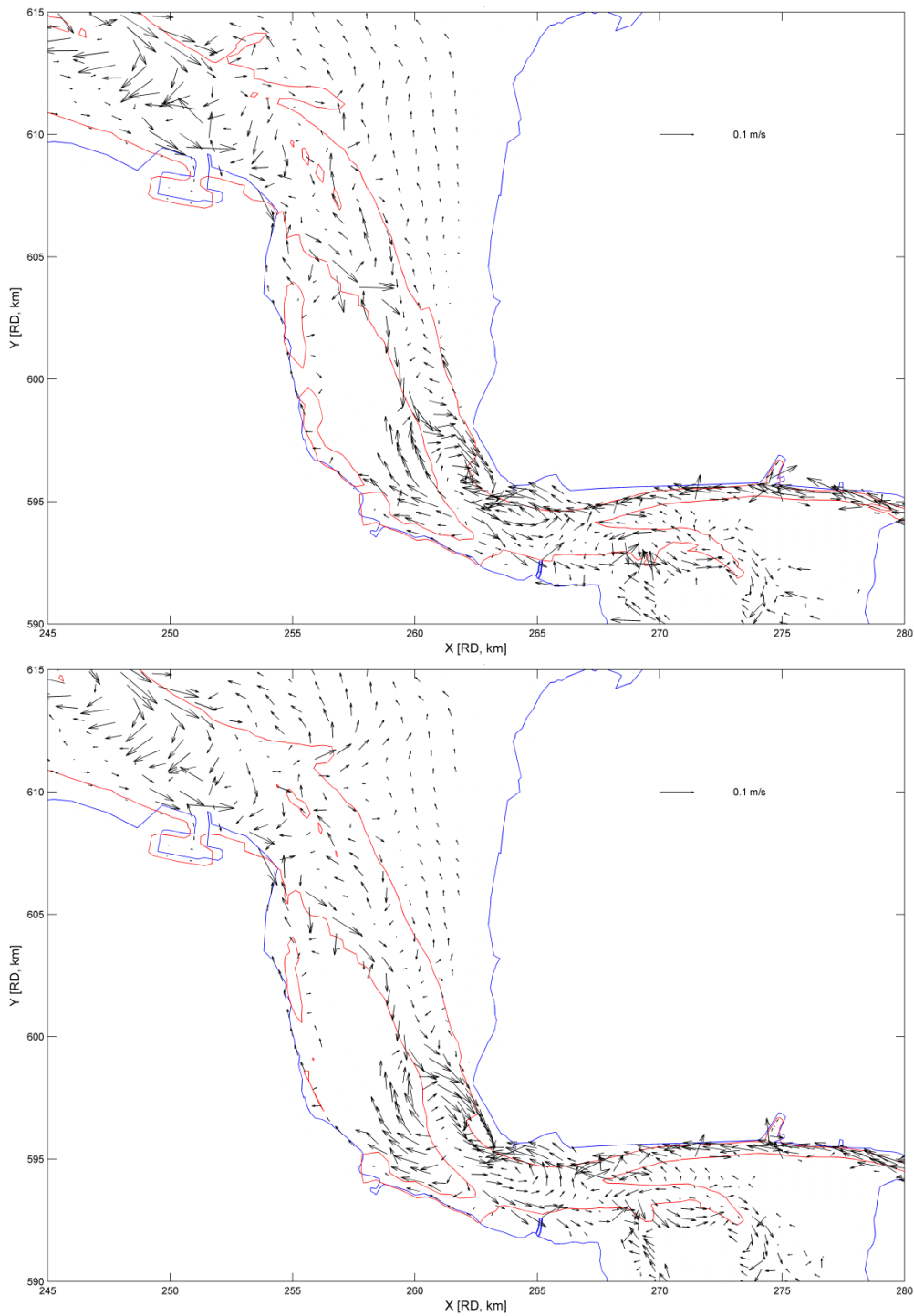


Figure 5.5 Monthly averaged residual flow for the month January 2012, using the 1985 bathymetry (top panel) and the 2005 bathymetry (lower panel).

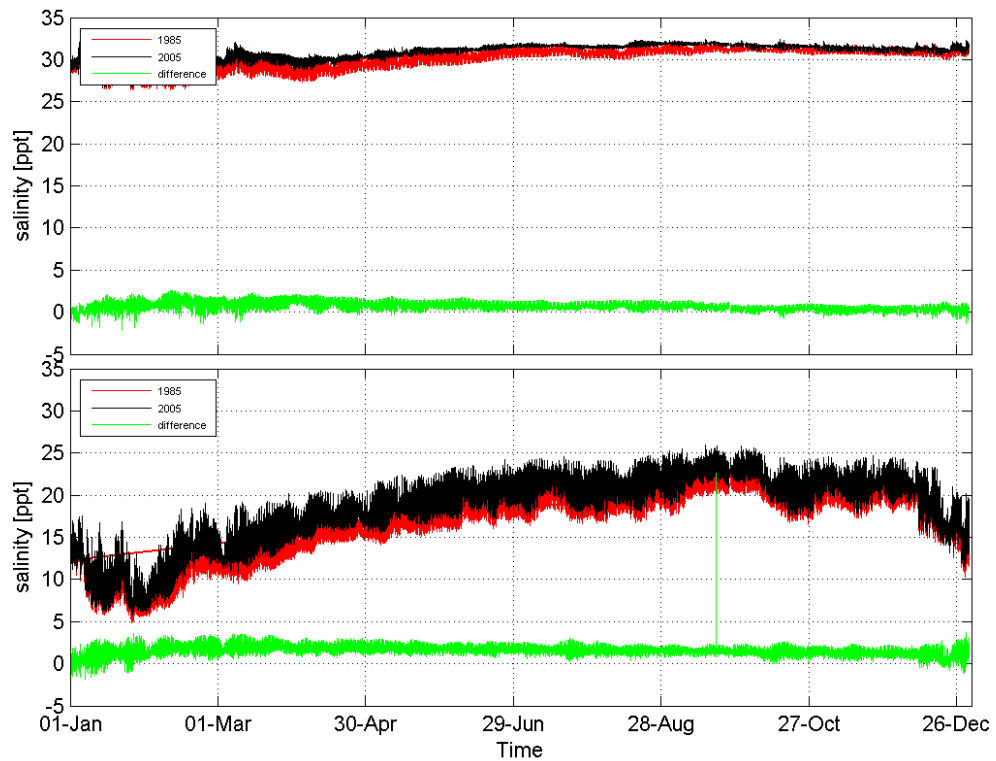


Figure 5.6 Salinity computed at HuibertGat (top panel) and Grootte Gat (lower panel) using the 1985 (red) and 2005 (black) bathymetry, and the increase from 1985 to 2005 (green).

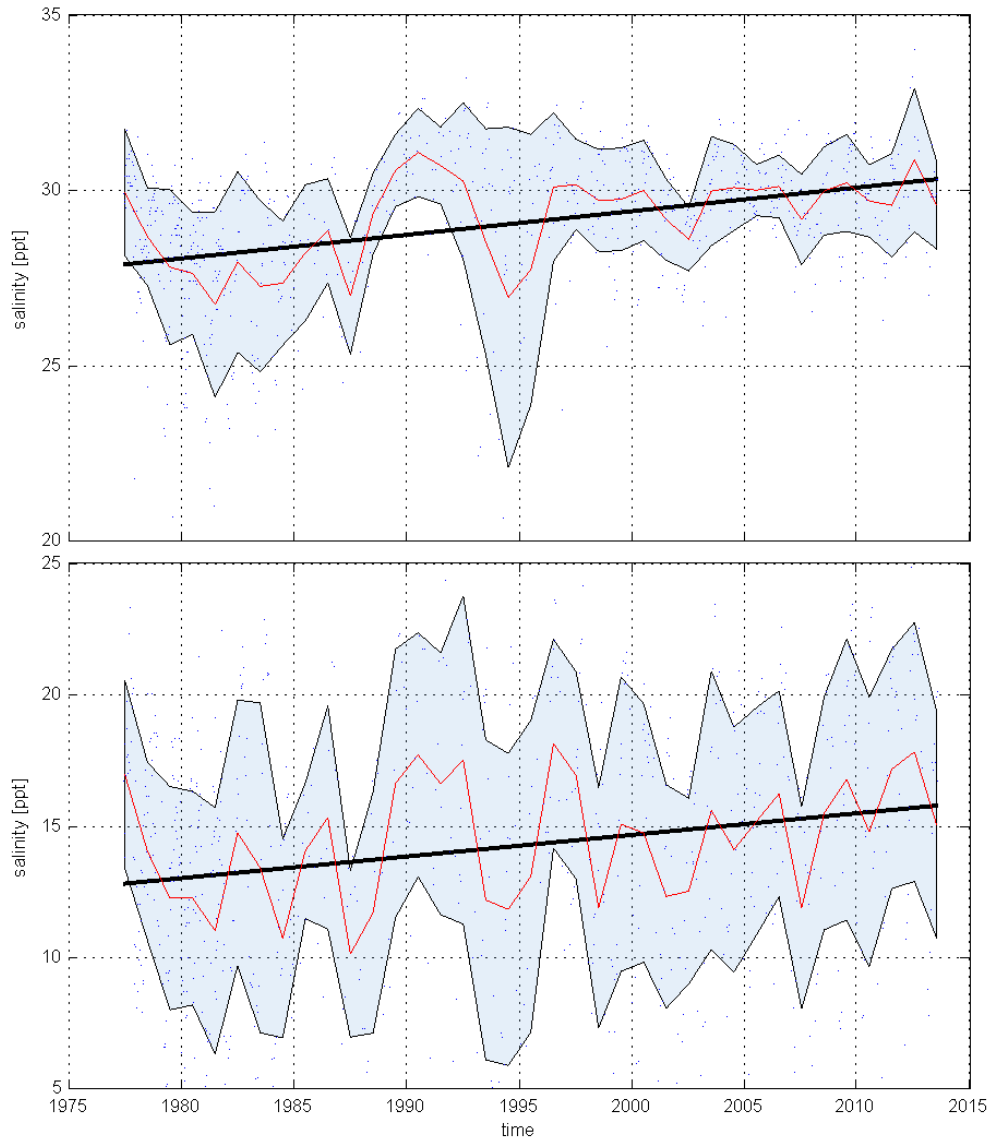


Figure 5.7 Salinity observations (dots) with least-squares linear fit (black line), annual average (red line), and standard deviation envelope (blue), collected as part of the MWTL program at Huibertgat (top) and Groote Gat (below).

## 5.3 The ER model

### 5.3.1 Scenario set up

The model resolution in the lower Ems River of the ER model is sufficiently detailed to implement various scenarios representing historic conditions of channel deepening. The hydrodynamics in the Ems Estuary have significantly changed in the past decades (since ~1950), as a result of channel deepening. However, there are no historic bathymetries (at sufficient spatial detail) and continuous waterlevel recordings available (only long-term observations of high water (HW) and low water (LW)). Therefore, the historic scenarios for the lower Ems River are based on historical channel deepening, and calibration of the waterlevels

is done at high water / low water (HW / LW) for the available stations in the lower Ems River. More details on the set up, calibration, and analysis are given in Schoemans (2013).

Table 5.1 Chronology of fairway deepening and other interventions in the lower Ems River, from Schoemans (2013), based on Herrling and Niemeyer, 2008, Krebs & Weilbeer, 2008, and pers. comm. Krebs (2013).

Included in model situation:				Year	Intervention in Lower Ems
2005	1985	1965	1945		
				Before 1939	Emden Fahrwasser at -6 m SKN
				1932 - 1939	Waterway depth: 5.5m m below MHW between Pogum and Leerort; 4.1m m below MHW between Leerort and Papenburg
				1939 - 1942	Maintaining Emden Fahrwasser at -7 m SKN.
				1942 - 1948	No maintenance between 1942 and 1945. After 1945 natural depth Emden Fahrwasser between - 5.8 and -6 m SKN.
				1957	Deepening Emden Fahrwasser to -8 m SKN
				1958 - 1961	Construction of 2.2 km training dam 'Seedeich', 12 km Geise training wall from Pogum to Geisesteerwert and 17 new groynes.
				1961 - 1962	Deepening of Leerort-Papenburg to 5 m below MHW. Narrowing of river between Herbrum - Papenburg by extension of groynes.
				1965	Emden Fahrwasser at -8.5 m SKN
				1983 - 1986	Deepening Lower Ems on trajectory Emden-Papenburg to 5.7 m below MHW
				1984 - 1985	Streamlining of river near Weekeborg and Stapelmoor (increase of radius), reduced river length with 1 km
				1991 - 1994	On-going deepening of Lower Ems on trajectory Emden - Papenburg to 6.3 m, 6.8 m and 7.3 m below MHW
				2001-2002	Construction of storm surge barrier Emssperwerk

The historic cases are set up as follows:

- 1) Historic bathymetries are constructed based on anecdotal information. This includes straightening of river bends and deepening, as tabulated in Table 5.1. Historic deepening are related to a certain reference level (MHW<sup>7</sup> or SKN<sup>8</sup>). These values change along the river and in time, and therefore the implementation is described in more detail below.
- 2) Because historic boundary conditions are not available, each historic scenario is forced with the 2005 boundary conditions. Since high and low waters vary with the 18.6 year nodal cycle, the 2005 hydrodynamic conditions are strictly speaking representative for 2005, 1986, 1968, and 1949. However, to avoid an apparent overestimation in the degree of accuracy of the historic scenarios, these years are approximated as 2005, 1985, 1965, and 1945.
- 3) The computed high and low waters are calibrated against observations by changing the hydraulic roughness. A typical value for the Manning's coefficient  $n$  in sand-dominated estuaries is  $0.02 \text{ s/m}^{1/3}$ . For muddy systems,  $n$  may be as low as  $0.01 \text{ s/m}^{1/3}$ . The apparent hydraulic roughness of muddy estuaries may be strongly influenced by the mud content in suspension and by fluid mud. Vertical gradients damp turbulent exchange, leading to larger flow velocities. For the 2005 calibration,  $n = 0.01 \text{ s/m}^{1/3}$  was indeed

<sup>7</sup> Mean High Water.

<sup>8</sup> Seekartennull or chart datum, CD.



needed in the lower Ems River to reproduce the present-day tidal propagation. Likely, before the strong increase in turbidity in the lower Ems River, a value of  $n = 0.02 \text{ s/m}^{1/3}$  should be more representative.

### Waterlevel conversion

Waterlevel measurements were available from the Federal Waterway Agency of Emden (WSA Emden) for 1985 and 1965. These measurements consist of the time and height of each high and low water. Mean high water (MHW) values were determined from this data. MHW is defined as the average height of all high waters recorded at a given place over a 19-year period. For example, for the 1985 model state, the 19-year averages for each gauge are calculated using the high waterlevels in the period 01-01-1976 till 31-12-1994 (9 years before and after 1985). In this way, 19-year averaged MHW values were determined for all waterlevel stations in the Emden Fairway (Emder Fahrwasser, Knock and Emden NS) and along the lower Ems River (Pogum, Terborg, Leerort, Weener and Papenburg). Because Knock, Terborg and Weener have started recording data fairly recently, the 19-year averages for these stations could only be determined for the 1985 model configuration. Unfortunately, no waterlevel data prior to 1949 was available (the existing German data is not available to Deltares). Instead, the 19-year averaged MHW values were estimated from a graph by Herrling and Niemeyer (2008), showing the historical trend of yearly MHW for stations along the lower Ems River. This was done by fitting a trend line by hand. The error for this method is approximately 5 cm. Figure 5.8 shows the obtained 19-averaged MHW values for all gauges. High waterlevels increase more or less linearly in up-estuary direction, from Knock to Papenburg, and MHW levels also increase in time.

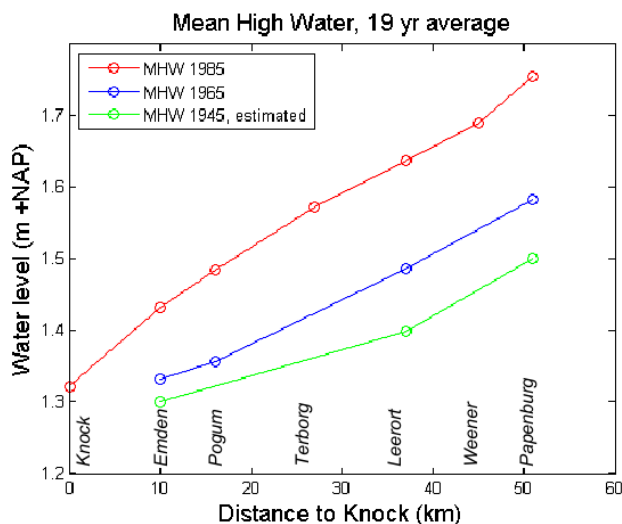


Figure 5.8 Measured (1985 and 1965) and estimated (1945) mean high waterlevels (19-year averaged values) for waterlevel stations in the Emden Fairway and along the lower Ems River, including trend lines.

While the channel depth in the lower Ems River was usually expressed in depth relative to MHW, the channel depth in the Emden Fairway was documented as a function of German chart datum SKN (See Karten Null). For the German North Sea coastline and the Ems-Dollard estuary, SKN is defined as the average spring low waterlevels or Lowest Astronomical Tide (Bundesamt für Seeschifffahrt und Hydrographie). The available waterlevel data did not include SKN values. Instead, for 1985 and 1965 the dates of full and new moon are used. Since spring tide generally lags behind in coastal areas, SKN values are obtained by averaging the low waterlevels measured 1-3 days after full/new moon. The 1945 SKN value for Emden was based on Herrling and Niemeyer (2008) showing the historical trend of

yearly MLW levels. Low waterlevels are fairly constant in Emden, therefore it was assumed that SKN levels are also constant. MLW levels in 1945 seem slightly higher than in 1965, so SKN waterlevel at this location was estimated slightly above the 1965 SKN value.

#### Depth reconstruction

The largest bathymetry change in the Emden Fairway (between Knock and Emden NS) took place between 1945 and 1965, when the approach to Emden harbour was deepened from  $\sim -8$  m NAP to  $\sim -10.5$  m NAP. This depth has been maintained since then, which is confirmed by the measured 2005 bathymetry. For the 1965 and 1985 model configuration, the observed 2005 depth of the Emden Fairway was used. For the 1945 model situation the depth of this stretch was reduced to  $\sim -9$  m NAP. The value of  $-9$  NAP is the port depth in 1942, which decreased to  $-8$  m by 1948 because of lack of maintenance dredging. The 1942 depth is chosen to represent 1945 because

- The depth of  $-8$  m was probably local and consisting of very fine sediment.
- The exact depth in 1945 is probably in-between  $-8$  and  $-9$  m, but its exact value unknown.

As can be seen in Figure 5.9, the stretch between Pogum and Leerort has remained at a constant depth of approximately  $-4$  m NAP between 1945 and 1985. However, the on-going deepening in an upper stretch of the lower Ems River (between Leerort and Papenburg) has lowered the bed level of the fairway from  $\sim -2.7$  m NAP in 1945, to  $\sim -3.5$  m in 1965, to a depth of  $\sim -4$  m in 1985. These depth changes have been included in the model conditions of 1945, 1965 and 1985, respectively. In the 1990's the entire river stretch from Emden to Papenburg was deepened to its present depth of approximately  $-6$  m NAP. No information about deepening measures was available upstream of Papenburg and east of Leerort (river Leda), therefore these river parts were not modified in the model.

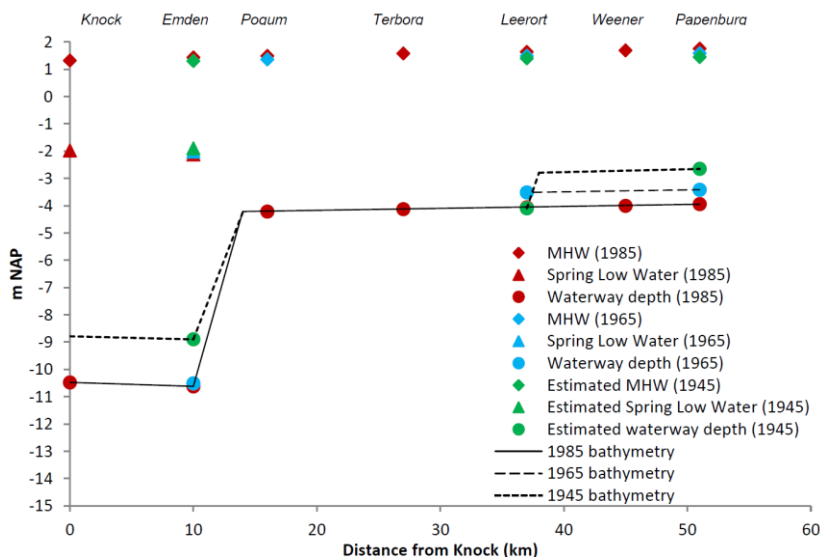


Figure 5.9 Reconstructed bathymetries of 1985, 1965 and 1945, based on channel deepening activities, mean high waterlevels and average spring low waterlevels. All values are given in m +NAP (=m +NN).

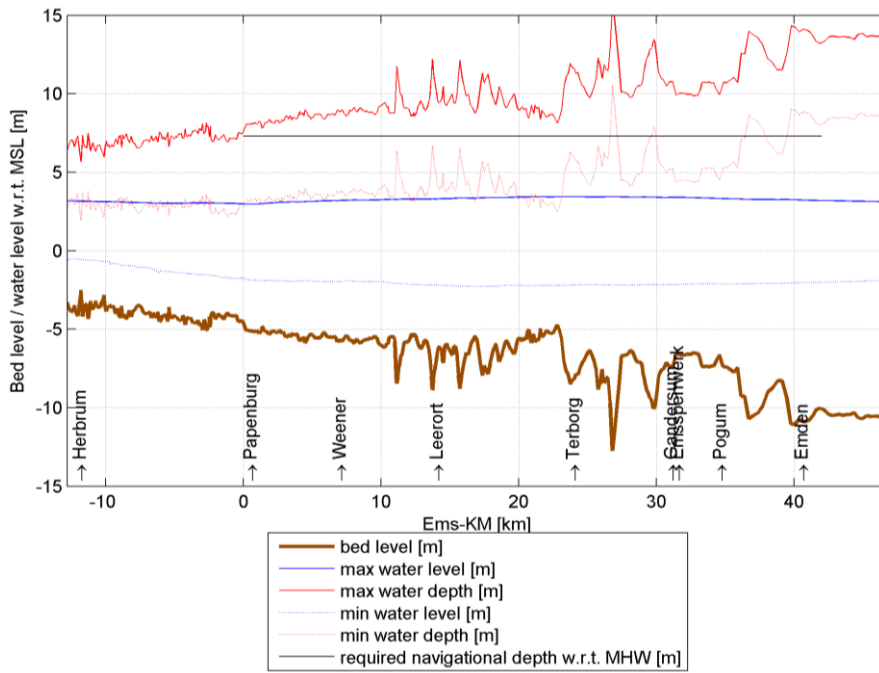


Figure 5.10 Bed level, water depth and waterlevel at HW and LW, and the required navigational depth (according to Table 5.1), for 2005. The bed level and waterlevels are relative to Mean Sea Level (MSL), whereas the water depth and required navigational depth is relative to the bed level

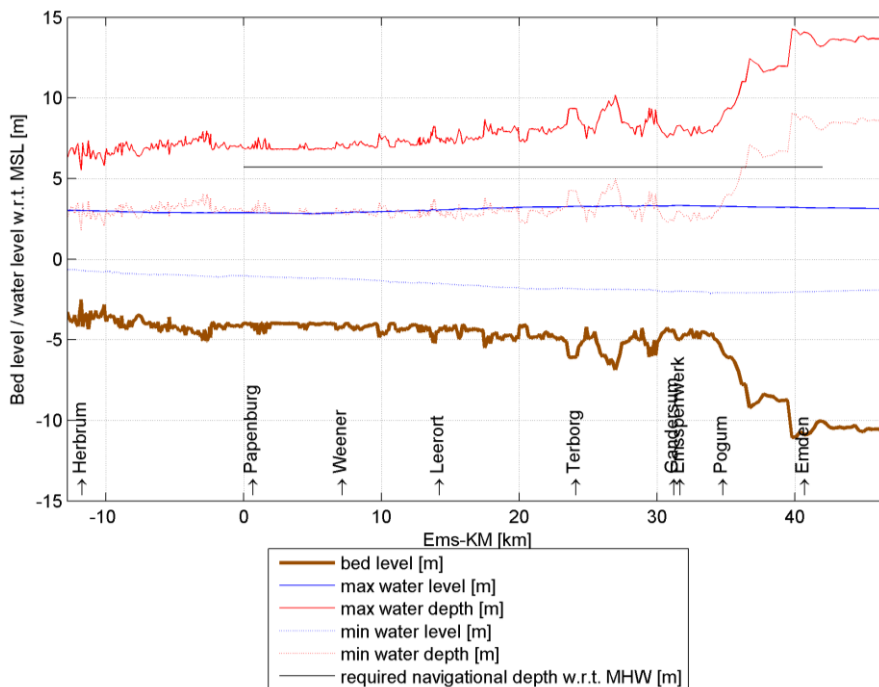


Figure 5.11 Bed level, water depth and waterlevel at HW and LW, and the required navigational depth (according to Table 5.1), for 1985. The bed level and waterlevels are relative to Mean Sea Level (MSL), whereas the water depth and required navigational depth is relative to the bed level

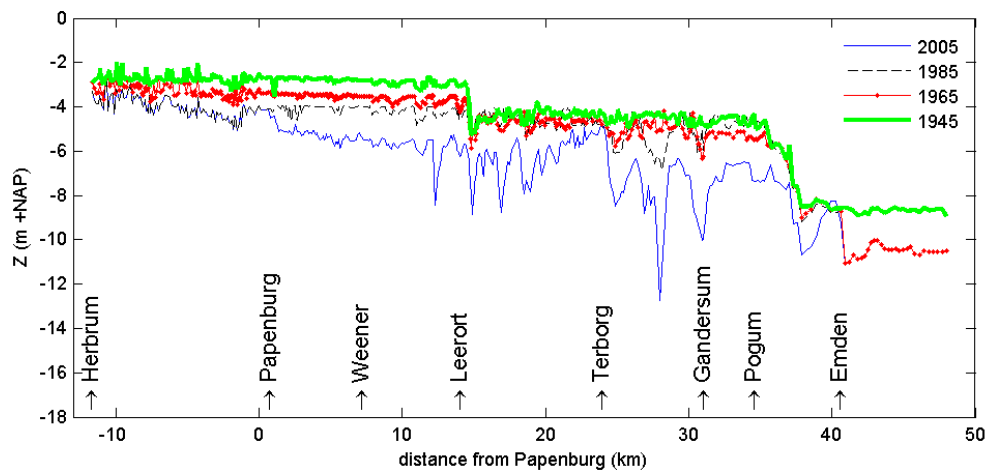


Figure 5.12 Water depth along the thalweg of the lower Ems River from Herbrum to Knock. The bed level has remained unchanged in the Emden Fairway in since 1965 (red overlaps black and blue lines)

The navigational depth in the ER model has been obtained by multiplying the 2005 measured bed level over the whole cross-section with an along-channel variable factor (between 0 and 1) until the channel depth corresponds to Figure 5.9. In 2005, the actual maximum water depth was typically about 1 m larger than the required navigational depth (Figure 5.10). Therefore the historic bed level is constructed in such a way that the maximum water depth is also about one meter larger than the required navigational depth (see Figure 5.11 for 1985; 1945 and 1965 not shown). The resulting model thalweg depths for 1945, 1965, 1985, and 2005 are summarised in Figure 5.12.

In addition to deepening, also the meandering of the lower Ems River has been reduced by re-creating the original channel (based on old meanders which can still be observed in the original bathymetry data). Most river bends were straightened before 1929 (reducing the river length with 1.8 km; Krebs, 2012), but in 1984-1985 the bends at Weekeborg and Stapelmoor were straightened. The 1945 and 1985 bathymetry therefore still contain these bends, whereas they are straightened in 1985 and 2005 (see Schoemans, 2013 for details).

### 5.3.2 Calibration

The historic scenarios (1945 – 2005) are run using identical hydrodynamic forcings (the year 2005, see the previous section) but with variable hydraulic roughness. The resulting HW and LW values (for a range of hydraulic roughness values) are compared per station to observed HW and LW values.

At Emden, the computed high and low waterlevel remain constant through time, with a minor influence of the bed roughness (Figure 5.13, top panel). The observed high and low waters do show a trend, with increasing HW and decreasing LW levels. This may partly result from a decreasing hydraulic roughness, but probably more by changes in tidal dynamics on a larger scale (the tidal range at Delfzijl increased 30 cm since 1960; see report 3).

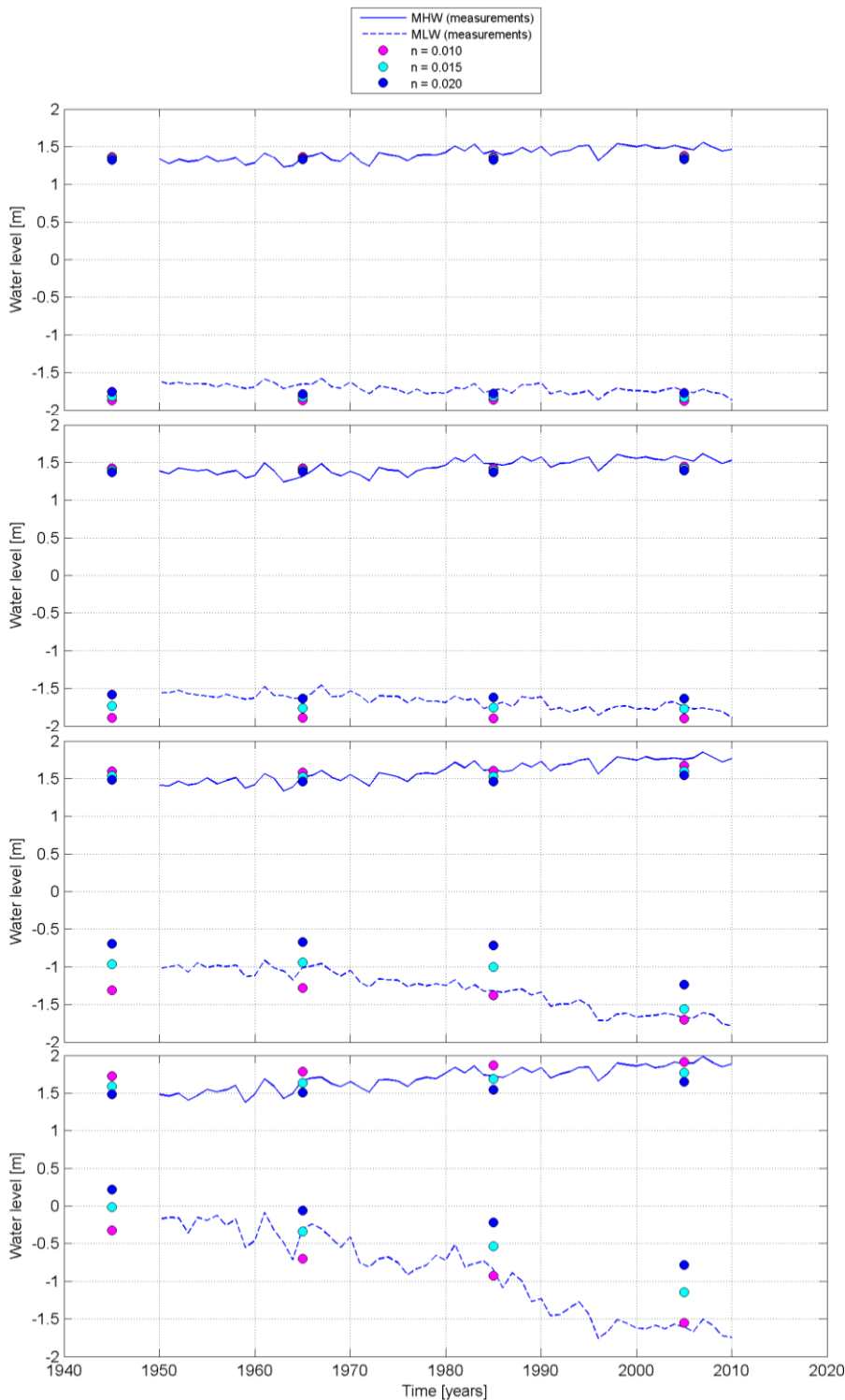


Figure 5.13 Model calibration runs with variable bed roughness. Observed (lines) and computed (dots) HW and LW at Emden (top), Pogum (second panel), Leerort (third panel), and Papenburg (lower panel). HW (LW) is defined as the yearly average of every high water (low water) per tidal cycle.

The increase in tidal amplitude is much more pronounced within the lower Ems River. This increase is reasonably reproduced with the model. The effect of the bed roughness is more pronounced for LW levels than for HW levels. The year 2005 is best reproduced with a low

Manning's  $n$  (Figure 5.13), in line with the model calibration (see section above). For the year 1985 some stations require a Manning's  $n = 0.01$  while others perform better with  $n = 0.015$ . The model simulations therefore suggest that the hydraulic roughness was already fairly low around this period, which is in line with Duinker's (1985) observations of fluid mud in 1976. However, the model is also sensitive to bathymetrical changes, and therefore errors in the estimates of the bathymetry may lead to overestimated effects of the hydraulic roughness. For 1965, the Manning's value seems to be around  $n = 0.015 \text{ s/m}^{1/3}$ , whereas in 1945 it was probably closer to  $n = 0.02 \text{ s/m}^{1/3}$ .

Conclusively, the change in tidal regime between 1945 and 2005 is reproduced with the model. Especially in the upper part of the lower Ems River, the contribution of hydraulic roughness is comparable to the contribution of deepening: both contribute to ~1m in the tidal range at Papenburg. In 2005, the required hydraulic roughness is low ( $n = 0.010 \text{ s/m}^{1/3}$ ) resulting from the fluid mud layers present in the lower Ems River. In 1965 – 1985, the hydraulic roughness is higher, probably  $n \approx 0.015 \text{ s/m}^{1/3}$ . For 1945 conditions, the hydraulic roughness is typical for a sand-dominated system, with  $n = 0.020 \text{ s/m}^{1/3}$ .

#### 5.4 Model accuracy

The historic scenarios are mainly developed to analyse historic changes in hydrodynamics (tidal propagation, salinity-driven flow) and sediment transport. For the calibration of changes in tidal propagation in the lower Ems River, only historic HW and LW levels are available. Therefore the HW and LW values are the target variables to determine the accuracy of the ER model. For the WED model, waterlevels as well as salinity data is available to verify its accuracy. Waterlevels provide target variables to determine how well the model reproduced changes in tidal dynamics. Residual flow is an important parameter for changes in sediment transport, but reliable, even more historic, data on residual flow velocities does not exist. The salinity can be used as an approximation. For the Ems River, no proxy is available to assess the accuracy of the residual flow velocity. This provides the following target variables to determine model accuracy:

- Waterlevels (WED model)
- High and Low Waters (ER model)
- Salinity (WED model)

The modelled changes in waterlevels in the Ems estuary (WED model) suggest that the changing morphology from 1985-2005 does not or negligibly influence waterlevels. This is confirmed by waterlevel observations, and therefore the model captures (the absence of) changes in tidal dynamics. The computed change in salt content corresponds to actual changes in salt content in the estuary, suggesting that the increase in estuarine circulation computed by the model for 1985 to 2005 is realistic.

The computed increase in waterlevel variations in the lower Ems River is probably caused as much by deepening as by reduction of the hydraulic roughness. Both the change in bed roughness (from Manning's  $n = 0.02$  to  $0.01$ ) and the change in bed level are realistic, and the resulting changes in waterlevels correspond to observations. It is therefore concluded that the hydrodynamic module of the ER model provides a sufficiently accurate tool to analyse changes in water depth and bed roughness on tidal dynamics and on sediment transport. This analysis is part of report 7.

## 5.5 Summary

Historic scenarios have been developed for the Ems estuary (WED model, two scenario's) and the lower Ems River (ER model, four scenarios): see Table 5.2. The scenario in the WED model is based on actual historic bathymetric data, whereas the ER model is based on semi-quantitative information. The historic scenario constructed for the WED model suggests that tidal dynamics in the estuary (excluding the lower Ems River) have changed relatively little in the past decades, but that estuarine circulation and salt intrusion have increased. The historic scenarios constructed for the ER model indicate that the tidal amplification in the lower Ems River (upstream of Emden) is caused by deepening (directly) and by a hydraulically smoother bed. Both deepening and lower roughness are probably equally important for the present-day tidal dynamics. Both scenarios reproduce the available data sufficiently accurate to use the hydrodynamic model scenarios as input for the sediment transport models. Using the six scenarios introduced in this chapter, the historic changes in hydrodynamics and sediment dynamics will be analysed in more detail in report 7.

Table 5.2 Summary of model scenarios

Scenario	Model	Hydrodynamics	Bed level	Numerical settings
2012 Ems Estuary	WED	2012	2005 (Figure 5.1)	Table 3.1
1985 Ems Estuary	WED	2012	1985 (Figure 5.1)	Table 3.1
2005 lower Ems River	ER	2005	2005 (Figure 5.12)	Table 4.1
1985 lower Ems River	ER	2005	1965 (Figure 5.12)	Table 4.1
1965 lower Ems River	ER	2005	1965 (Figure 5.12)	Table 4.1
1945 lower Ems River	ER	2005	1945 (Figure 5.12)	Table 4.1

## 6 Summary and recommendations

In order to generate numerical model tools to quantify historic changes in hydrodynamics, sediment transport, and water quality in the Ems-Dollard estuary, three models were modified and validated (the WED model) or set up, calibrated and validated (the ER and ERD model). The WED model will also be used to quantify measures to improve the hydrodynamics and sediment dynamics in the estuary (report 11).

### 6.1 The Ems Estuary

The WED model is specifically set up to compute long-term changes in suspended sediment dynamics over the lower reaches of the Ems estuary (from the sand-dominated area North of Eemshaven to the muddy Dollard estuary). Because of its (relatively poor) resolution in the lower Ems River, and the offline coupling of hydrodynamics and sediment transport (see report 5), the model is expected to be less suitable for simulating the dynamics of the lower Ems River. The computed salinity agrees better with the observed salinity than in the KPP Eems-Dollard model (set up for 2005), probably because the fresh water sources are more realistically implemented. However, the modelled salinity can be further improved, as will be discussed at the end of this chapter. A validation against flow velocity observations reveals that at one station, the computed and observed flow velocity are comparable while at a second station, the observed flow asymmetry is underestimated. The model underestimation is probably related to bathymetric variations at spatial scales smaller than the model resolution, which are not resolved by the model. However, since these asymmetries are local, it is not expected that they significantly impact the sediment dynamics in the estuary. Wave forcing is computed with the wave model SWAN, generating a more pronounced gradient in the wave height distribution (and therefore bed shear stress) than the 2005 application of the WED model. With better reproduction of salinity and more accurate wave simulations, the new hydrodynamic model forms a solid basis for sediment transport and water quality modelling, reported in parallel reports.

### 6.2 The lower Ems River

The ER and ERD models are designed to model hydrodynamic and sediment transport processes within the lower Ems River (and changes therein). These aims require a high resolution, but also a model grid better aligned with the lower Ems River compared to the WED model. The newly developed models are calibrated against waterlevels, and validated against salinity (ERD only) and velocity observations. The observed waterlevels could only be numerically reproduced using a very low roughness value. This is in line with expectations, since the hyper turbid conditions in the lower Ems River strongly reduce the hydraulic drag (Winterwerp, 2011). The model is subsequently used to explore the impact of historic changes in the river. No detailed historic depth charts were available documenting historic changes in bed level in the lower Ems River, and therefore anecdotal information on channel deepening has been used to reconstruct the bathymetry. Since deepening was related to local High Water or Low Water values, which change in time and space, observations of waterlevels were needed to reconstruct the bathymetry. The resulting bathymetry was used with the same forcing as the original calibration and calibrated against yearly averaged historic waterlevel observations by varying the bed roughness. This revealed that the low hydraulic roughness conditions in the present-day lower Ems River were already present in 1985 (agreeing with observations). The decrease in bed roughness from 1945 to 2005



strongly suggests that the overall hydraulic drag has decreased (i.e. the river has become muddier), in line with expectations.

### 6.3 Model applicability

The model chain developed in this report, report 5 (sediment transport) and report 6 (water quality) will be applied to explore mechanisms responsible for changes in suspended hydrodynamics, sediment concentrations and water quality in the Ems Estuary in the past decades (report 7) and as a result of potential measures (report 11). In Chapter 2, a number of processes were defined which are important for the model to reproduce, in order to be suitable to explore the effect of changes in the system. The most important hydrodynamics processes were defined as:

- a) Tidal propagation and changes in tidal propagation in the Ems Estuary and lower Ems River as a result of deepening
- b) Residual flows resulting from river discharge, wind and salinity, and changes therein as a result of deepening

The present-day hydrodynamics have been validated against available data on waterlevels, flow velocity, and salinity (and qualitatively against residual flow). The waterlevels and flow velocity provide information on the tidal dynamics in the system. The main features of the tidal dynamics and asymmetries of the tide are sufficiently resolved by the model to represent the present-day tidal dynamics. Historic scenarios can be compared to a much more limited dataset, and data-model comparison is more qualitative. Therefore the model results should be used mainly in a relative sense: the model provides insight in relative changes in the system, but may not resolve the absolute values. In the Ems River, the model reproduces historic high and low waters, as well as an evolution in hydraulic roughness corresponding to expectations. In the Ems Estuary, the present-day tidal waterlevels are reproduced within several percent and flow velocity (including flow asymmetry) within 10%. The computed changes in waterlevels are low, in agreement with observations. As a result, both models are tools with which the relative changes in tidal dynamics as a result of bathymetric changes can be explored.

Residual flows are more difficult to validate because this requires long-term observations, which are subsequently difficult to compare to observations because residual flows are very sensitive to bathymetry (and therefore requires a high resolution model for a proper comparison). An approximation for the residual flows is the salinity. The salinity is compared qualitatively to observations. In the Ems Estuary, most observation stations are snapshot observations without intra-tidal or spring-neap information. The typical salinity levels are reproduced, but there are differences which are probably the result of (a combination of) model boundary conditions, observation errors and the model itself. The historic changes in salinity are small but present, which is in line with historic observations. As a result, also the residual circulation (especially gravitational circulation) has changed, with a more pronounced up-estuary near-bed flow. In the lower Ems River, salinity-induced residual flows are probably less important than in the Ems Estuary, because of the shallow water (typically less than 5 m). Salinity-induced residual circulations increase in magnitude with depth, and are therefore stronger in the Ems Estuary than in the lower Ems River. The computed salinity in the lower Ems River is mostly determined by the fresh water flux from the Ems River and mixing in the river itself. Despite some discrepancies, the available observations reasonably correspond to computed salinities (ER and ERD models). Although the simulated salinity may be improved

in both the WED and the ER(D) models, all three models resolve the salinity (and changes in salinity) with sufficient accuracy to use the model for the scenario studies (report 7 and 11).

#### **6.4 Recommendations**

Although the WED model reproduces observed waterlevels and absolute flow velocities, the salinity distribution could be improved. With the presently available data, it is not possible to determine whether deviations between observed and modelled salinity is the result of model input (river discharges, but probably most importantly the seaward boundary) or modelled processes / parameter settings related to mixing. One improvement could be to improve the salinity in the model used to generate boundary conditions (which provides accurate waterlevels, but being a two-dimensional model, the salinity is less well resolved). Determining the reason for mismatches between observed and modelled salinity requires more observational data with sufficient coverage in space, depth, and in time. The WED model has been limitedly evaluated for residual flows, because data on residual flow is scarce. This requires more long-term measurements.

The ER model is sensitive to the bed roughness, for which a constant value has been used. In reality, the bed roughness is probably spatially varying, related to fluid mud occurrences. The available data to prescribe such conditions to the model is limited, and would also require additional calibration / validation data in the form of flow velocity observations. The physically most realistic solution is to develop a full coupling between the sediment transport model and the bed roughness.



## 7 Literature

Alkyon (2008). Effect of dumping silt in the Ems estuary, 3D model study. Hydromorphological study for EIA of Eemshaven and EIA of fairway to Eemshaven. Technical report A1836, June 2008

Battjes, J. and J. Janssen, 1978. "Energy loss and set-up due to breaking of random waves,." In Proceedings 16th International Conference Coastal Engineering, ASCE, pages 569–587. 44, 128, 133, 192

Booij, N., Ris, R.C. and Holthuijsen, L.H. (1999), A third-generation wave model for coastal regions, Part 1, Model description and validation, Journal of Geophysical Research, Vol. 104, No. C4, p. 7649–7666

Cleveringa, J. 2008. Ontwikkeling sedimentvolume Eems-Dollard en het Groninger wad: Overzicht van de beschikbare kennis en gegevens. rapport A2269. Alkyon, Marknesse. 47 pp.

Duinker, J.C., Hillebrand, M.T.J, Nolting, R.F. and Wellershaus, S. (1985). The river Ems: Processes affecting the behaviour of metals and organochlorines during estuarine mixing. Netherlands Journal of Sea Research, 19 (1): 19-29.

Harezlak, V., W. Stolte, en A.J. Nolte (2014). Objectiveren van onzekerheid van gebiedsmodellen voor waterkwaliteit en ecologie. Deltares report 1207726-000, 112 p.

Haskoning (2013). Maatregelstudie Eems-Dollard, Economie en Ecologie in balans: Hydrodynamisch berekeningen en effectbepaling herstelmaatregelen Eems-Dollard. BC4649-100/R0002/MvH/JEBR/Nijm, 52 p.

Hasselmann, K., T. P. Barnett, E. Bouws, H. Carlson, D. E. Cartwright, K. Enke, J. Ewing, H. Gienapp, D. E. Hasselmann, P. Kruseman, A. Meerburg, P. Müller, D. J. Olbers, K. Richter, W. Sell and H. Walden, 1973. "Measurements of wind wave growth and swell decay during the Joint North Sea Wave Project (JONSWAP)." Deutsche Hydrographische Zeitschrift 8 (12). 44, 125, 127, 132

Herrling, G. and Niemeyer, H.D. (2008). Comparison of the hydrodynamic regime of 1937 and 2005 in the Ems-Dollard estuary by applying mathematical modelling. Harbasins Report.

Holthuijsen, L.H. (2007), Waves in oceanic and coastal waters, Cambridge University Press.

Krebs, M. and H. Weilbeer, 2008. Ems-Dollart Estuary. Die Kueste 74, p. 252-262.

Krebs, M. (2012). Historical developments in the Ems estuary and its area. Overview of morphological human-induced changes to the Ems River and estuary. WSA Emden, Germany. NCK presentation.

Pawlowicz, R., Beardsley, B. and Lentz, S. (2002), Classical tidal harmonic analysis including error estimates in MATLAB using T-TIDE, Computers & Geosciences 28, 929-937.

Rijkswaterstaat, 2009. Programma Rijkswateren 2010-2015 Uitwerking Waterbeheer 21e eeuw, Kaderrichtlijn Water en Natura 2000 Beheer- en Ontwikkelplan voor de Rijkswateren 2010-2015 (366 p.)

Schoemans, M. (2013). Tidal changes in the Lower Ems (1945-2005): reconstructing the effects of channel deepening and bottom roughness. BSc report, Utrecht University.

Talke, S.A., H.E. de Swart, and H.M. Schuttelaars. 2009. Feedback between residual circulations and sediment distribution in highly turbid estuaries: an analytical model. *Continental Shelf Research* 29: 119–135. doi:10.1016/j.csr.2007.09.002.

Van Vledder, G., Zijlema, M. and Holthuijsen, L.H. (2010), Revisiting the JONSWAP bottom friction formulation, *Proceedings of the 32nd International Conference on Coastal Engineering*, 1(32).

Van Kessel, T., W. Stolte, J. Dijkstra (2013). Development and application of effect chain model Ems-Dollard period 2009 – 2012. Deltares report 1206237.

Winterwerp, J.C. (2011). Fine sediment transport by tidal asymmetry in the high-concentrated Ems River: indications for a regime shift in response to channel deepening. *Ocean Dynamics* 61:203-215.

## A Waterlevels WED model

Figure description:

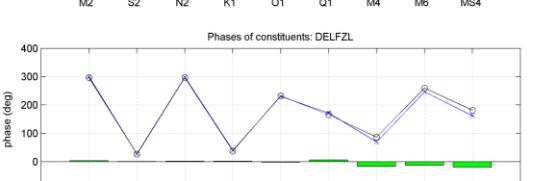
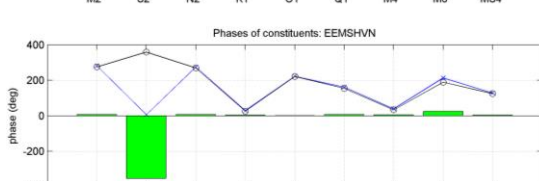
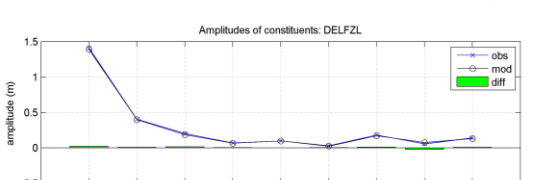
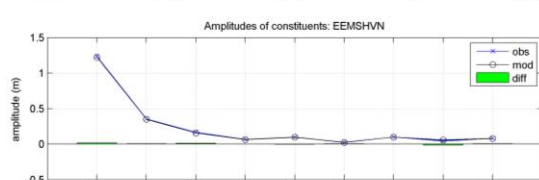
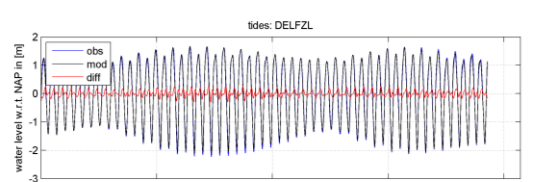
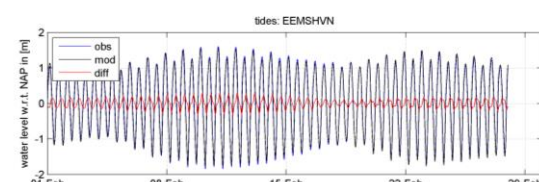
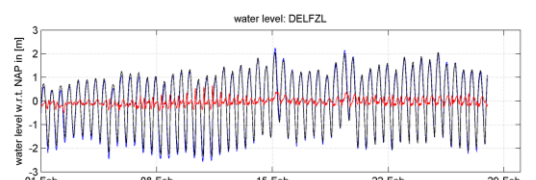
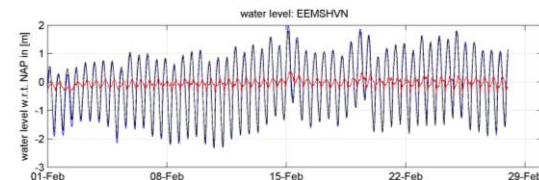
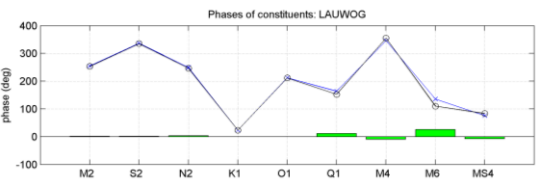
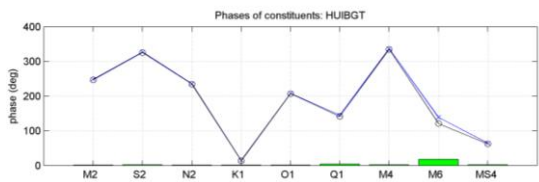
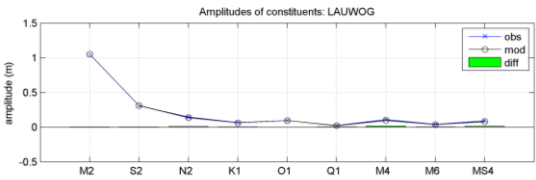
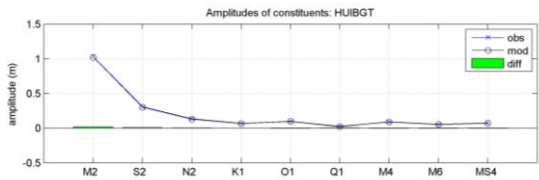
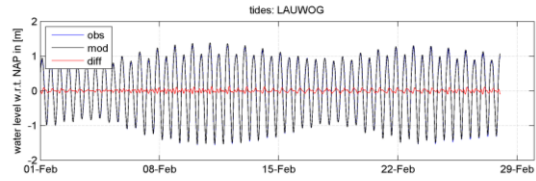
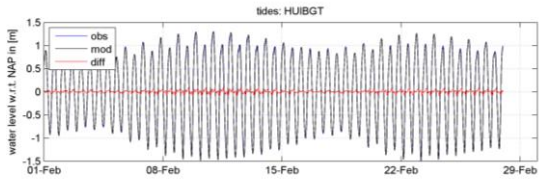
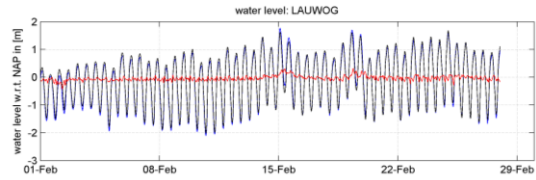
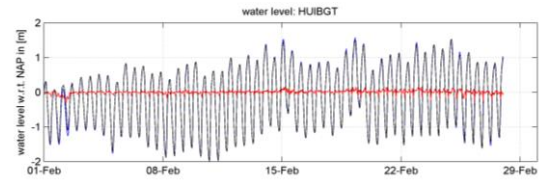
Top panel: computed and observed waterlevel (in m above MSL), and difference between observed and computed value.

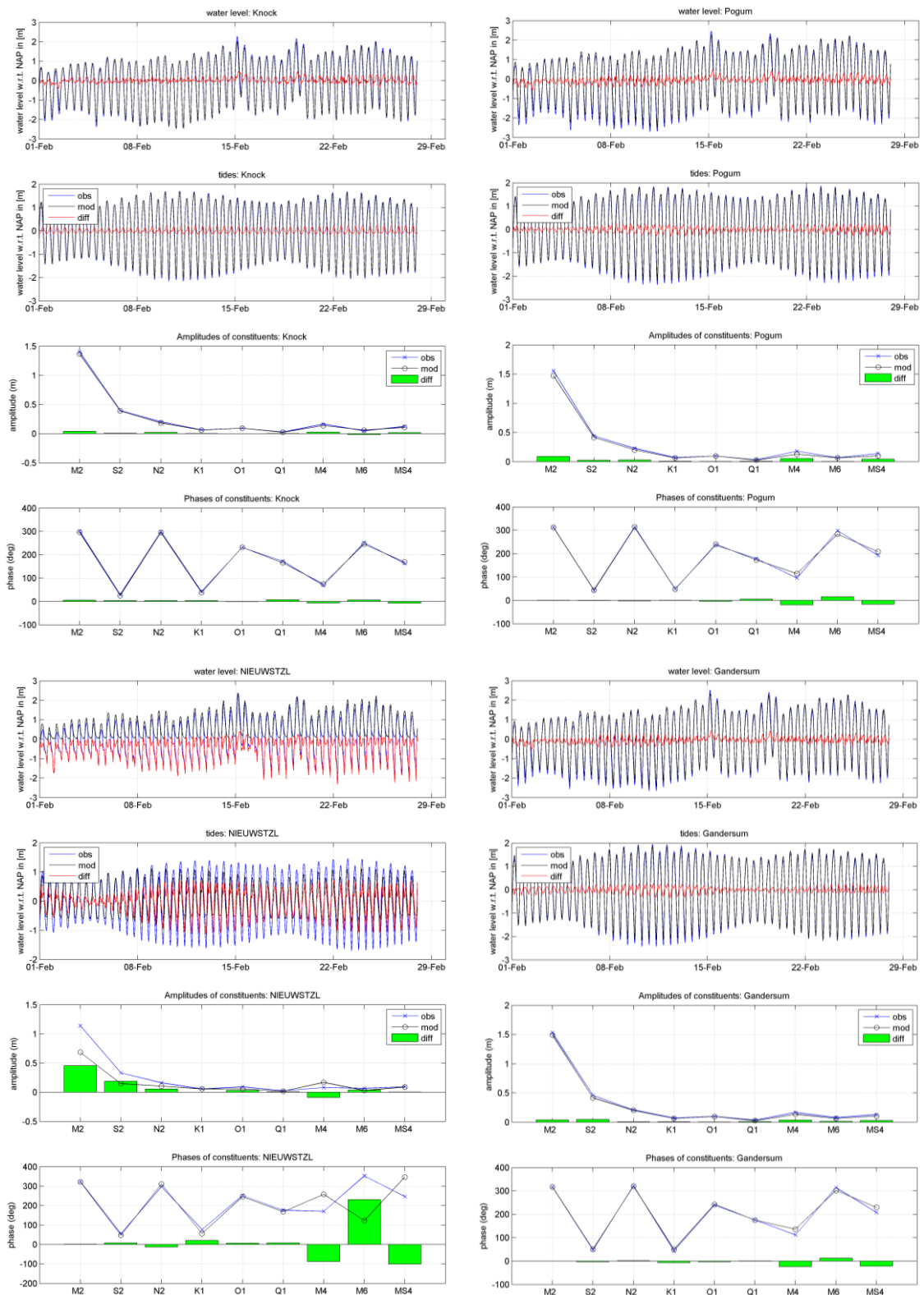
Second panel: computed and observed tidal amplitude(in m above MSL), and difference between observed and computed value.

Third panel: Observed and computed tidal amplitude per constituent, and difference between observed and computed value

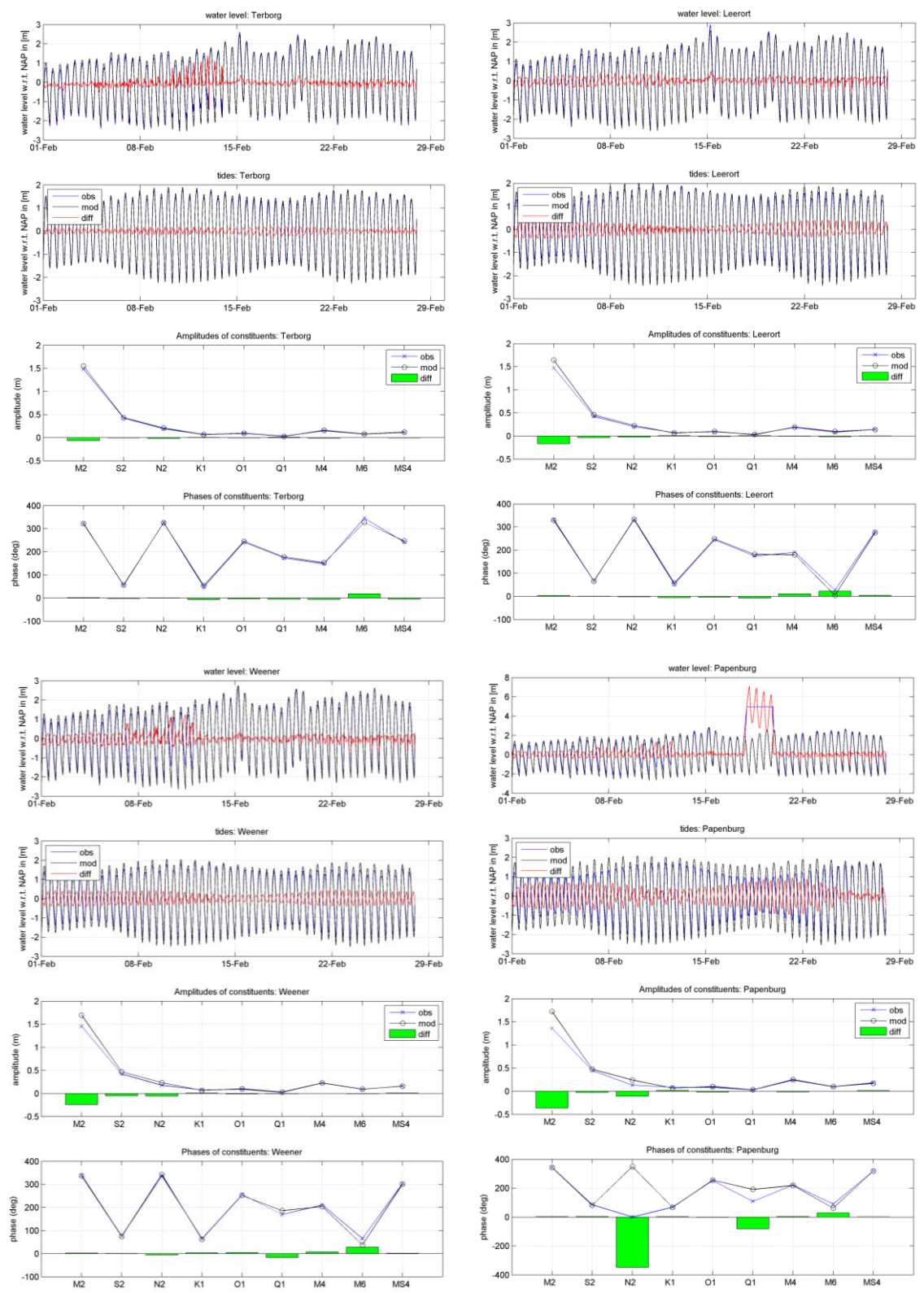
Fourth panel: Observed and computed tidal phase per constituent, and difference between observed and computed value

## A.1 2012

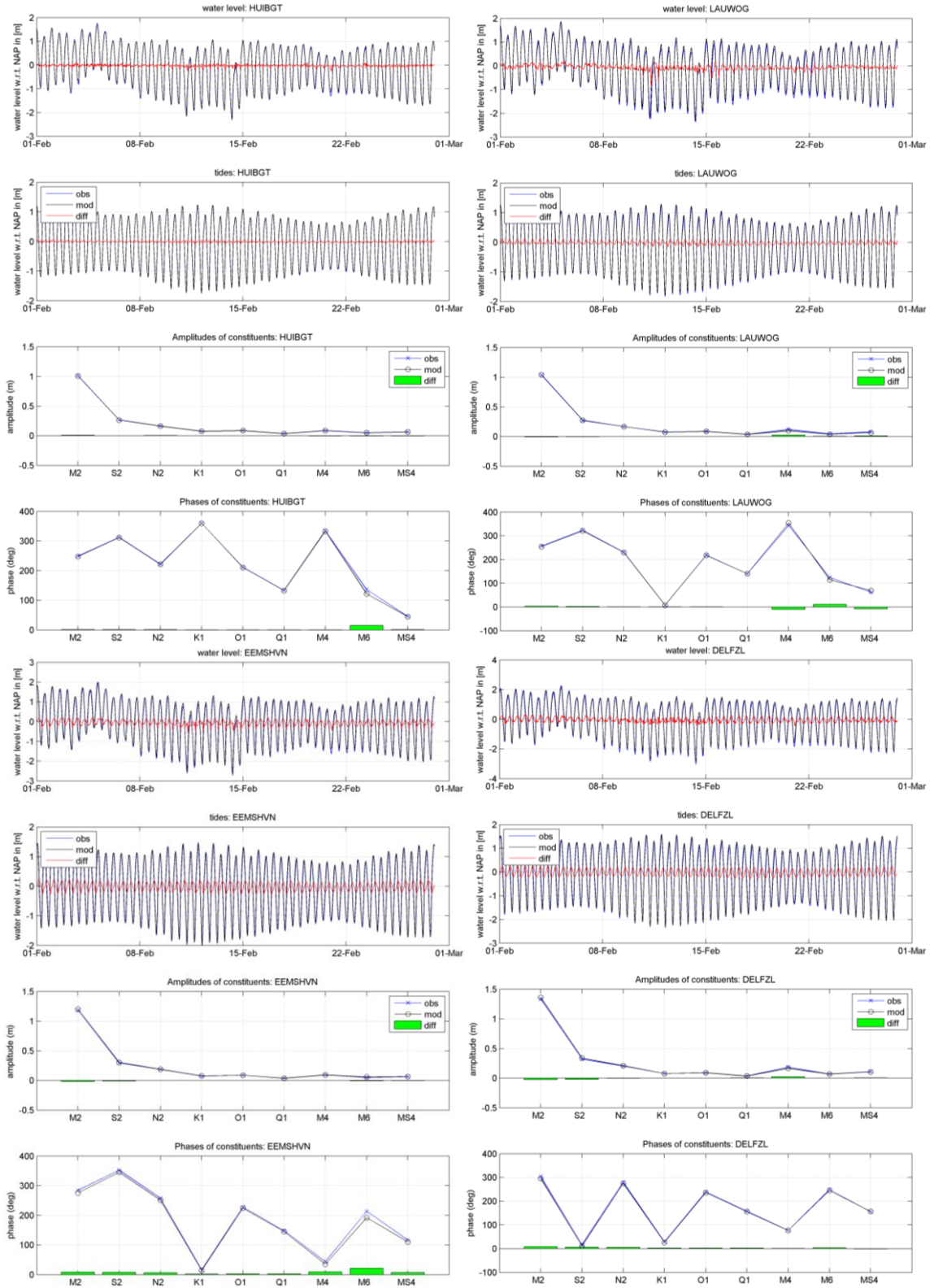


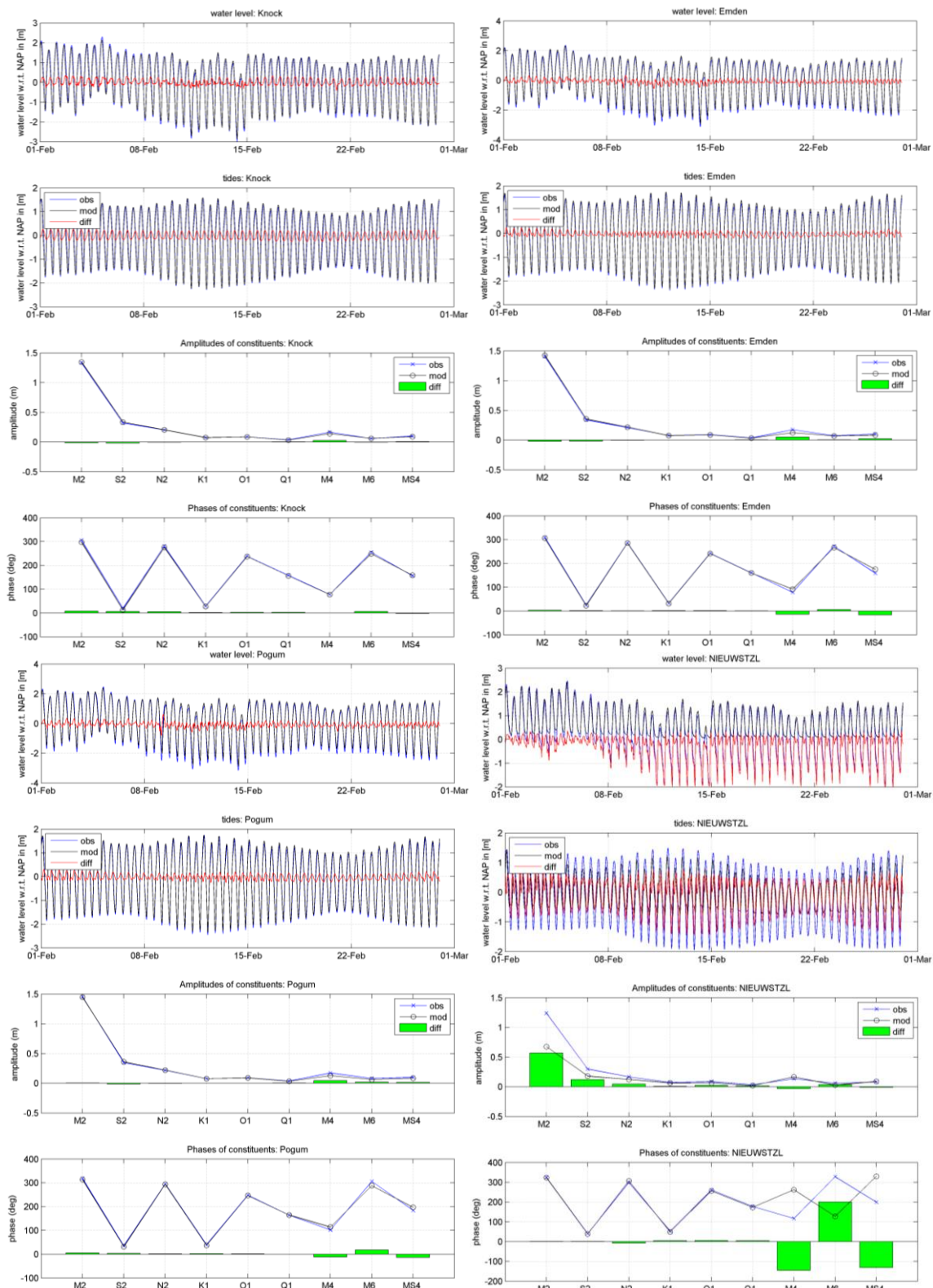




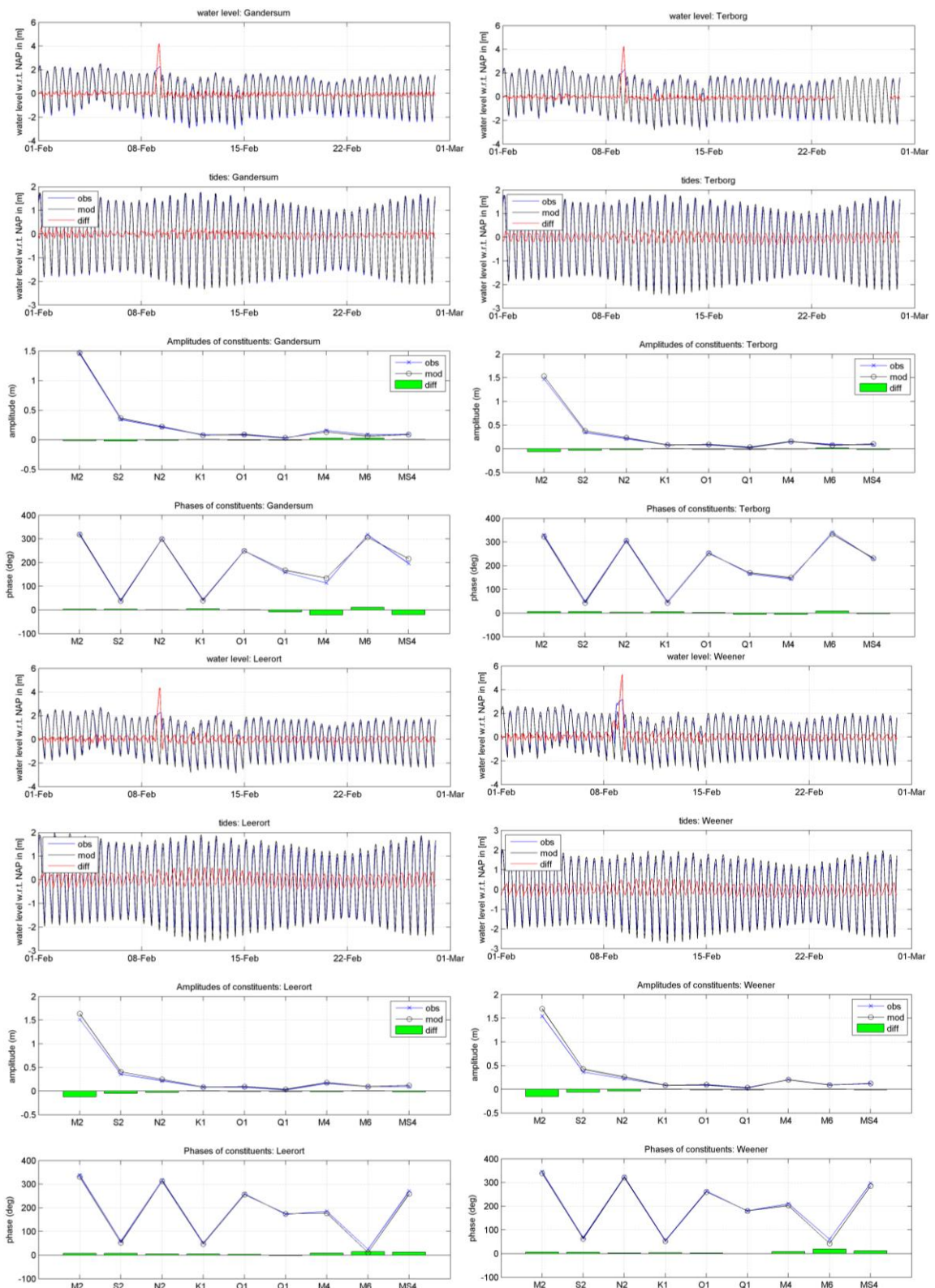


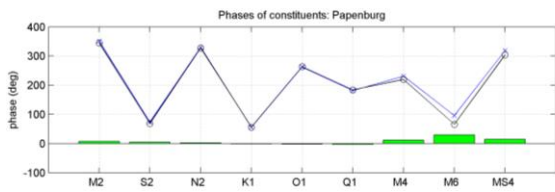
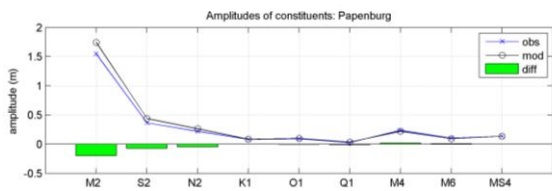
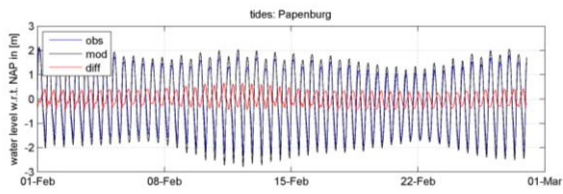
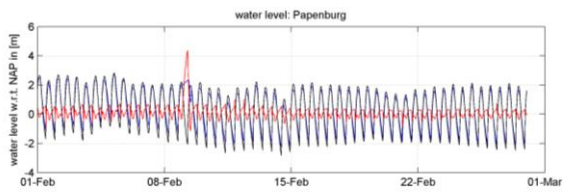
A.2 2013





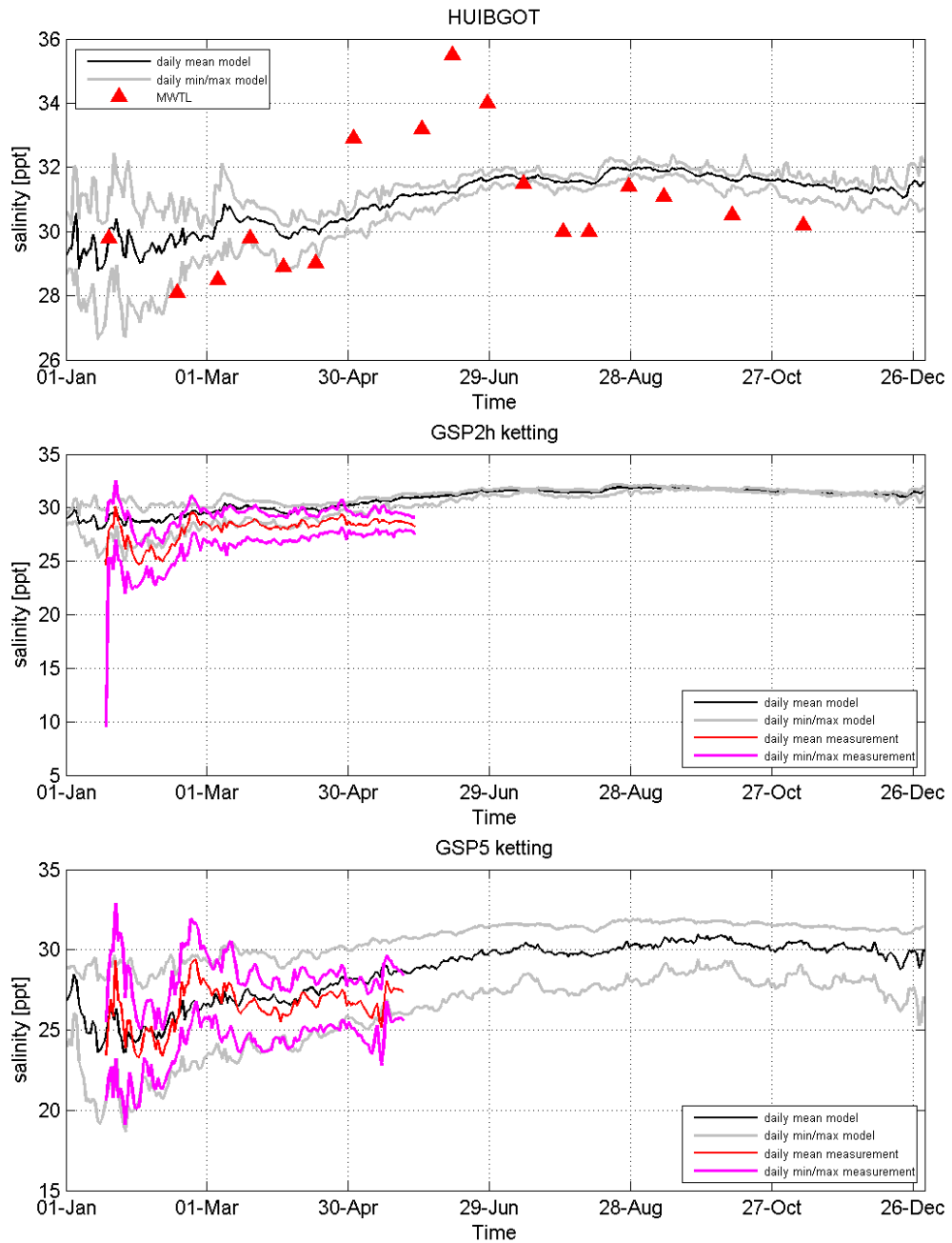


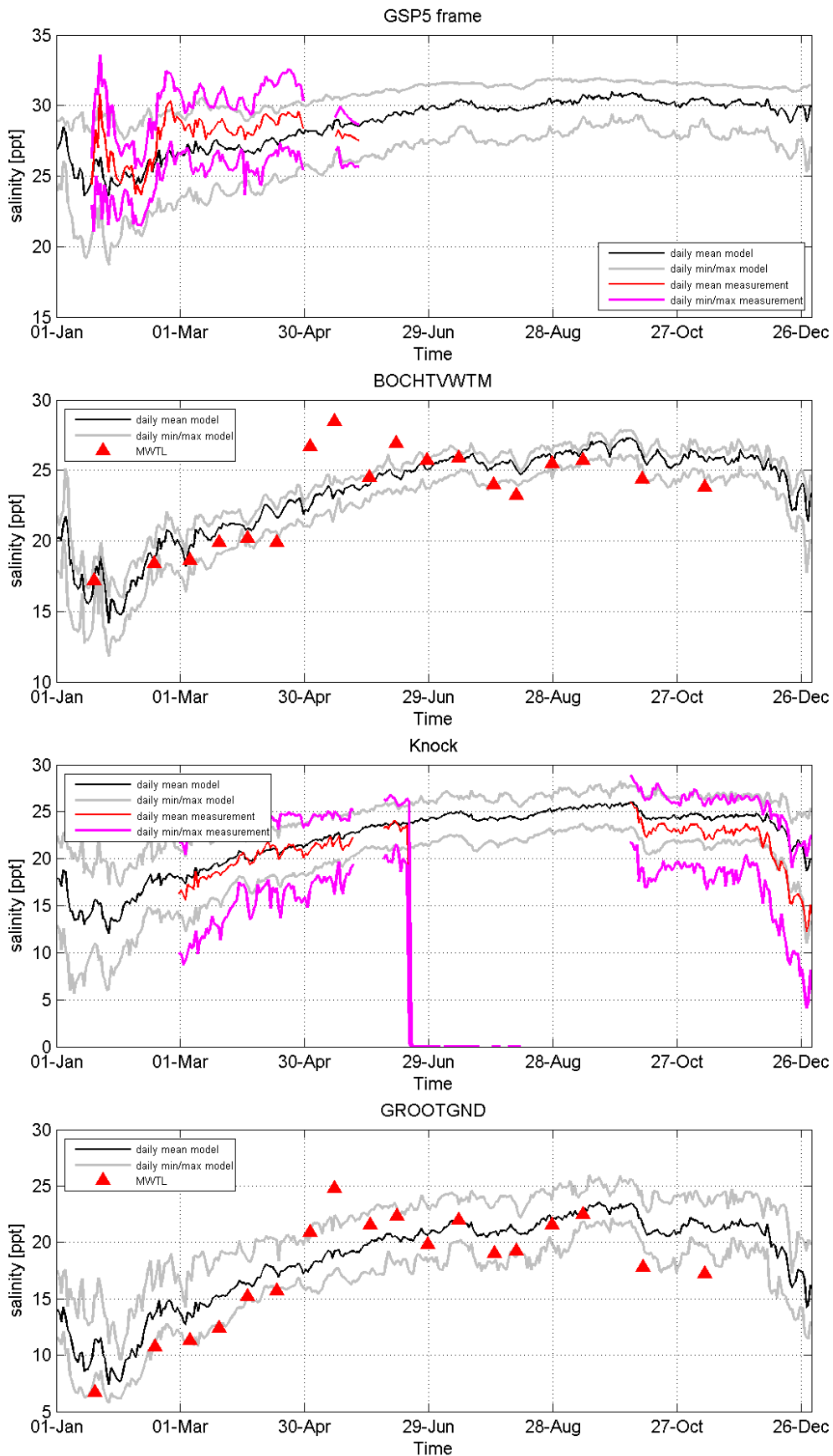


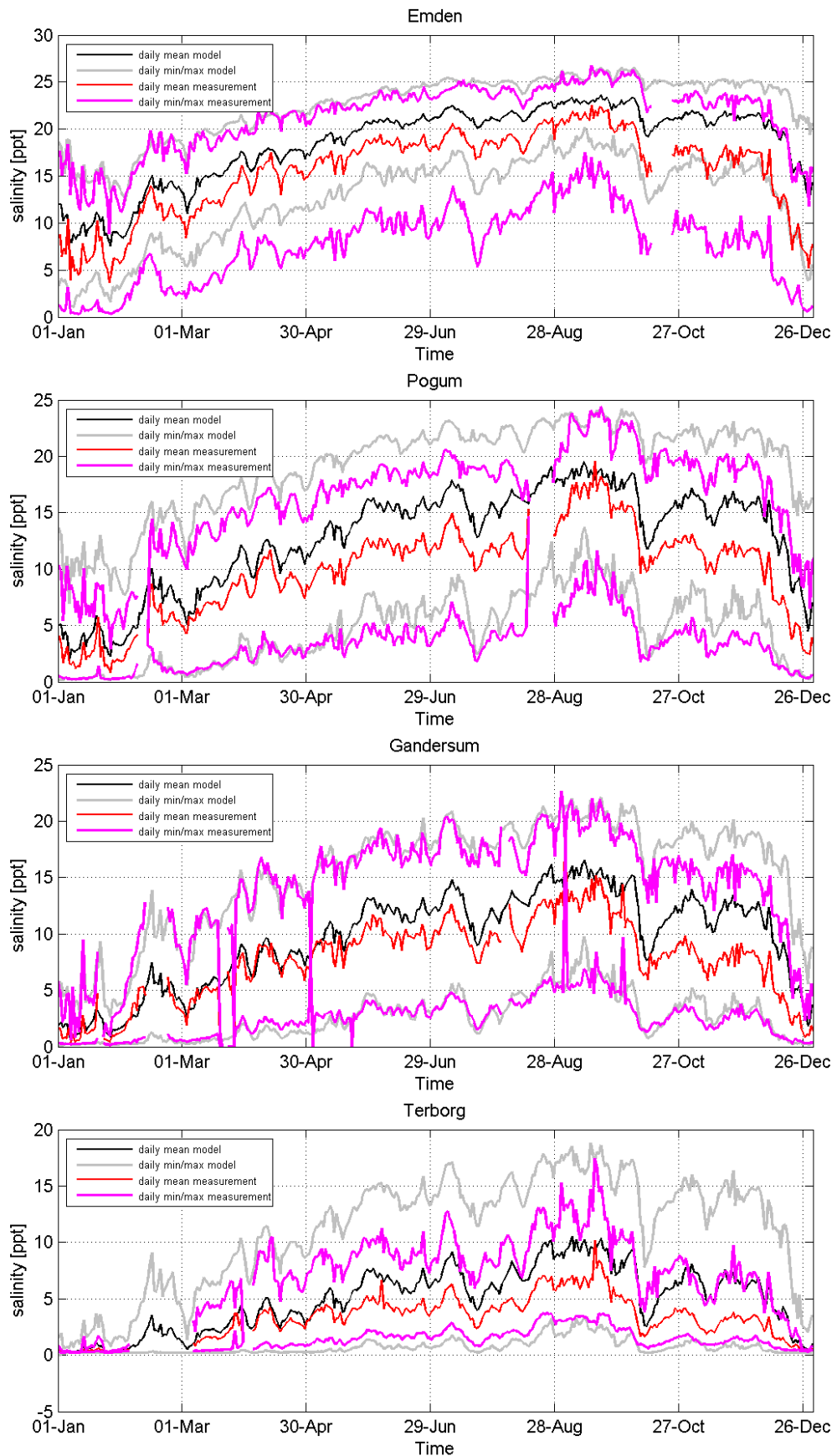


## B Salinity WED model

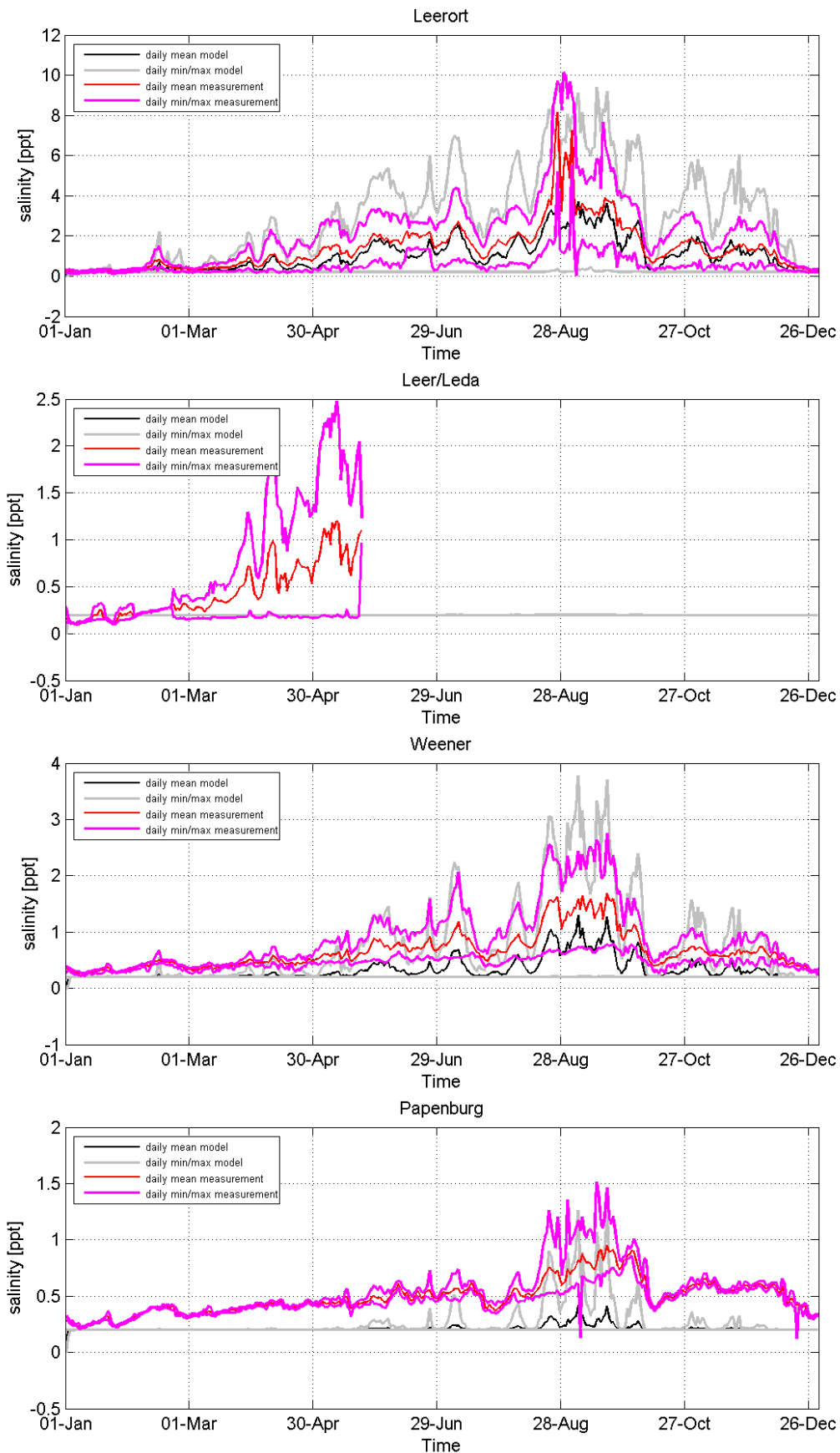
### B.1 2012

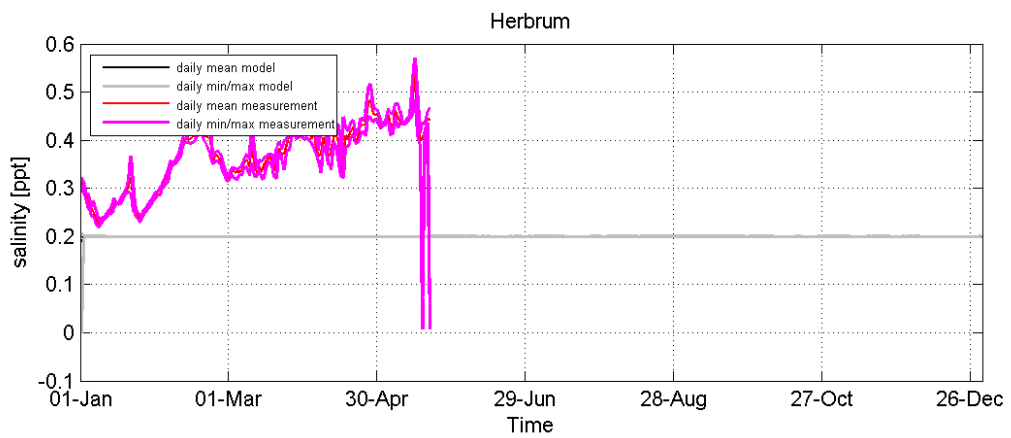




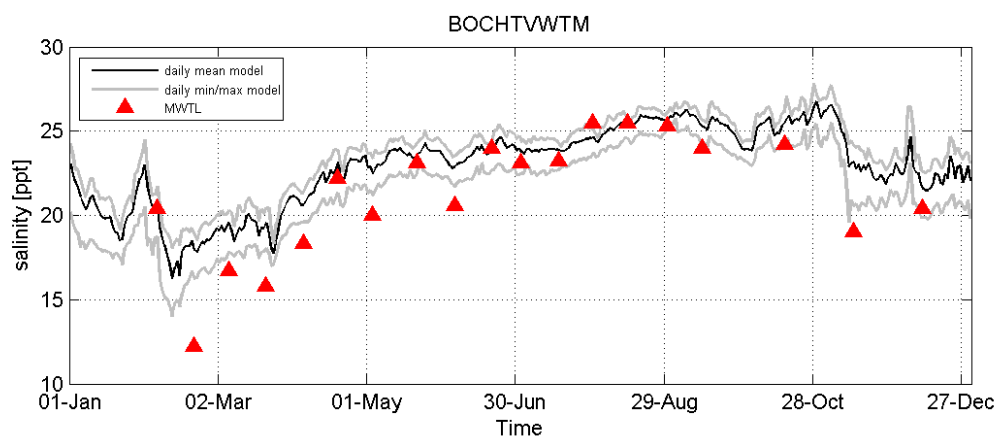
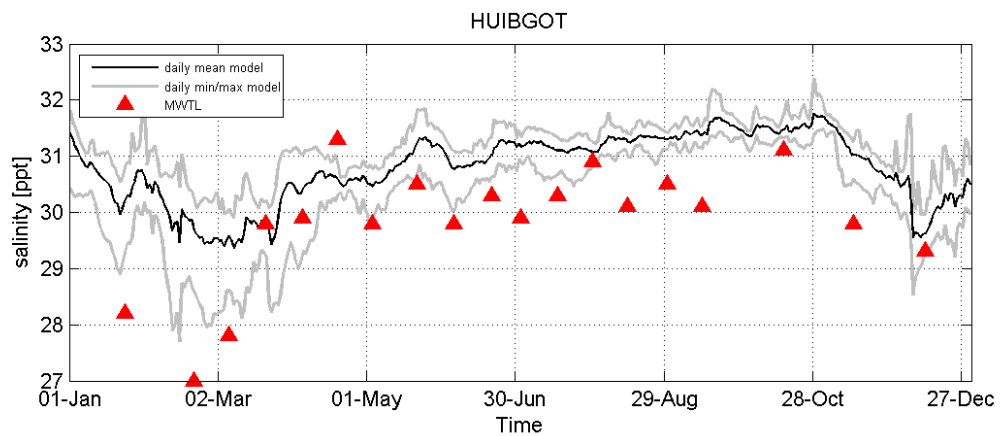


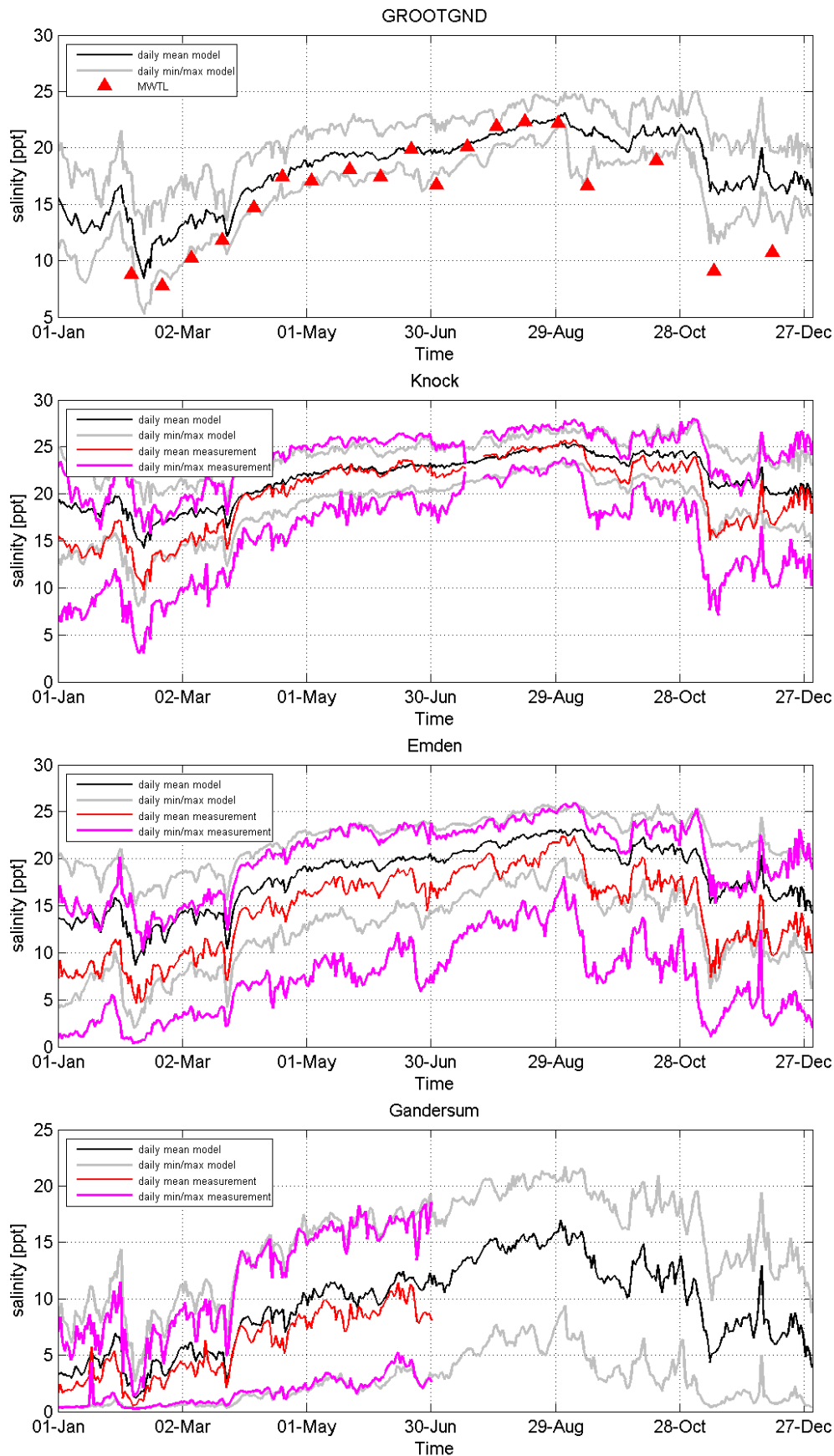


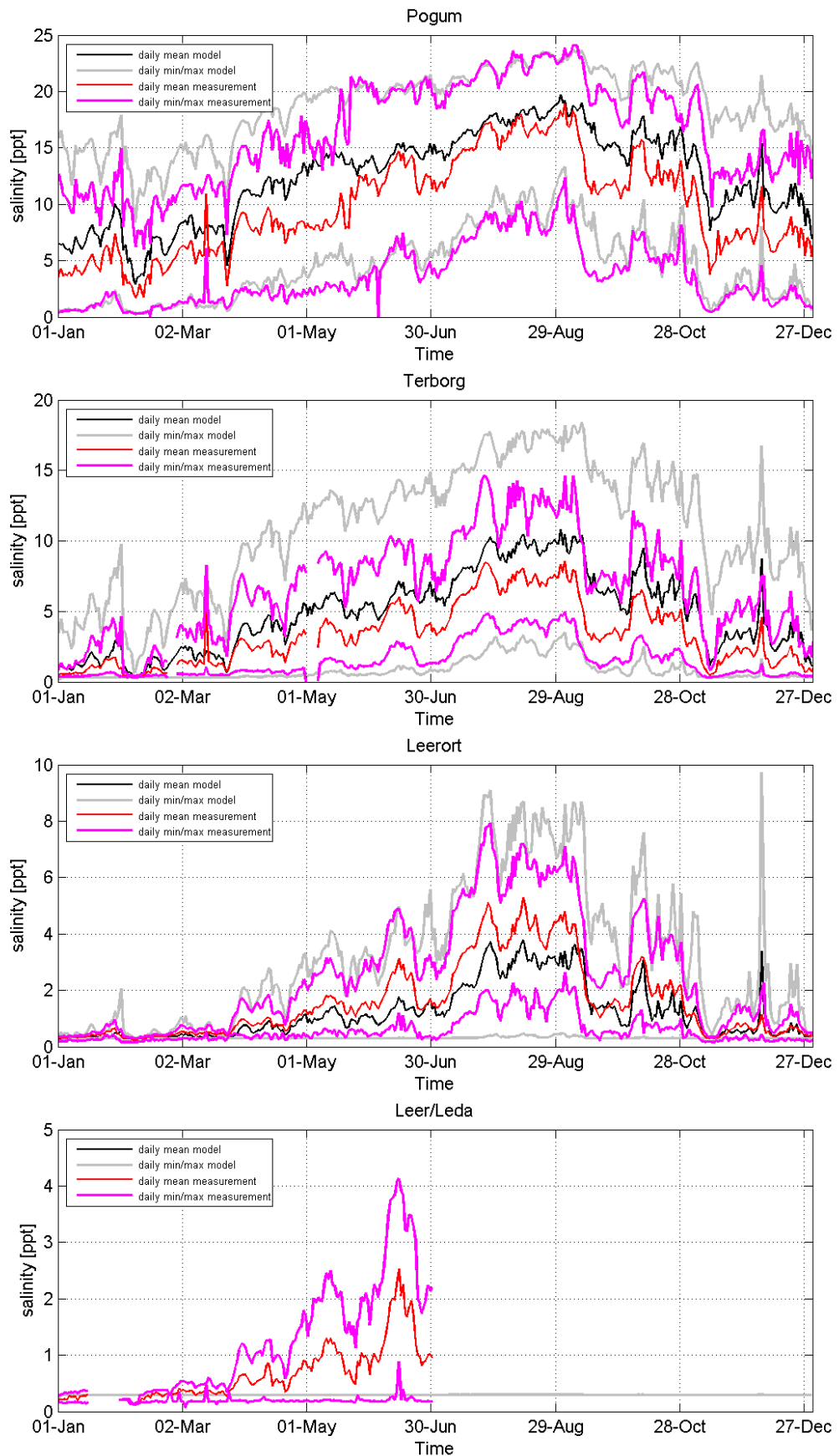


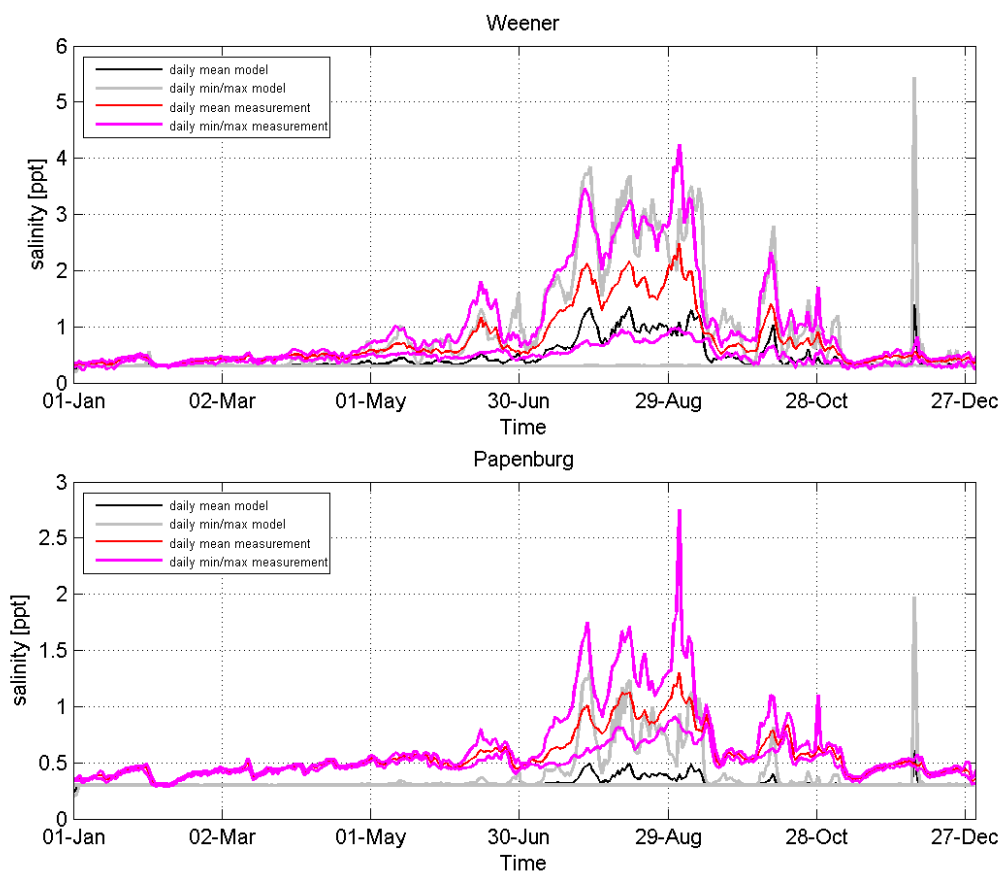


**B.2 2013**









## **C Calibration waterlevels, ERD model, frequency domain**

Figure description:

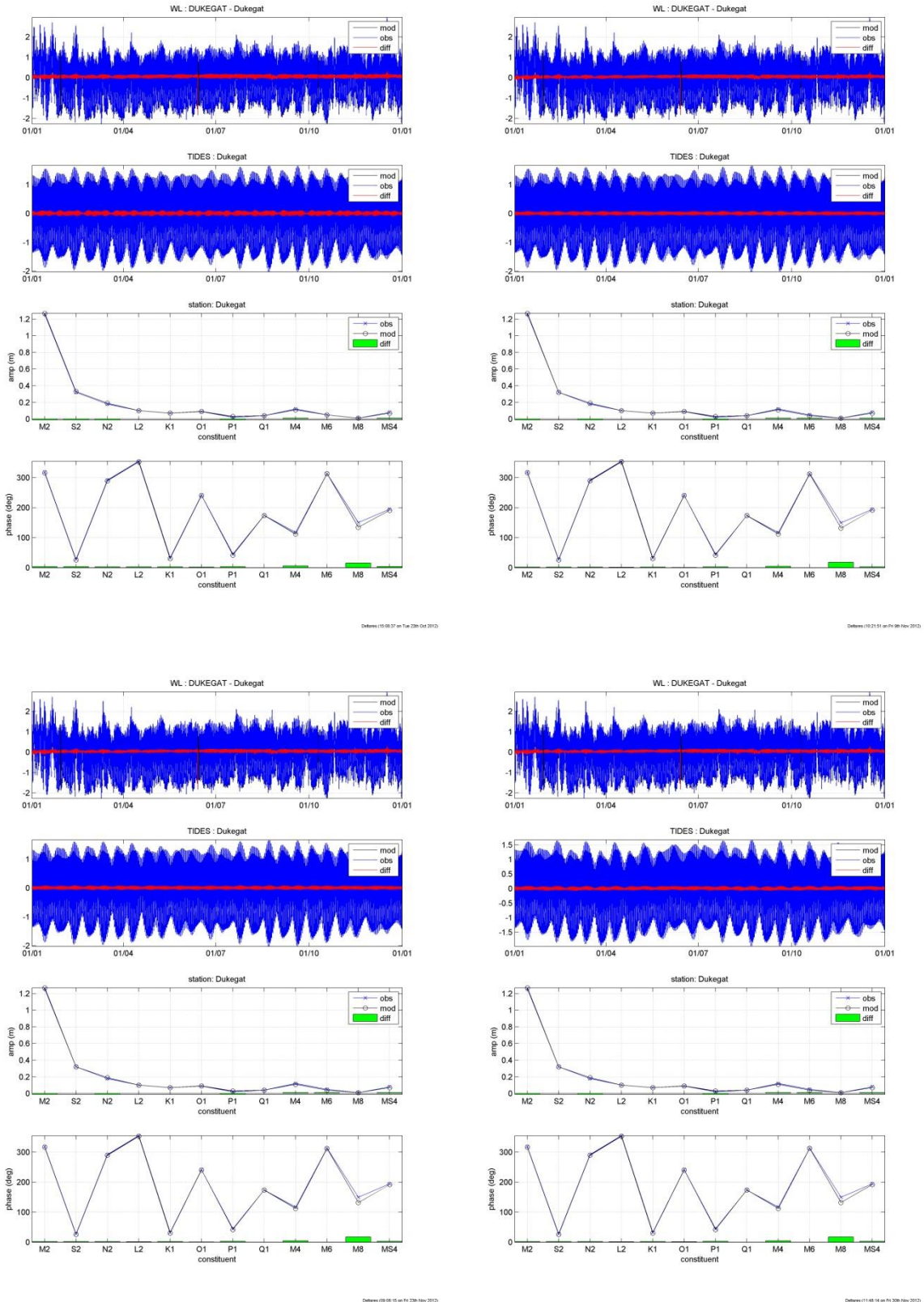
Top panel: computed and observed waterlevel (in m above MSL), and difference between observed and computed value.

Second panel: computed and observed tidal amplitude(in m above MSL), and difference between observed and computed value.

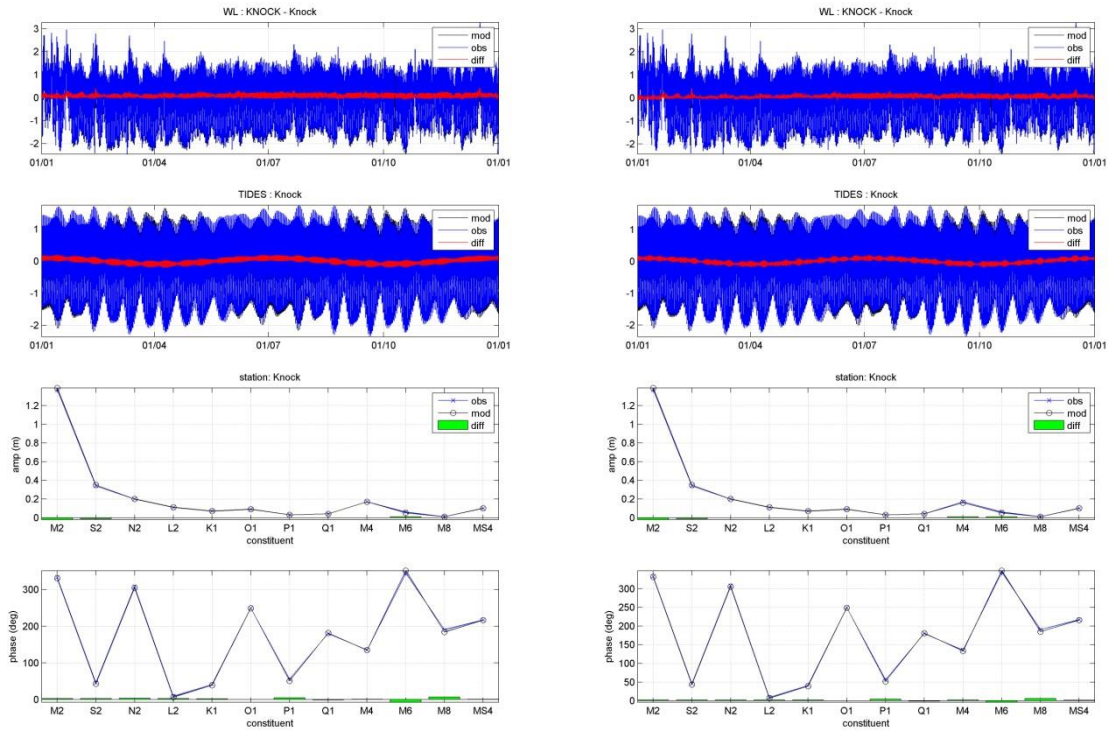
Third panel: Observed and computed tidal amplitude per constituent, and difference between observed and computed value

Fourth panel: Observed and computed tidal phase per constituent, and difference between observed and computed value

## C.1 Dukegat (top left: Cal 01, top right: Cal09, lower left: Cal14, lower right: Cal 16)



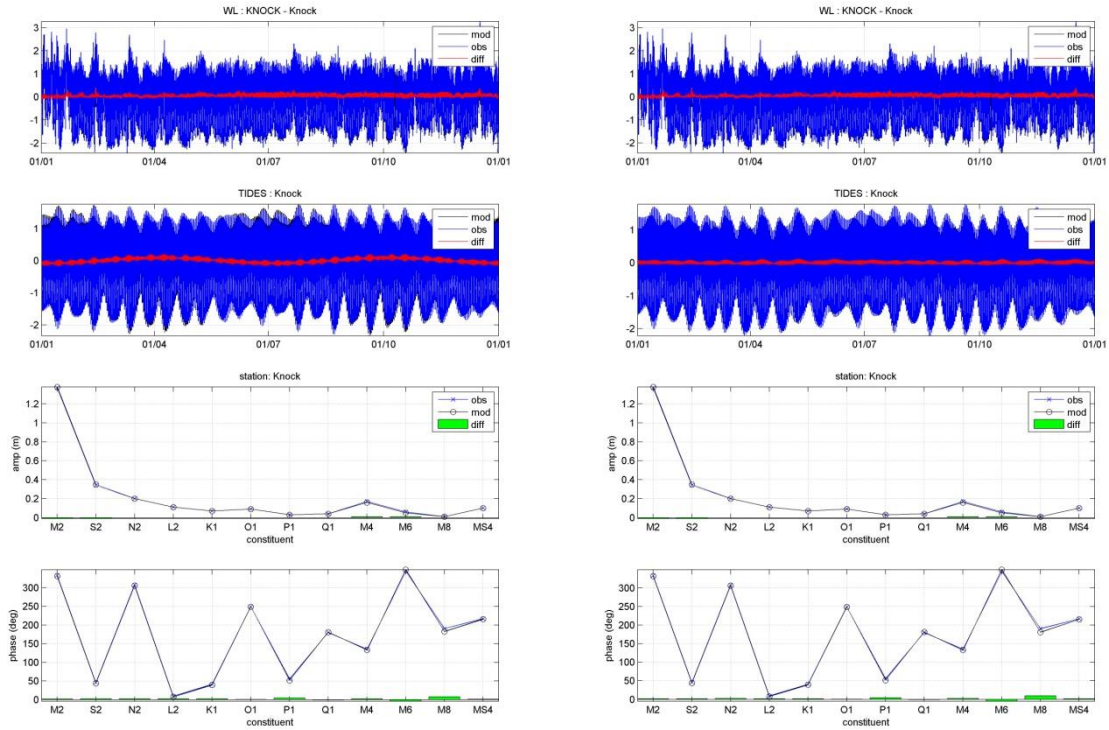
c.2 Knock (top left: Cal 01, top right: Cal09, lower left: Cal14, lower right: Cal 16)



Deltares | 15:13:00 on Tue 22th Oct 2012

Deltares | 15:22:39 on Fri 9th Nov 2012

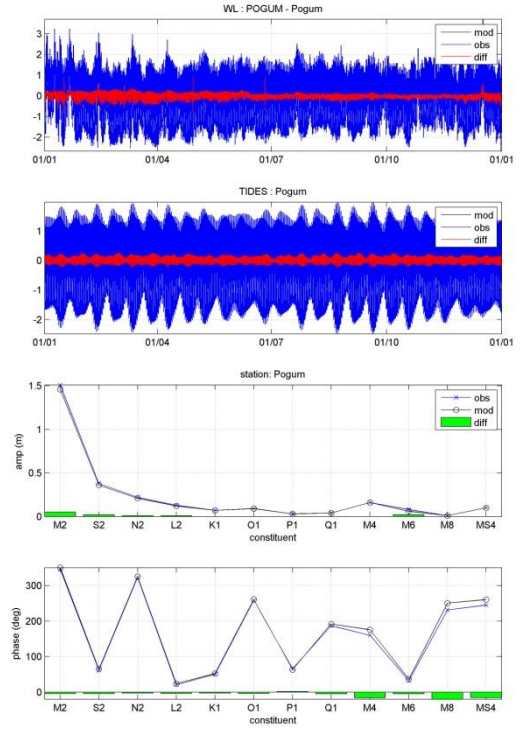
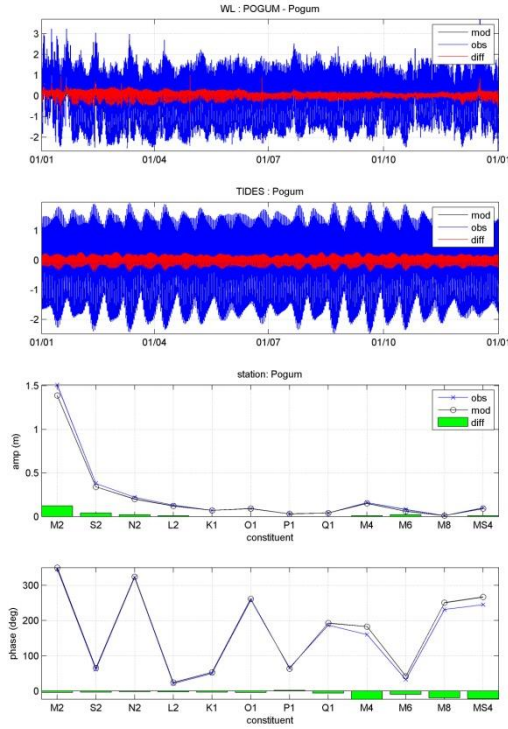




Deltares (2011.12.14 on Fri 22th Nov 2012)

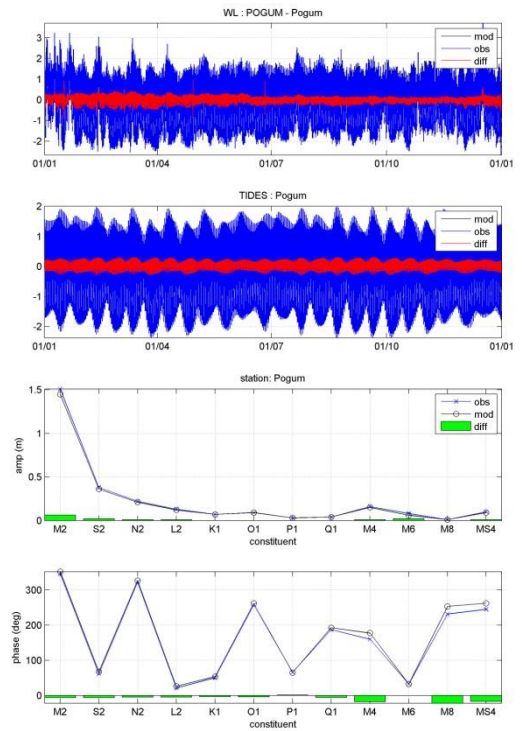
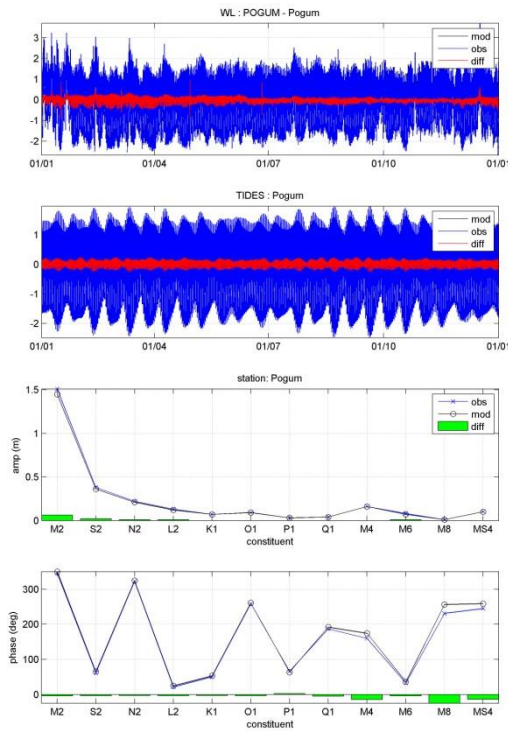
Deltares (11.09.20 on Fri 22th Nov 2012)

c.3 Pogum (top left: Cal 01, top right: Cal09, lower left: Cal14, lower right: Cal 16)



Deltares 10-11-10 on Tue 23th Oct 2012

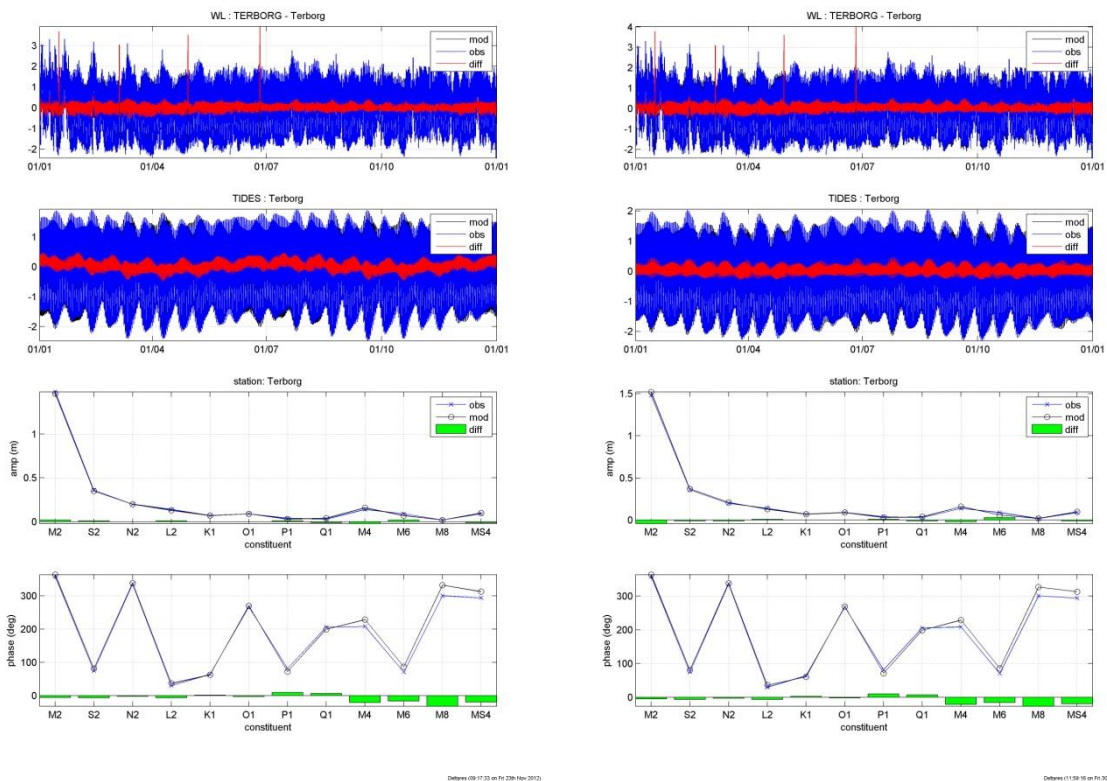
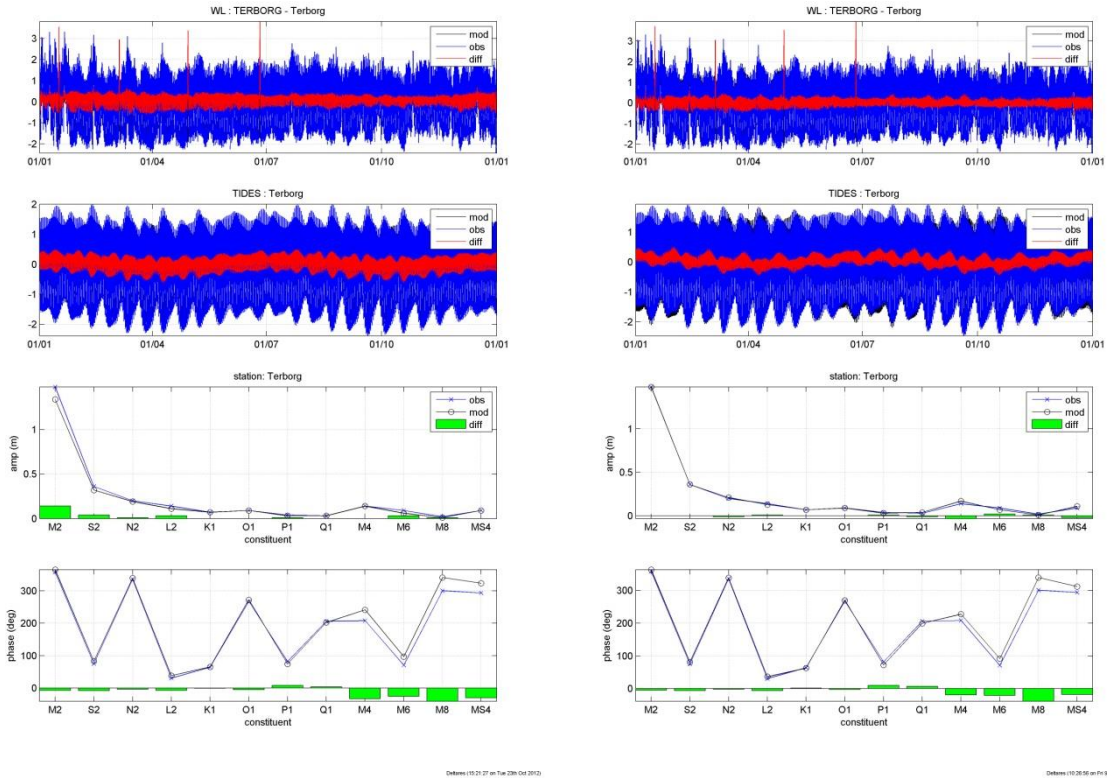
Deltares 10-11-10 on Fri 26th Nov 2012



Deltares 09-14-12 on Fri 23th Nov 2012

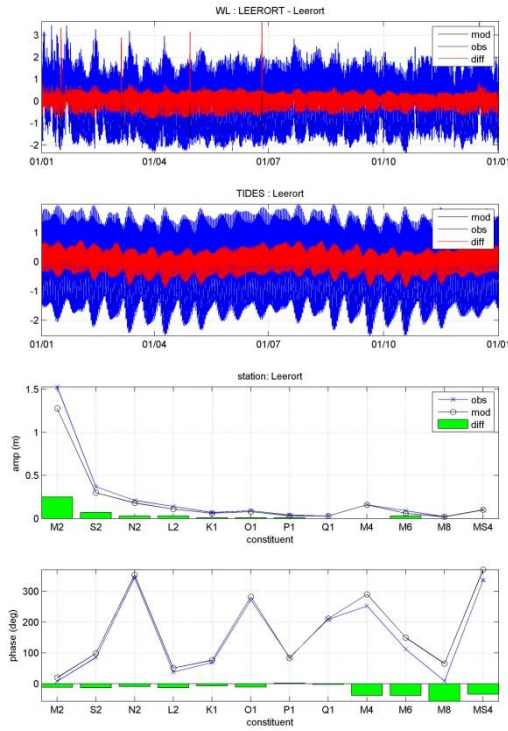
Deltares 11-02-12 on Fri 26th Nov 2012

## c.4 Terborg (top left: Cal 01, top right: Cal09, lower left: Cal14, lower right: Cal 16)

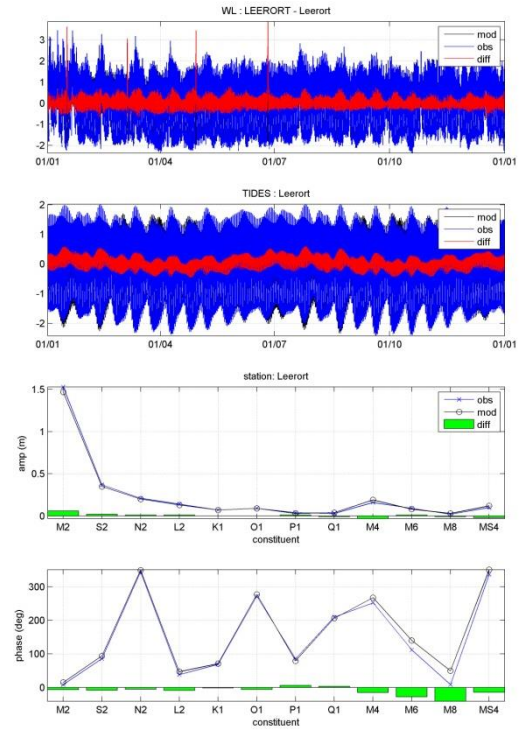




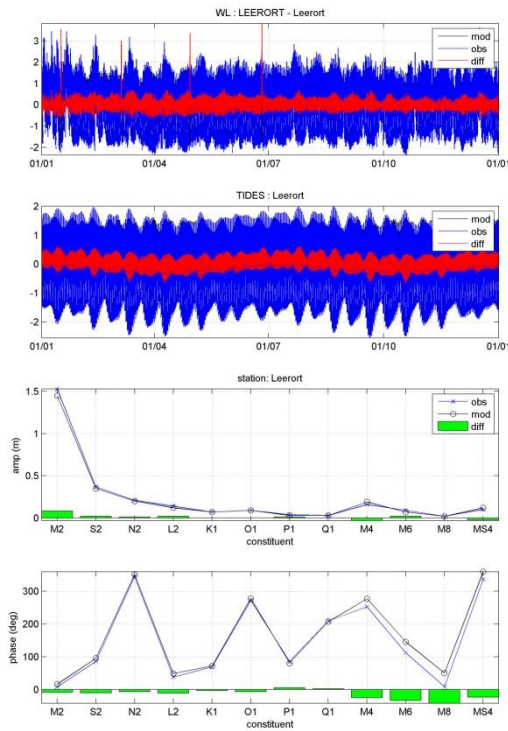
c.5 Leerort (top left: Cal 01, top right: Cal09, lower left: Cal14, lower right: Cal 16)



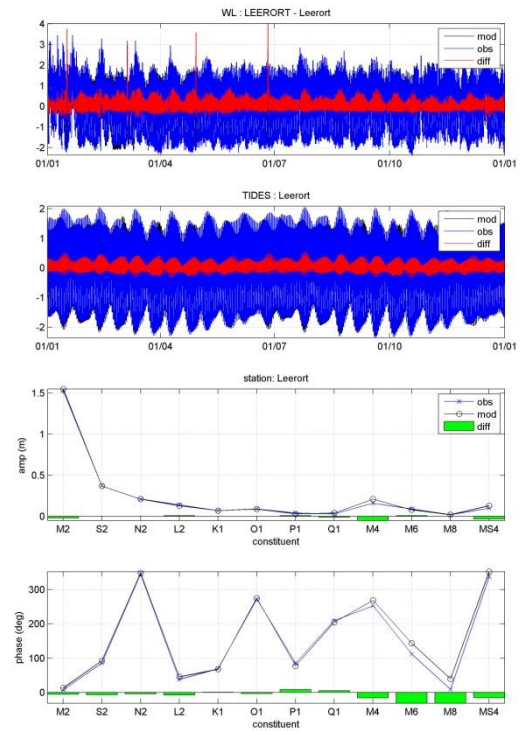
Deltares 13.02.12 on Tue 23th Oct 2012



Deltares 13.02.12 on Fri 26th Nov 2012

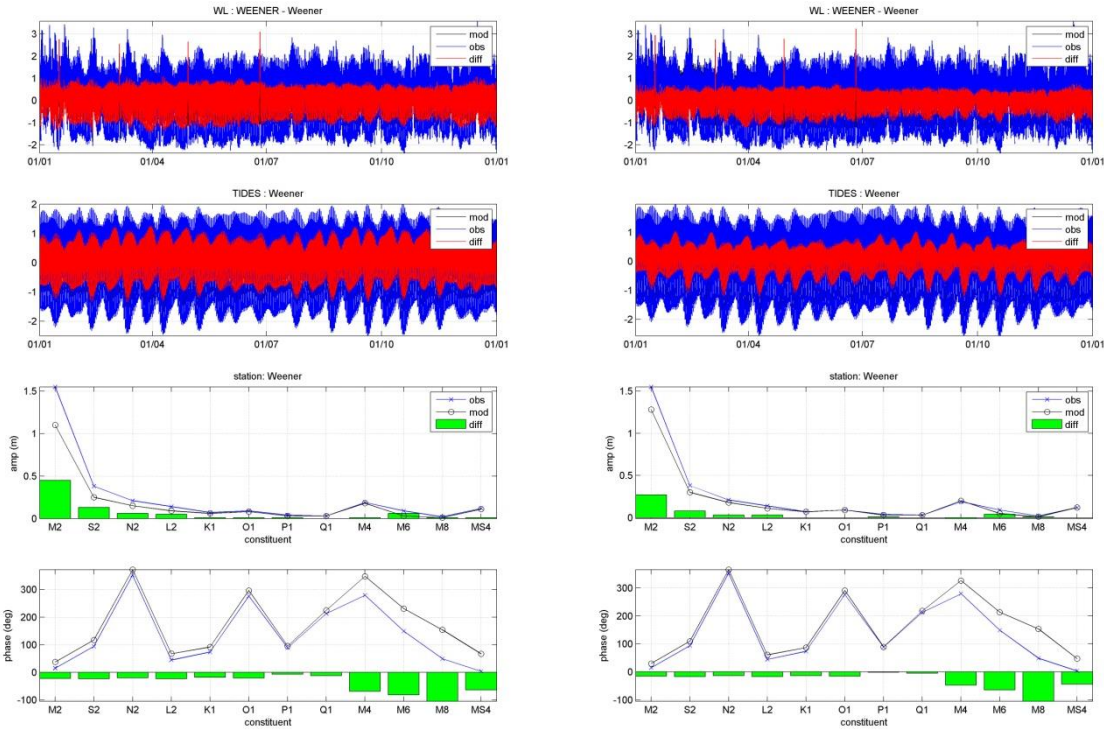


Deltares 09.02.12 on Fri 23th Nov 2012



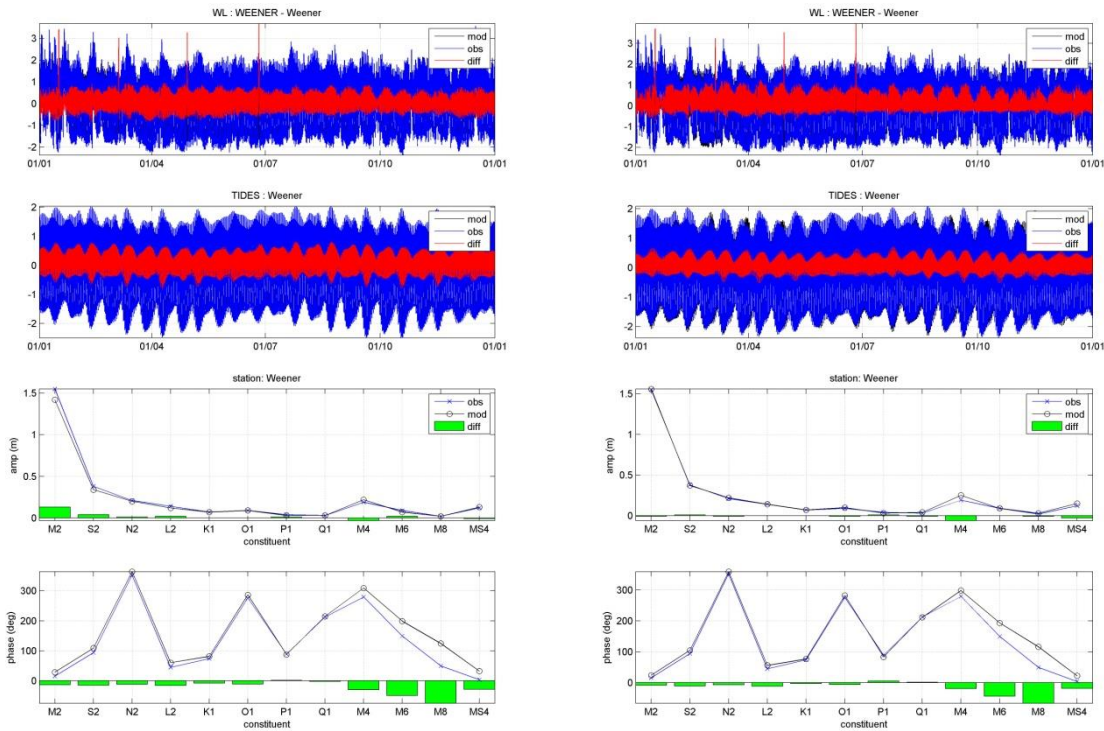
Deltares 13.02.12 on Fri 26th Nov 2012

## c.6 Weener (top left: Cal 01, top right: Cal 09, lower left: Cal 14, lower right: Cal 16)



Deltares (12.03.02) on Fri 22th Oct 2014

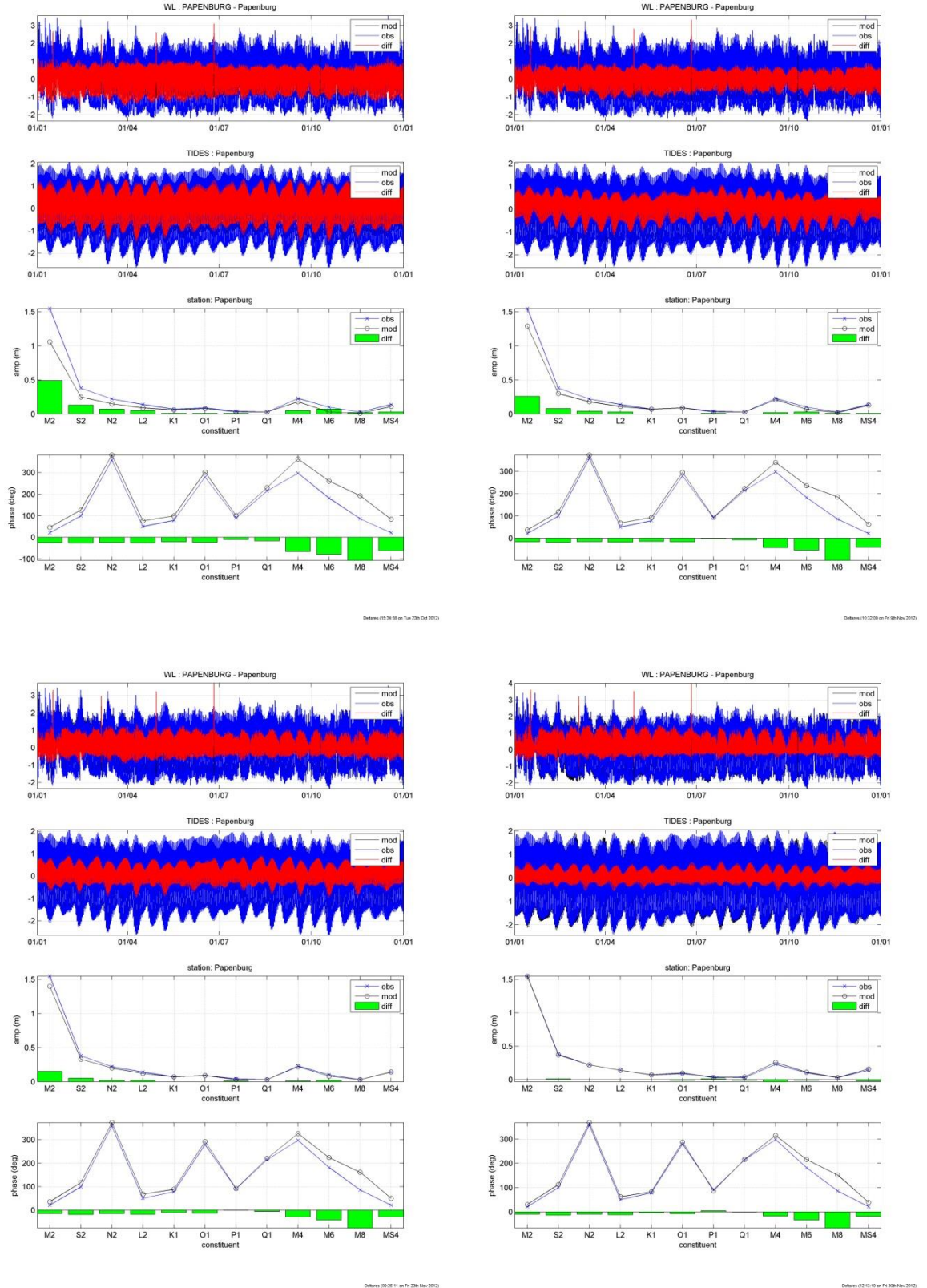
Deltares (12.03.02) on Fri 22th Nov 2014



Deltares (12.03.02) on Fri 22th Nov 2014

Deltares (12.03.02) on Fri 22th Nov 2014

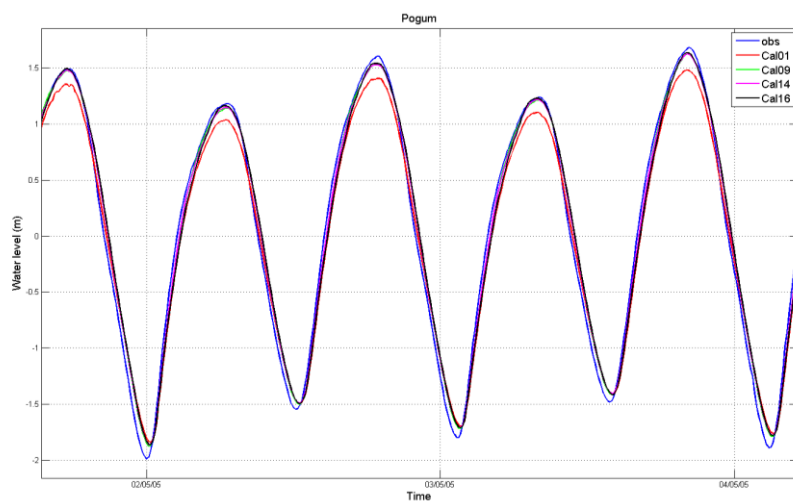
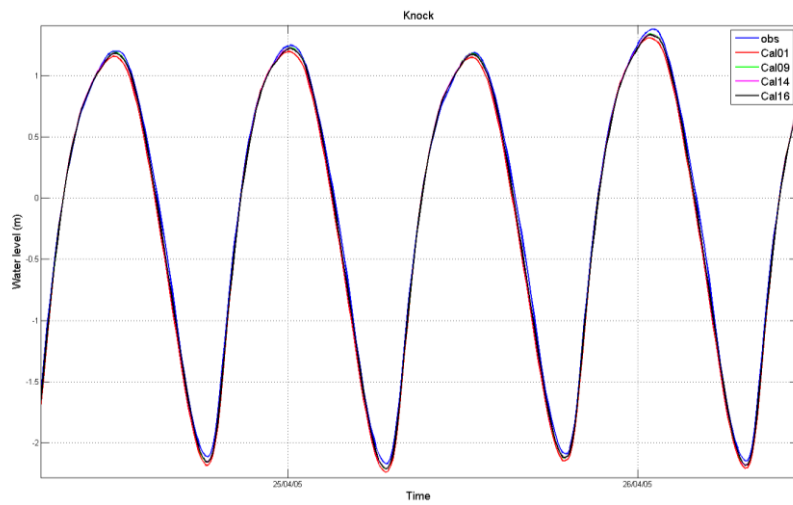
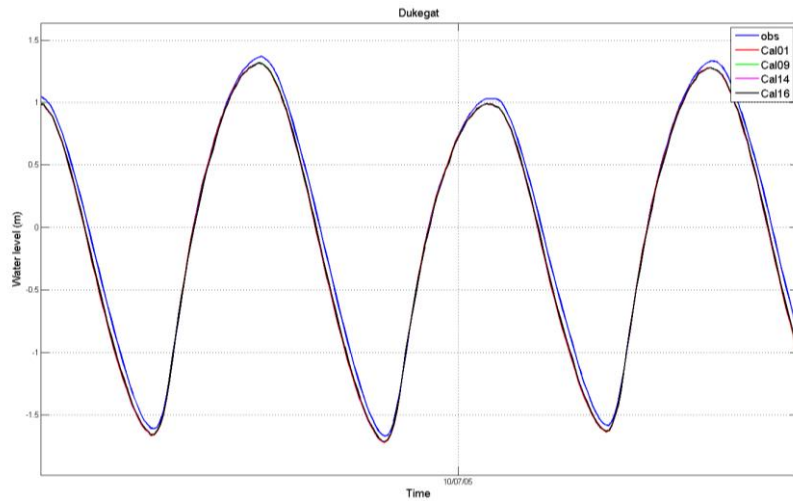
c.7 Papenburg (top left: Cal 01, top right: Cal 09, lower left: Cal 14, lower right: Cal 16)



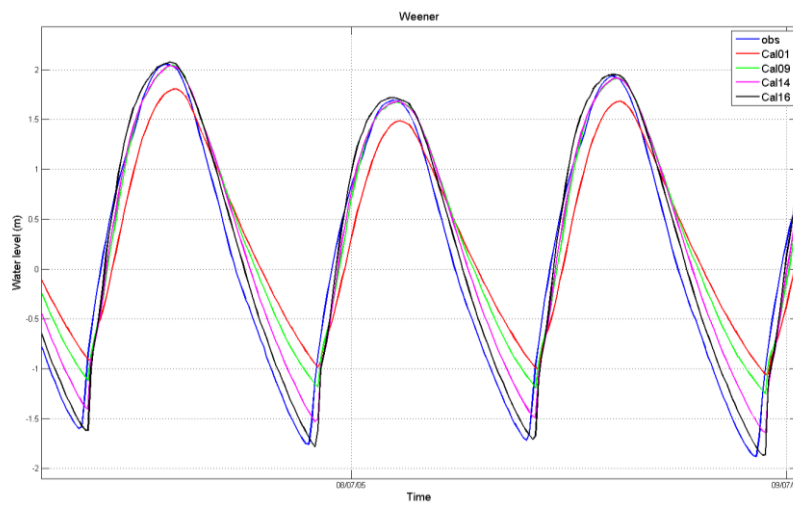
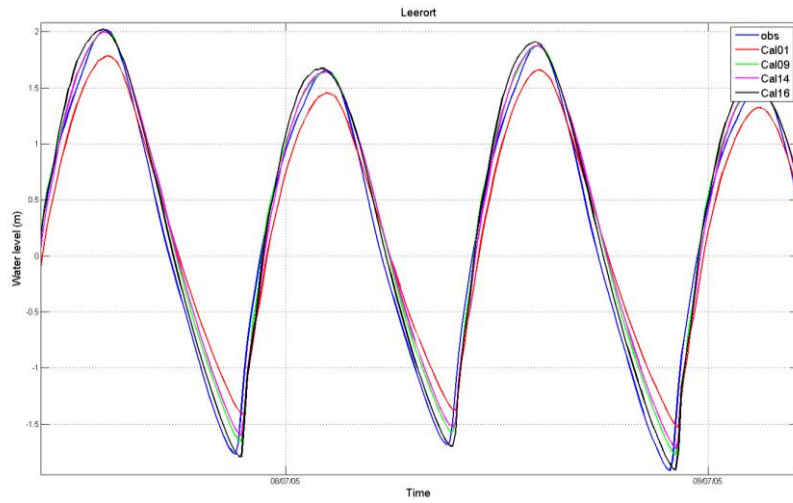
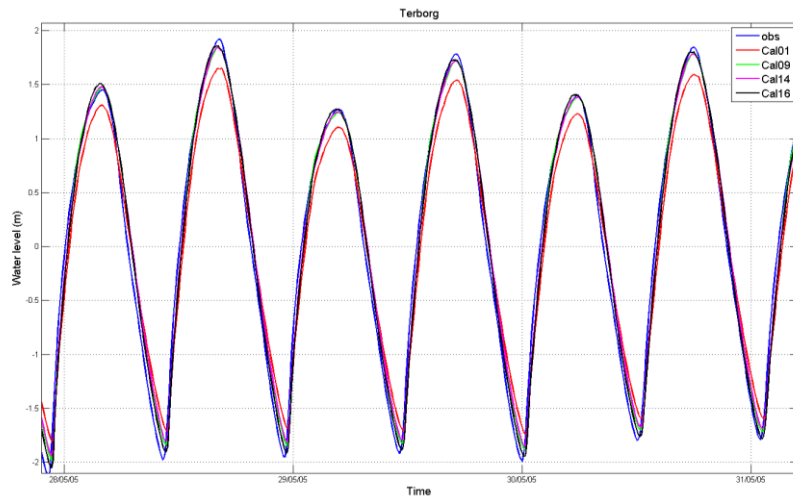


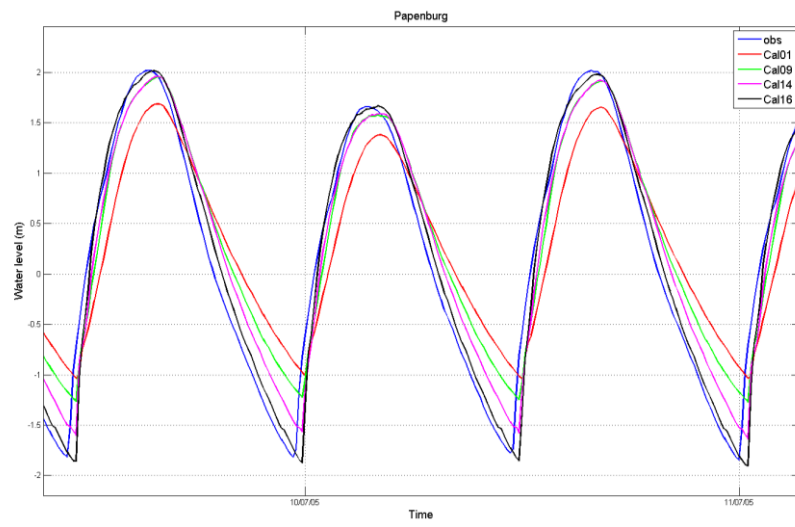


## D Calibration waterlevels ERD model, time domain







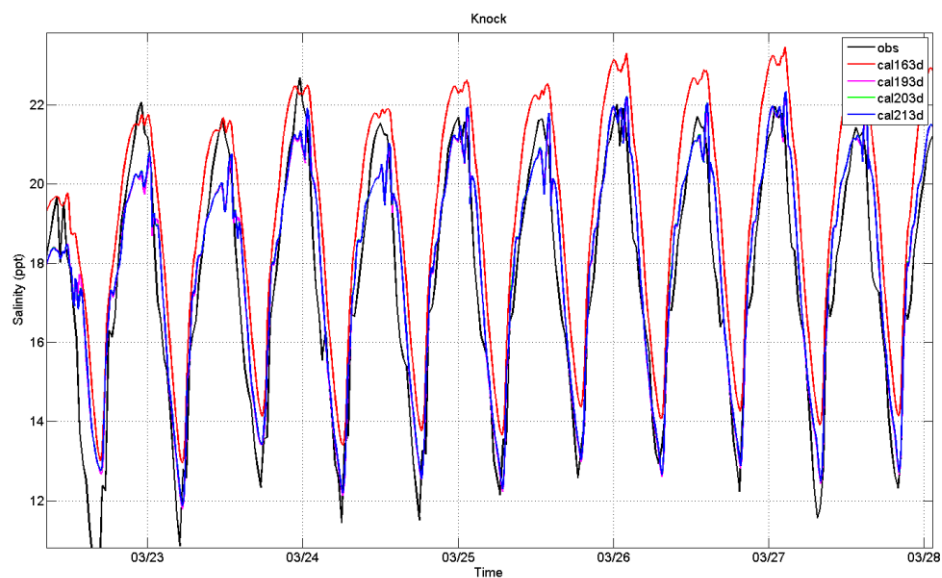
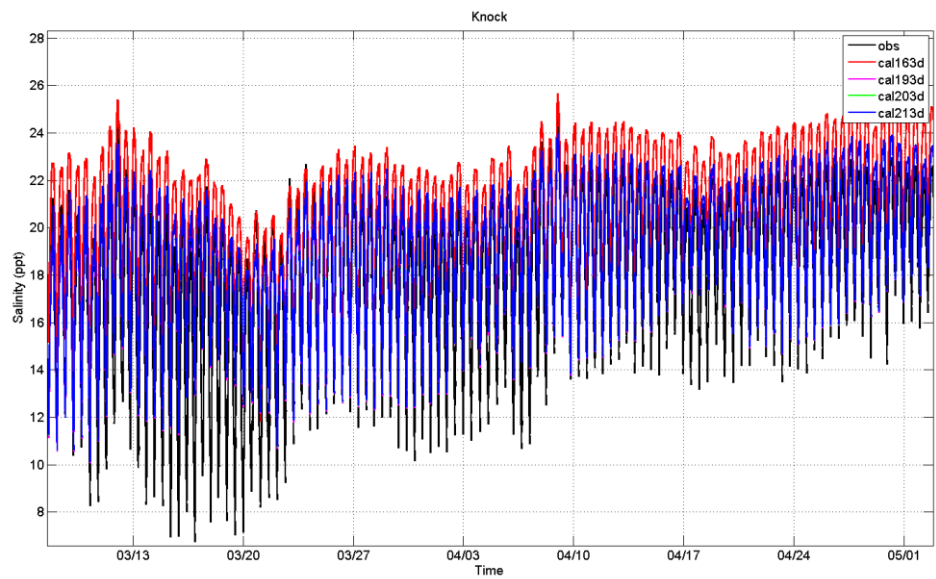




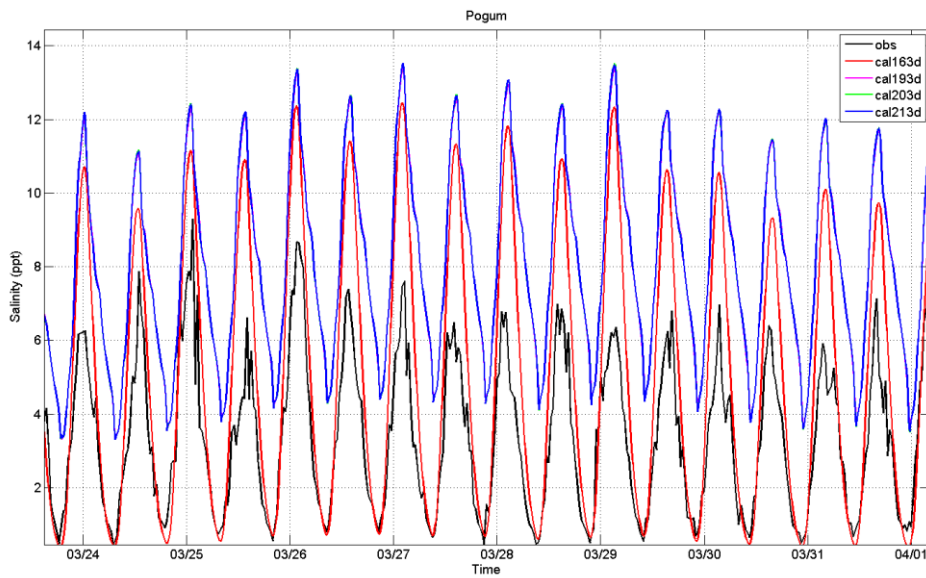
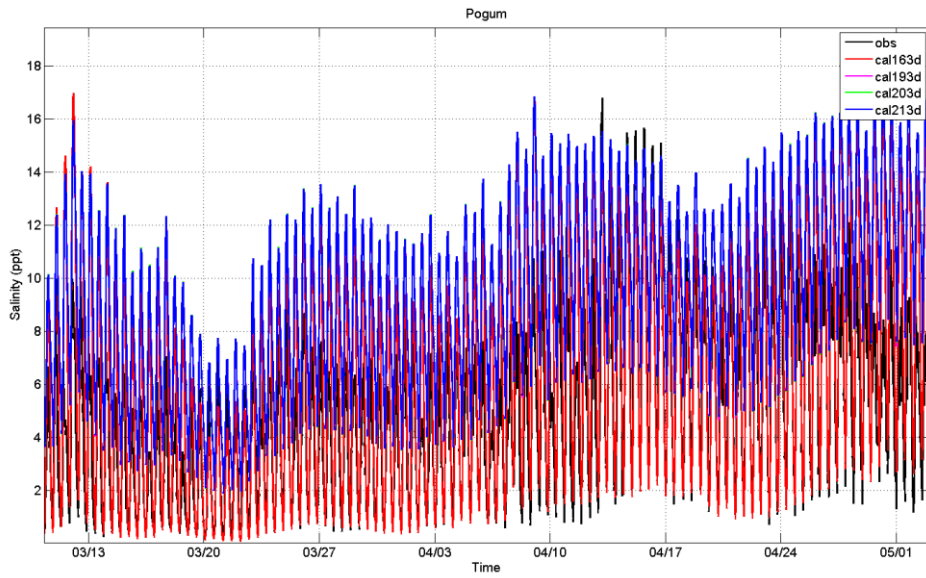
## E Salinity ERD model

Measured (black) and computed salinity at a Knock, Pogum, Terborg, and Leerort. Results for cal193d and cal203d are poorly visible because they overlap with cal213d.

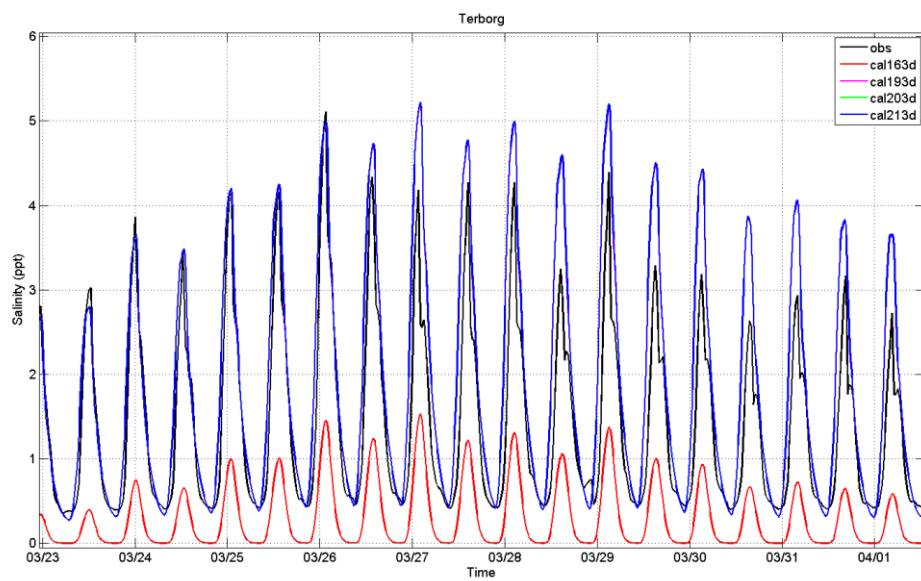
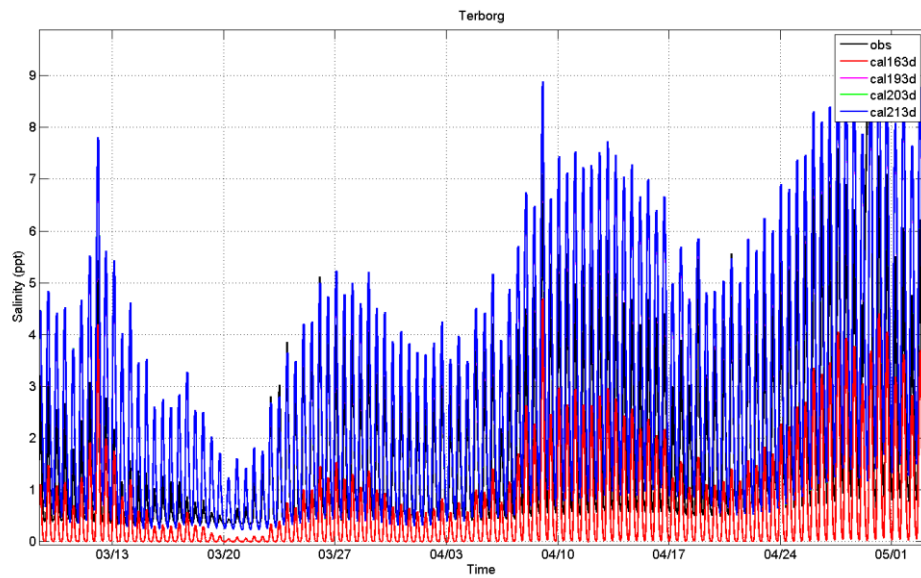
### E.1 Knock



## E.2 Pogum



E.3 Terborg



## E.4 Leerort

